9-8

SANDIA REPORT

SAND95–1551/1 • UC–706
Unlimited Release
Printed August 1995

1994 Triggered Lightning Test Program: Measured Responses of a Reinforced Concrete Building Under Direct Lightning Attachments

Volume 1: Test Description and Data Summary

George H. Schnetzer, Jerry Chael, Raymonard Davis, Richard J. Fisher, Philip J. Magnotti

Prepared by
Sandia National Laboratories
Albuquerque, New Mexico 87185 and Livermore, California 94550
for the United States Department of Energy
under Contract DE-AC04-94AL85000

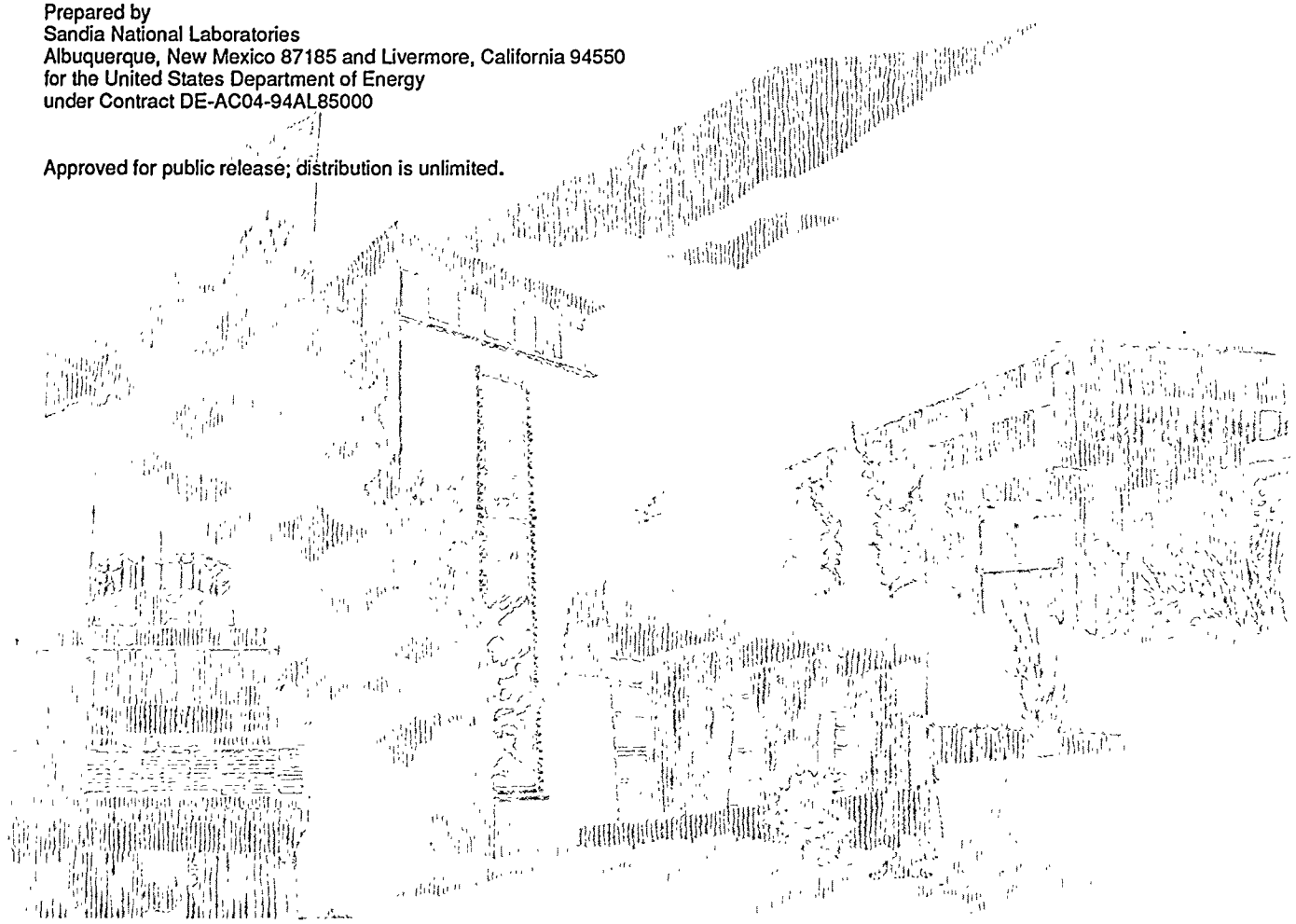

Issued by Sandia National Laboratories, operated for the United States Department of Energy by Sandia Corporation.

Available to DOE and DOE contractors from
Office of Scientific and Technical Information
PO Box 62
Oak Ridge, TN 37831

Prices available from (615) 576-8401, FTS 626-8401

Available to the public from
National Technical Information Service
US Department of Commerce
5285 Port Royal Rd
Springfield, VA 22161

NTIS price codes
Printed copy: A05
Microfiche copy: A01

DISCLAIMER

SAND95-1551/1
Unlimited Release
Printed August 1995

Distribution
Category UC-706

1994 Triggered Lightning Test Program: Measured Responses of a Reinforced Concrete Building Under Direct Lightning Attachments

Volume 1: Test Description and Data Summary

George H. Schnetzer, Jerry Chael, and Raymonard Davis
Electromagnetic Analysis and Test Department
Sandia National Laboratories
Albuquerque, NM 87185-0865

Richard J. Fisher
Engineering Consultant

Philip J. Magnotti
U.S. Army Armament Research, Development and Engineering Center
Picatinny Arsenal, NJ 07806-5000

Abstract

A rocket-triggered lightning test was carried out during the summer of 1994 on a specially designed steel reinforced concrete test building located at Ft. McClellan, Alabama. Currents, voltages, and magnetic fields were measured at 24 instrumented locations during 42 return strokes triggered to designated points on the structure and its lightning protection systems. As was found during an earlier similar lightning test of an earth covered munitions storage building, the buried power service conduits carried a much larger fraction of incident stroke current away from the building than did the intended grounding elements of the lightning protection system. Electrical breakdown and subsequent arcing occurred repeatedly to create dominant current paths to earth that were not accounted for in pretest linear modeling. Potential hazard level transient voltages, surprisingly more resistive than inductive in nature, were recorded throughout the structure. Also surprisingly, strikes to a single grounded protection mast system resulted in internal environments that were generally comparable to those occurring during strikes to roof-mounted air terminals. A description of the test structure, experimental procedures, and a full set of the resultant data are presented in this two-volume report.

Acknowledgments

The authors acknowledge the technical contributions of M. E. Morris and K. O. Merewether of Department 2753, SNL, and J. D. Struck of ARDEC during the test structure design phase of this project. Important on-site logistical and technical support was provided throughout the fielding period by ARDEC's T. Tran, K. Haynes, and R. Branstetter of the SOTS facility at Ft. McClellan, Alabama. Special thanks are due to B. J. Hawley for her extensive help in the plotting of the test data. The excellent discussions with and substantial input from M. E. Morris, K. O. Merewether and B. J. C. Burrows, (formerly of the Lightning Test and Technology Center, Culham Laboratory, United Kingdom) are gratefully acknowledged. The enthusiastic management support and encouragement provided by M. E. Morris of SNL and by M. A. Chiefa and J. E. Grenert of ARDEC's Fire Support Armaments Division is acknowledged to have contributed substantially to the success of the entire project.

Contents

Illustrations

Illustrations (Continued)

Illustrations (Continued)

Tables

Acronyms

ARDEC	U.S. Army Armament Research, Development, and Engineering Center
AT	air terminal (lightning rod)
CTG	cloud-to-ground (lightning)
CVR	current viewing resistor
CVT	current viewing transformer
EM	electromagnetic
EMT	electrical metal tubing (conduit)
FM	frequency modulated
FOL	fiber optic link
GRE	ground ring electrode
LPS	lightning protection system
LTA	launch tube assembly
M&A	maintenance and assembly
OD	outside diameter
PVC	polyvinyl chloride (pipe)
rebar	concrete reinforcing bar
RTL	rocket-triggered lightning
SATTLIF	Sandia Transportable Triggered Lightning Instrumentation Facility
SNL	Sandia National Laboratories
SOTS	U.S. Army Security Operational Test Site
TP	test point

1994 Triggered Lightning Test Program: Measured Responses of a Reinforced Concrete Building Under Direct Lightning Attachments

1.0 Introduction and Summary

1.1 Introduction

During the past six years Sandia National Laboratories (SNL) and the U.S. Army's Armament Research, Development, and Engineering Center (ARDEC)[1] have been carrying out a collaborative investigation of the interaction mechanisms of lightning with munitions and their associated handling and storage facilities. One fundamental program objective is the development of an improved understanding of the performance of various elements of conventional lightning protection systems (LPS's) employed at such facilities. In support of this objective, rocket-triggered lightning tests were performed on a specially prepared and instrumented earth-covered nuclear munitions storage bunker during the summer of 1991 [1]. In 1993, measurements were made of the electromagnetic environment at the earth's surface 10 and 20 meters from the ground strike points of triggered lighting flashes [2].

In 1994, tests were performed on a specially designed and constructed facsimile of a weapon maintenance and assembly (M&A) building. This structure was designed jointly by ARDEC and SNL to incorporate many of the design and constructional features found in real M&A buildings that most influence electromagnetic responses at critical points throughout the structure. Furthermore, the test structure was designed to allow the inclusion or removal of various key features during the course of the testing. In this way, assessment of the influence of each feature of interest could be accomplished through direct comparison of test results with and without its presence, all other factors being the same. Because one of the most significant questions was the effect on overall current flow within a structure attributable to the degree of connectivity between the individual steel concrete reinforcing rods (rebar) within the walls, the building was divided into two volumes, separated electromagnetically by a steel barrier. On one side of the barrier, the so-called "bad" side, the rebar within the walls was of a type in which the individual steel rods were coated with an epoxy layer, thereby ensuring that they were normally isolated electrically from one another at their crossover junctions throughout the walls and floor. On the other, "good," side, the rebar intersections were welded together at regular intervals.

Construction of the building was the responsibility of ARDEC and was accomplished by them using the U. S. Army Corps of Engineers as their contracting and construction supervision agency. The test structure was completed in September 1993 at ARDEC's

[1] Fire Support Armaments Center (FSAC), U.S. Army Research, Development & Engineering Center; Picatinny Arsenal, New Jersey 07806-5000.

Security Operational Test Site (SOTS), located at Ft. McClellan, Alabama. This is the same site at which previous triggered lightning tests in this program were carried out in 1991 and 1993. Technical planning of the 1994 experiments was developed jointly by SNL and ARDEC, with the testing itself being conducted by SNL personnel using the Sandia Transportable Triggered Lightning Instrumentation Facility (SATTLIF) [3] with on-site technical and logistical assistance from ARDEC.

1.2 Summary

The SATTLIF arrived at the test site on April 19. Setup and checkout of the facility and instrumentation of the building were completed by early May. However, administrative impediments to the shipping of the triggering rockets delayed their arrival until June 6. Test readiness was achieved on June 7 and continued without interruption throughout the duration of the summer lightning season until September 2. During that period, which represented an unusually poor season for thunderstorms in Alabama, triggering operations were carried out during the occurrence of overhead storms on seven different days. Data were acquired during four storms, in which a total of 10 flashes, comprising 51 individual return strokes, were successfully triggered to designated points on the test structure. Peak amplitudes of stroke currents ranged from 4.2 to 29.6 kA, while the range of return-stroke current rise times was from 0.06 to 7.0 μs.

Data were acquired at all 24 planned test points and for attachments to all five planned terminus points on the structure and its LPS systems. In addition to the incident lightning flash currents, response currents were measured in the walls, on the lightning protection system down conductors, on the two 100-ft long buried electrical power conduits, on the buried LPS ground ring electrode around the structure, and at several miscellaneous points inside the building. Voltages with respect to the floor rebar were recorded on the simulated overhead crane rail, on the metallic ventilation stack, and on elements of the interior power distribution system. Also measured were the transient potentials developed between the wall and floor rebar at six locations around the inside perimeter of the building. Magnetic fields were recorded at floor level in the two corners of the building that were adjacent to the exterior LPS down conductors. A complete set of waveforms from all the measurements considered to be reliable is presented in Volume 2 of this report for documentation purposes and for use in future analyses. In the remainder of this volume, the design and construction of the test structure is described, along with the test procedures and instrumentation. In Section 3, the data for each type of measurement are summarized and discussed in turn.

An extended list of preliminary conclusions based on the level of analysis reported herein is given in Section 4. While in general the results form a self-consistent set and are compatible with pretest expectations, occasional exceptions exist, and not all aspects of the data have as yet been fully understood. A refined interpretation of the data and a reliable appreciation of their more significant implications will require considerable additional data processing, analysis, modeling, and painstaking comparison on a point-by-point basis under the numerous combinations of variations that were tested.

2.0 General Test Description

2.1 Objective

The primary objective of the test was the acquisition of a set of measurements of the direct-strike lightning responses (voltages, currents, and magnetic fields) throughout the test structure for use in validating SNL's analytical and computer models of this type of building. The secondary objective was to evaluate the influence of various alternative construction features and the relative effectiveness of certain conventionally employed LPS concepts and components.

2.2 Description of the Test Structure

The outside dimensions of the structure were 25 ft by 18 ft by 12 ft. It was constructed of 8-in-thick poured reinforced concrete walls; 4-in poured reinforced concrete floor; and flat 20-gauge corrugated steel roof, supported by steel rafters. The rafters were electrically bonded at regular intervals to the rebar network in the walls. To facilitate evaluation of the effects of variations in wall rebar grid intersection connectivity, the structure was partitioned into two electromagnetically isolated cells by means of an expanded steel grating (1/4-in by 1-in holes) between the two halves. This barrier was bonded to the wall rebar and ceiling rafters at 8-in intervals. In one half of the structure, a crane rail was simulated by means of a steel I-beam suspended from metal hangars tied to the overhead rafters. In the other side, a 10-in-diameter light gauge galvanized steel ventilation pipe was included. The ventilator duct passed through the roof and terminated 3 feet above the floor and was arranged so that it could be either isolated electrically from or bonded to the metal roof. Simulated incoming electrical power service was provided in the form of two 100-ft lengths of buried 3-½-in OD steel conduit. Each conduit was buried at a depth of 3 feet and rose vertically under the structure to penetrate the floor near its respective corner of the interior and terminate in a steel electrical service box mounted on the front wall. To preclude direct contact of the conduits with the floor or its rebar until purposely intended during the course of testing, the conduit penetrations through the floor were made through sections of polyvinyl chloride (PVC) pipe. Interior electrical service distribution was simulated by steel electrical metal tubing (EMT) conduits mounted along the walls in each half of the structure using dielectric fasteners to prevent any electrical contact with the rebar within the walls.

Special provisions were made during construction to allow either electrical isolation or intentional controlled bonding between different parts of the structure and the LPS. The options included

- connecting of floor-to-wall rebar,
- bonding of incoming electrical power service conduit to the buried LPS ground ring electrode, and
- bonding of the vent-pipe to the metal roof.

Figure 2-1 summarizes the main features of the test structure. No windows were included, since those of real M&A buildings are generally covered with metal security screens in a manner that makes them essentially closed electromagnetically at lightning frequencies.

The wall and floor reinforcement consisted of a network of No. 5 (0.625-in diameter) steel reinforcing rod on 8-in centers in both directions. The wall rebar in the "good" side consisted of standard steel rods, welded together on 32-in centers in both directions (every fourth intersection). The intervening intersections between the welds were wire-tied together according to standard construction practice. In the "bad" half, the rebar material was of a type that is coated with an approximately 80-mil-thick layer of epoxy to prevent normal electrical contact between the individual rebar members. Also, in that section, the intersections were secured with nylon cable ties. The thickness of the wall concrete was 8 in. The front and side walls were tied together electrically and mechanically as shown in Figure 2-2.

In the floor, the rebar was of the standard uncoated type on the good side and of the epoxy coated type on the bad side and was also laid on 8-in centers in both directions. On the good side, it was welded at every fourth joint and wire-tied elsewhere. The floor of the bad-side incorporated epoxy-coated rebar, with the intersections being secured with nylon cable ties at each intersection. The 4-in-thick concrete floor was poured on a nominal 6-in-thick limestone gravel base above the underlying red clay soil.

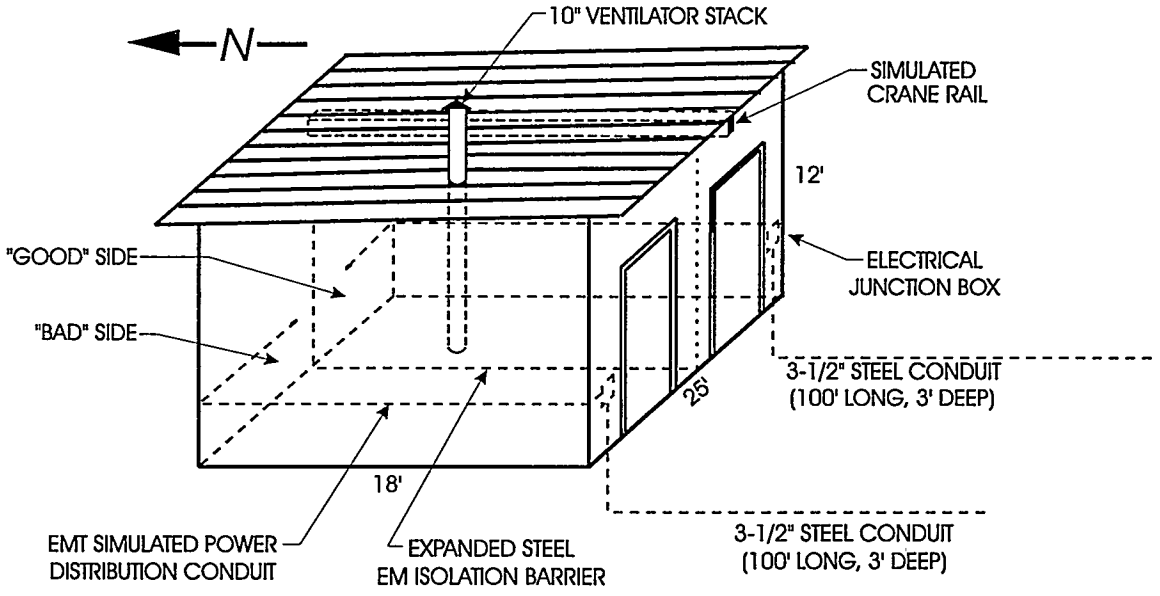

Figure 2-1. Main features of the simulated munitions handling building

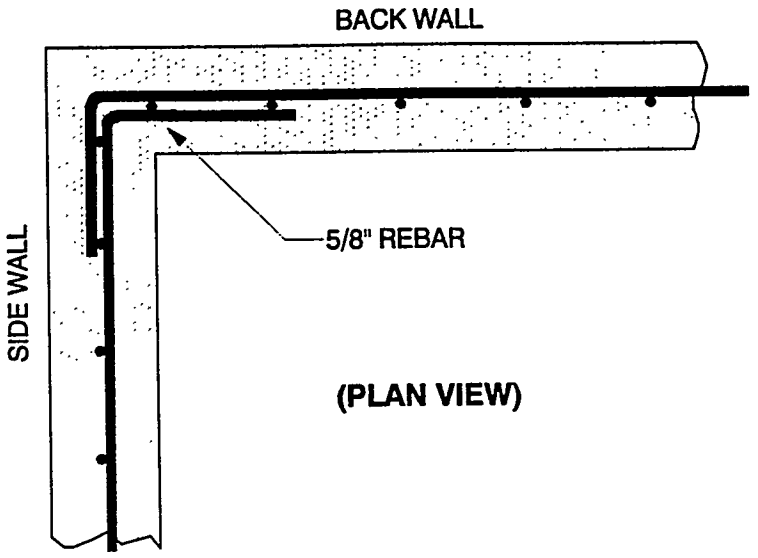

Figure 2-2. Details of concrete rebar connections at corners of the structure. In the "good" side, the connections were welded; in the "bad" side, the rebar was insulated by an epoxy coating and secured by nylon cable ties.

To maintain electrical isolation between the walls and the floor except when they were to be intentionally connected, the bottoms of the walls where they fit into the footer pockets were encased by an insulating layer of 1/2-in-thick woven phenolic dielectric material. The details of this arrangement are shown in Figure 2-3. For those tests in which intentional bonding of the wall and floor rebar was desired, the 28 pairs of matching exposed ends of wall and floor rebar rods around the interior perimeter were connected together using 1-in-wide braided grounding strap and stainless steel hose clamps. PVC pipe penetrations were provided in six places through the back walls of each half of the structure to accommodate the various fiber optic cables and pneumatic control lines from instrumentation located in the interior.

Each half of the structure was provided with a 36-in by 80-in steel door, the frame of which was bonded to the rebar in its surrounding wall but not in the floor (except when the floor and wall rebar were intentionally connected). The interior of the structure was made light-tight so that time exposure photographs could be made inside the building to detect any arcing that might occur during lightning attachments to the exterior.

The lightning protection system consisted of 2-ft high lightning air terminals mounted one on each corner of the roof and a similar one on the top of the ventilator shaft, copper down conductors located at diagonally opposite corners of the structure, and a buried ground ring electrode (GRE). At each corner occupied by a down conductor, the GRE and down conductors were connected to 1/2-in diameter, 10-ft-long copper ground rods. The GRE, down conductors, and interconnecting cables between the air terminals were #1/0 gauge, 24-strand, 1/2-in diameter copper. The GRE, which is often referred to in the lightning literature as a "counterpoise," was buried at a depth of 36 to 48 inches around

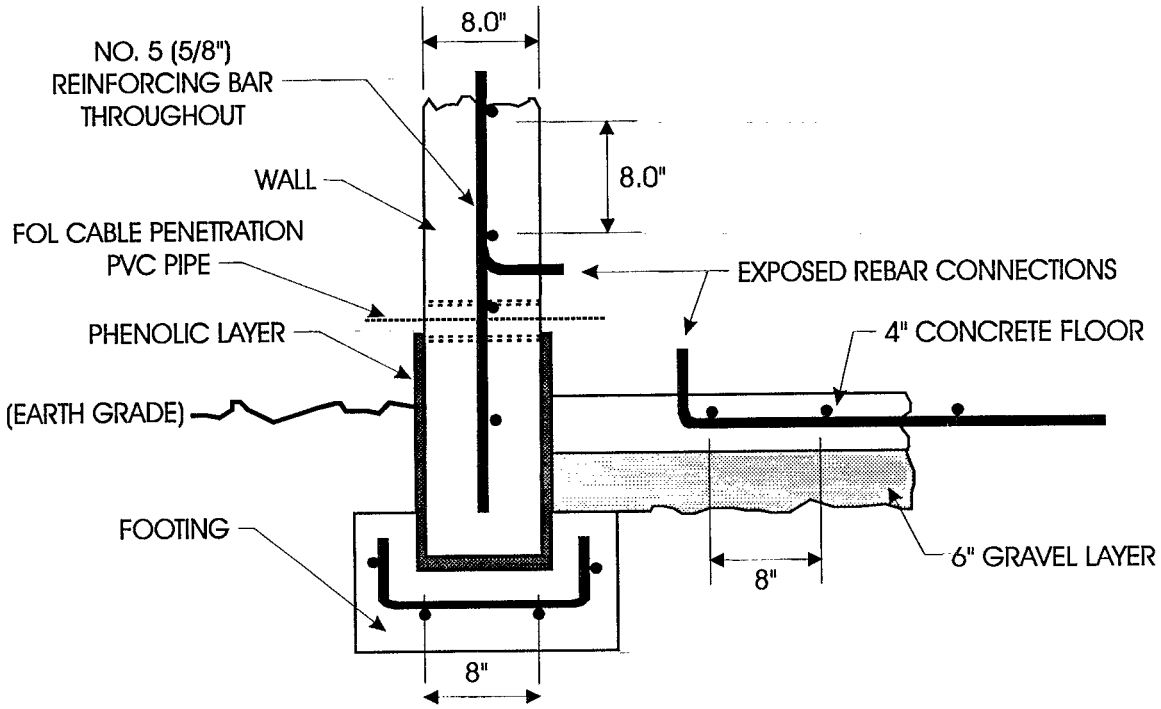

Figure 2-3. Details of construction of the wall/floor joints

the structure approximately 2 to 3 feet out from the bottom of each wall. In the baseline configuration, the buried 100-ft electrical conduits were not connected directly to the GRE, but provisions were made inside the building to allow their intentional bonding during some of the testing. (Refer to Section 2.3, in which the measurement points and various configurations tested during different storms are described.) The details of the baseline LPS are shown in Figure 2-4.

The LPS was modified for testing purposes during one storm. In this version, the air terminals and down conductors were removed from the building and ventilator stack. Instead, a single 49-ft high lightning protection mast was installed at the front center of the building approximately 5 ft out from the edge of the roof. The pole consisted of a telescoping antenna mast with outside diameters of about 1 in at its topmost section and 2½ in at its base. The bottom of the mast was connected to the incident lightning current sensing instrumentation, which in turn was connected to the buried GRE using a 1-in braided ground strap. One flash, comprised of 7 individual return strokes, was triggered to the top of this mast.

The test site was located in the same immediate area where the 1993 triggered lightning experiments were carried out to measure the environments close to the ground strike points of lightning channels. The soil in this vicinity is of heavy red clay composition with an average conductivity of approximately 1.8×10^{-3} S/m [2]. The site layout is shown in Figure 2-5. The photographs in Figure 2-6 show the test building from two views, and Figure 2-7 shows the SATTLIF as deployed for these tests.

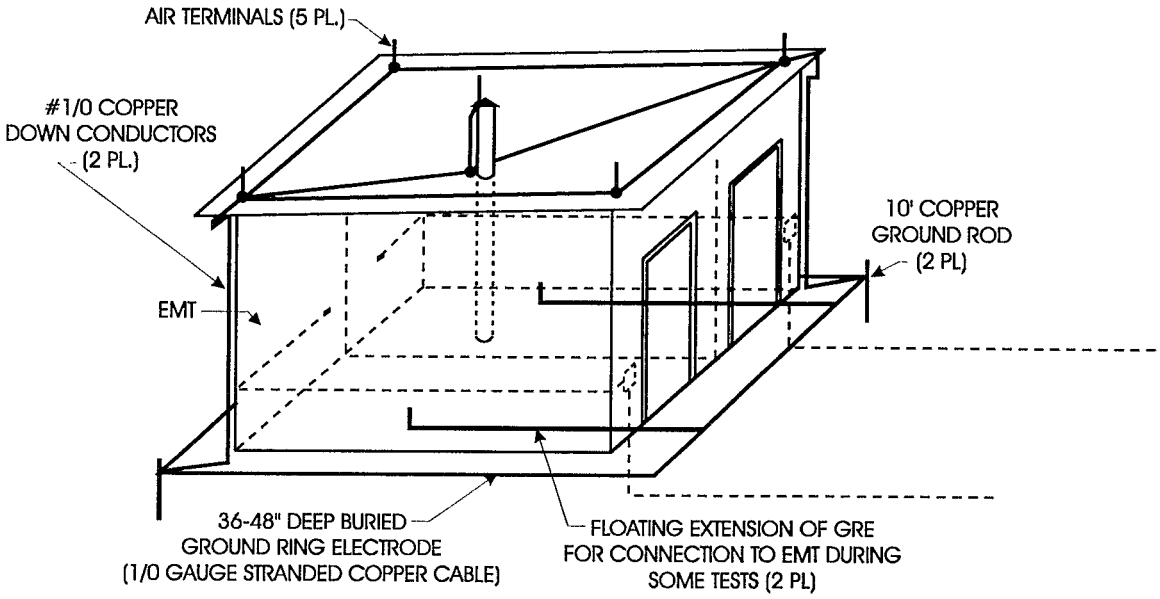

Figure 2-4. Diagram of the lightning protection system installed on the test structure during part of the present tests. During Storm 4, a single 49-ft high mast system was tested for comparison with the one shown in this figure.

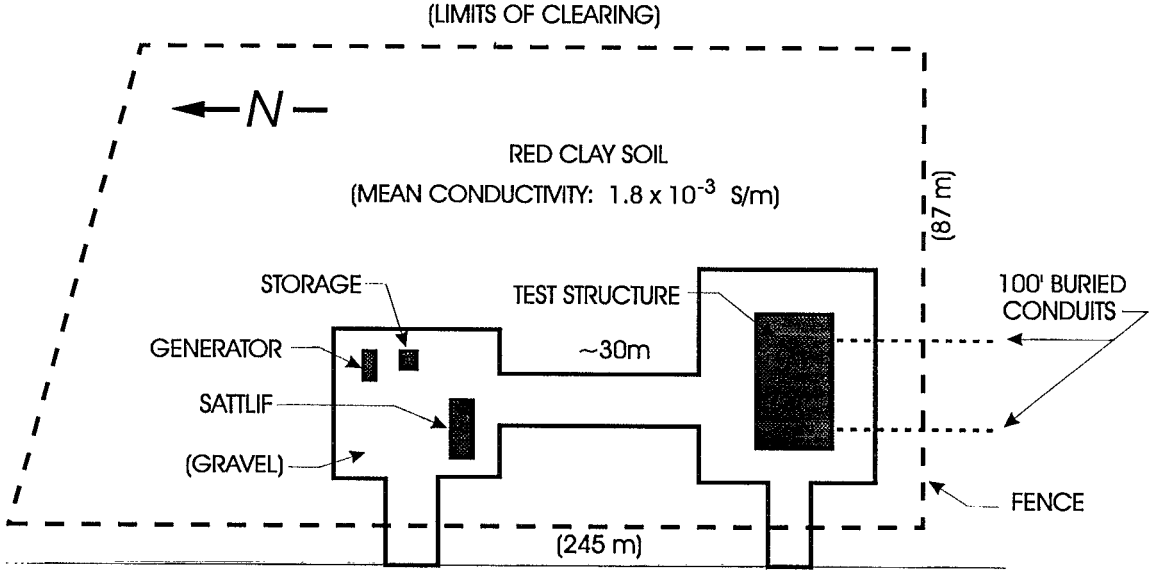

Figure 2-5. Overview of the test site

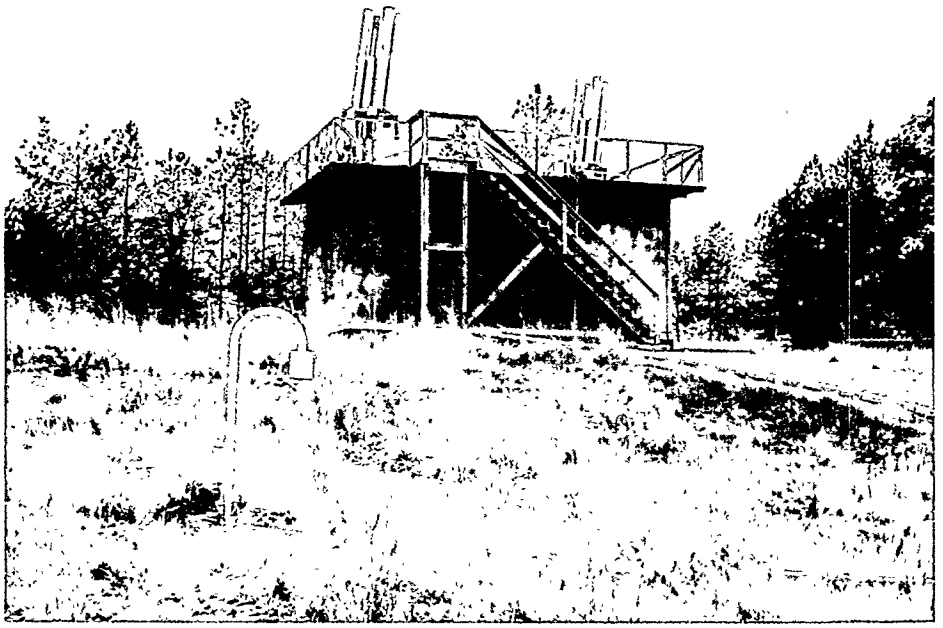

(a)

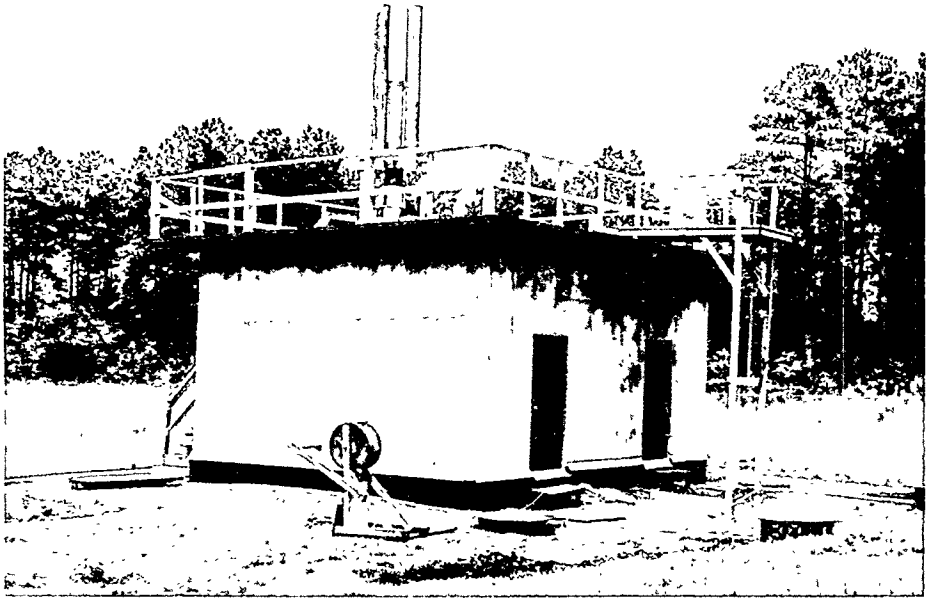

(b)

Figure 2-6. (a) View of the test structure with rocket launchers installed on the roof. Visible from this angle are the north and east walls. (b) View showing the south wall (front of the building) and west wall. Note the dark portion along the base of the walls, which is the phenolic insulating material installed to provide electrical isolation between the walls and the floor and ground.

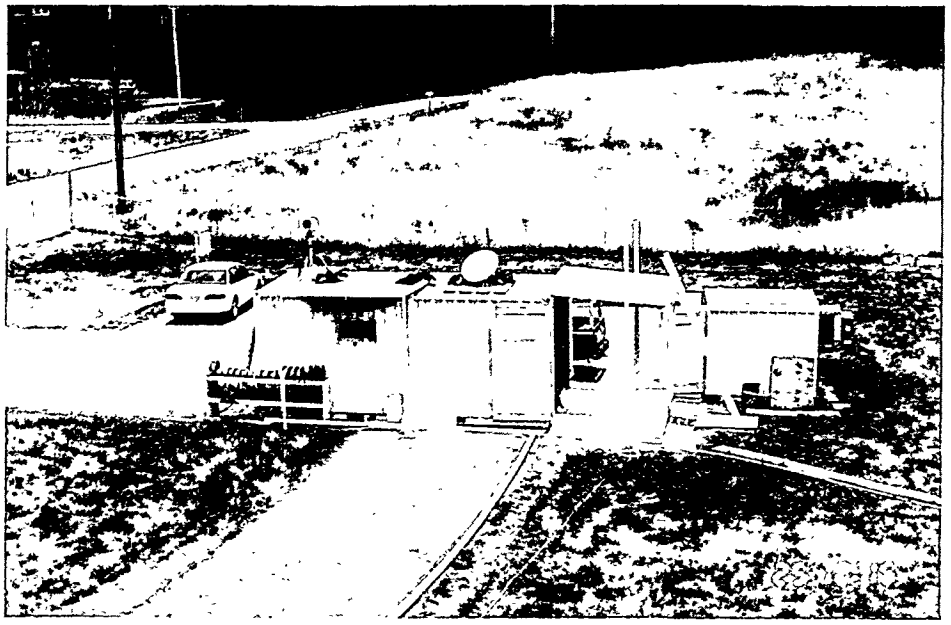

(a)

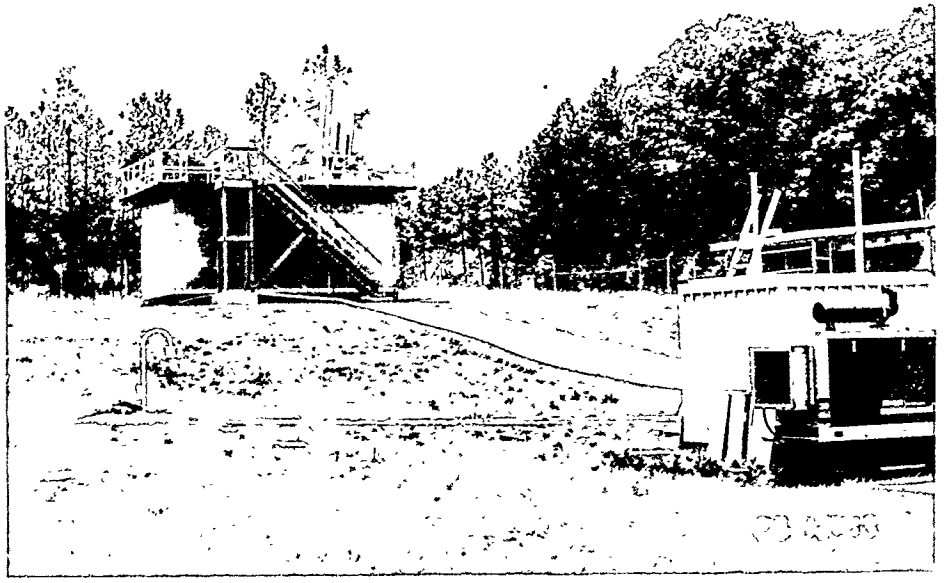

(b)

Figure 2-7. (a) View of the SATTLIF and its auxiliary equipment from the roof of the test structure; (b) the test structure and portion of the generator and storage container taken from a point near the top right portion of the photograph shown in (a).

2.3 Test Point Description

In addition to the incident return-stroke and continuing current components of the triggered flashes, measurements were made of currents flowing within and voltages developed between various structural members of the building and its lightning protection system. The transient magnetic field at floor level was also recorded near the interior corners nearest the down conductors in each half of the structure. Data were acquired on a total of 24 test points over the course of four separate thunderstorms, which produced ten triggered flashes to various designated attachment points on the test building and its LPS. The triggered flashes, all of which were of the negative cloud-to-ground (CTG) type,[2] produced in excess of 50 return strokes, with a range of peak current amplitudes from about 4 to 30 kA and 10-to-90 percent rise times of between 0.06 and 7.0 μs.

A full list of the measurement test points is given in Table 2-1. In the table, the channel type designations "S" (for "slow") and "F" (for "fast") correspond to the 400-kHz frequency modulated (FM) magnetic tape channels and 6-MHz digitizing oscilloscope channels, respectively, that were assigned as listed. (Instrumentation details are discussed in Section 2.5.) The listed priorities of the measurements were applied during the testing of any given building configuration, which included the particular test points in question.

Figure 2-8 is a plan view of the test structure on which has been superimposed the physical location of each of the test points. The arrows next to some of the test points in the figure correspond to the direction of positive current flow represented in the acquired data for each respective sensor. The ultimate polarity of the recorded responses at each test point depends not only on the actual direction of current flow at that location, but also on how the sensor was installed. A negative-going data record from any test point corresponds to electron flow in the same direction as the arrow. For example, in the case of TP7, which was installed on the LPS down conductor cable on the southeast corner of the building, a negative going signal would imply the flow of electrons down the LPS cable and into the GRE. Such a result would be consistent with expectations for a negative CTG flash.

During testing it was arranged that lightning flashes were triggered to five separate attachment points. These are listed along with their designations in Table 2-2. A summary is given in Table 2-3 of the attachment points and configurations of the building as they were tested during each storm.

[2] Globally, more that 90 percent of all cloud-to-ground lightning is of negative polarity, that is, of the type that effectively lowers negative charge from the cloud to earth.

Table 2-1. Test Point Definition

Test Point	Description	Channel Type[1]	Priority[2]
	Current		
1	Buried Conduit	S	1
2	Buried Conduit	S	1
3	Conduit Entry	S/F	1
4	Conduit Entry	F	2
5	GRE[3]	S/F	1
5'	GRE	S/F	1
6	GRE	S/F	1
6'	GRE	S/F	1
7	GRE	S/F	1
8	GRE	S/F	1
9	GRE Stub, Good Side	S	1
9'	GRE Stub, Bad Side	S	2
10	Wall-to-Floor Rebar	S	1
11	Wall-to-Floor Rebar	S	1
12	Wall-to Floor Rebar	S	1
13	Wall-to-Floor Rebar	S	1
14	Wall-to-Floor Rebar	S/F	1
15	Wall-to-Floor Rebar	S/F	1
	Voltage		
16	Wall-to-Floor Rebar	F	1
17	Wall-to-Floor Rebar	F	1
18	Wall-to-Floor Rebar	F	1
19	Wall-to-Floor Rebar	F	1
20	Crane-to-Floor	F	1
21	Vent-to-Floor	F	1
22	Distribution Conduit/Floor	F	2
	Magnetic Field		
23	Field[4]	S/F	2
24	Field	S/F	2

[1] S = FM tape channel; F = LeCroy digitizer channel; S/F = digitizer with tape backup.
[2] Priority applies to those shots on which the listed TP is included.
[3] Ground Ring Electrode system.
[4] Floor level, 1 ft from walls in corners of each side adjacent to exterior down conductors; sensor axis at 45° with respect to the walls.

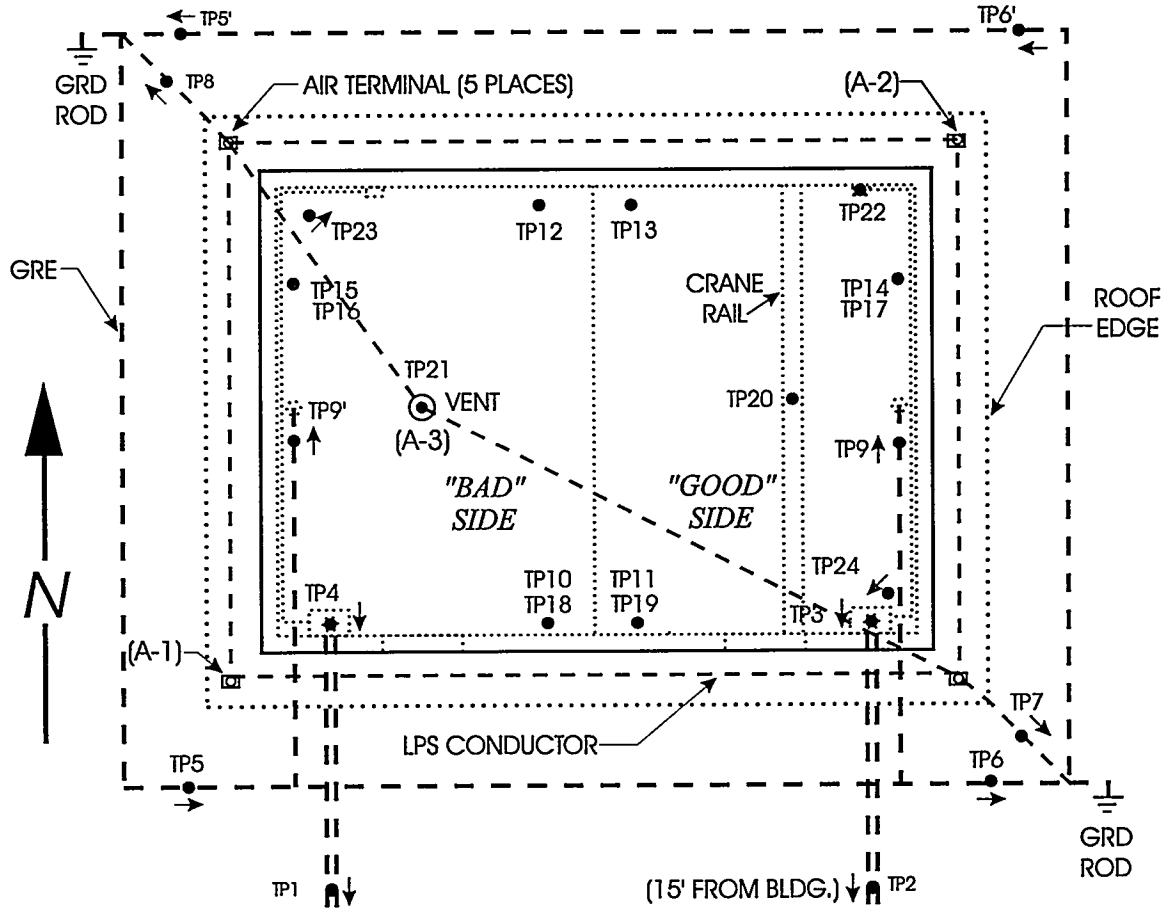

Figure 2-8. Map of test point locations throughout the test structure

Table 2-2. Triggered Lightning Attachment Points

Point	Location	Remarks
A-1	SW AT	
A-2	NE AT	
A-3	Vent Stack AT	
A-4	Conduit Riser Stub	Remove AT's and conductors
A-5	LPS Mast	Remove AT's and conductors

Table 2-3. Building Configurations Tested During Various Storms

Storm No.	Attachment Point	Configuration and Test Points
1	A-1 A-2	Floor and wall rebar connected; vent bonded; buried conduit floating[1]; TP's: 1-2, 5, 5', 6, 7-8, 10-15, 20-24
2	A-1 A-3	Floor and wall rebar disconnected; vent unbonded; conduit floating; TP's: 1-2, 5, 5', 6, 6', 7-8, 16-24
3	A-2 A-4	Floor and wall rebar disconnected; vent bonded; conduit grounded to GRE inside structure; TP's: 1-2, 3-4, 5-9, 16-24
4	A-4 A-5	Floor and wall rebar connected; vent bonded; LPS AT's and conductors removed; TP's: 1-2, 5-5, 6'-6', 7-8, 10-15, 20-24

[1]Buried conduit electrically disconnected from GRE.

2.4 General Test Procedures

During the course of naturally occurring thunderstorms in the immediate vicinity of the test structure, small weather modification rockets were fired into the overhead clouds at times when the atmospheric electrical conditions were appropriate for successful lightning initiation. Each rocket was equipped with a specially designed spool, which deployed a thin trailing wire as the rocket ascended. The bottom end of the wire was connected to the aluminum frame of the launch tube assembly (LTA). The resulting flash in each successful instance was therefore directed to earth via the intended attachment point, at which location the incident current was measured.[3]

Figure 2-9 is a diagram of the LTA and the manner in which the incident lightning current was measured. The instrumentation box indicated in the figure was an electromagnetically tight steel enclosure containing the sensor, signal conditioning electronics, and fiber optic transmitters employed in recording the incident flash current. Details of this instrumentation are addressed in Section 2-5.

[3] See Section 3 of Reference 3 for a discussion of the rocket-triggered lightning technique employed here and its associated phenomenology.

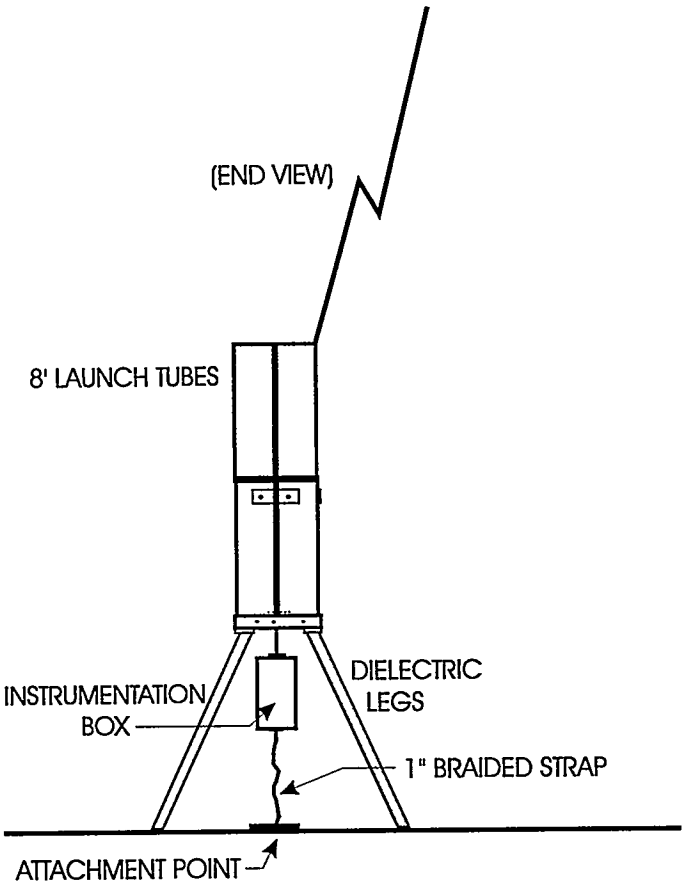

Figure 2-9. Diagram of launch tube assembly and its connection to a designated attachment point via the current sensing instrumentation

Prior to each storm, the building was configured and instrumented as desired according to Table 2-3, and two independently controlled launch tube assemblies were erected immediately above the desired attachment points. Photographs of the LTA's in place on the roof above attachment point A-1 and on the ground positioned over A-4 are shown in Figure 2-10. When proper triggering conditions were met, rockets were launched from each LTA in turn until lightning had been successfully initiated to both points. This procedure was continued until either adequate data had been acquired or storm conditions had deteriorated to the point that lightning could no longer be produced. Figure 2-11 is a photograph of flash 94-15, which was triggered to attachment point A-4, the riser stub connected to the 3-½-in buried conduit 50 feet from the building. In the photograph the building lies between the camera and A-4, so the ground terminus of the flash is not visible.

Following each storm, the acquired data were down loaded into permanent files, the magnetic tape channel data were digitized and stored, and all the data were plotted and reviewed. Based on the results, decisions were made about the adequacy of the data at each test point and whether any modifications should be made in the test plans covering subsequent storms. The building was then reconfigured and otherwise prepared for the next storm.

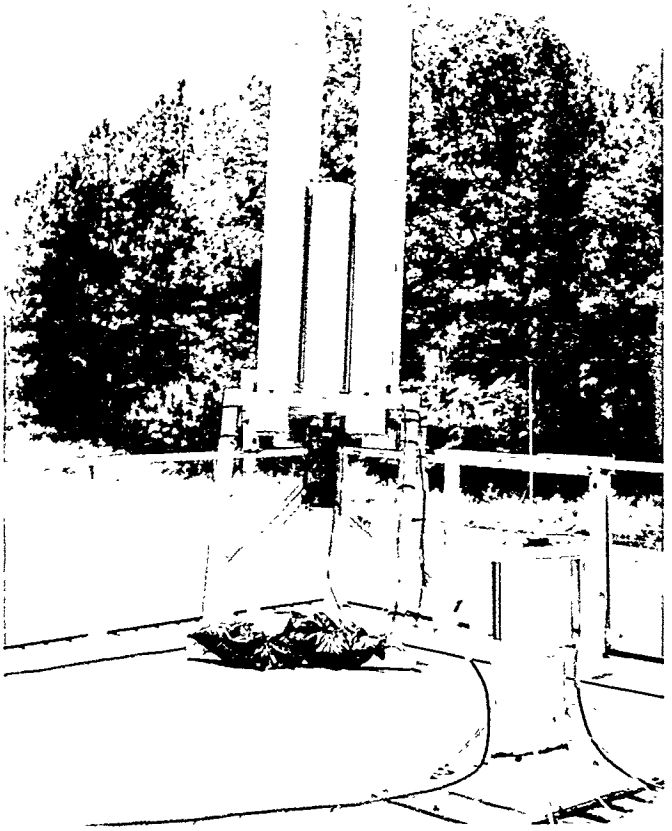

(a)

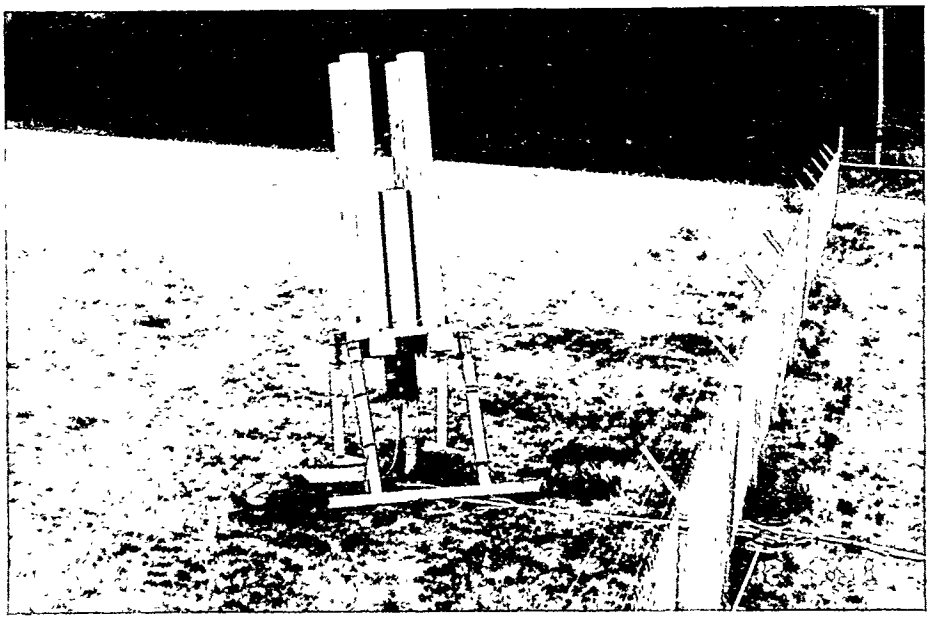

(b)

Figure 2-10. (a) LTA installed above attachment point A-1 on the roof of the test structure. Vent stack with its lightning rod and bonding straps installed is visible in the foreground. (b) LTA installed over the riser stub from the 3½-in east buried steel conduit 50 ft from the south wall of the test structure.

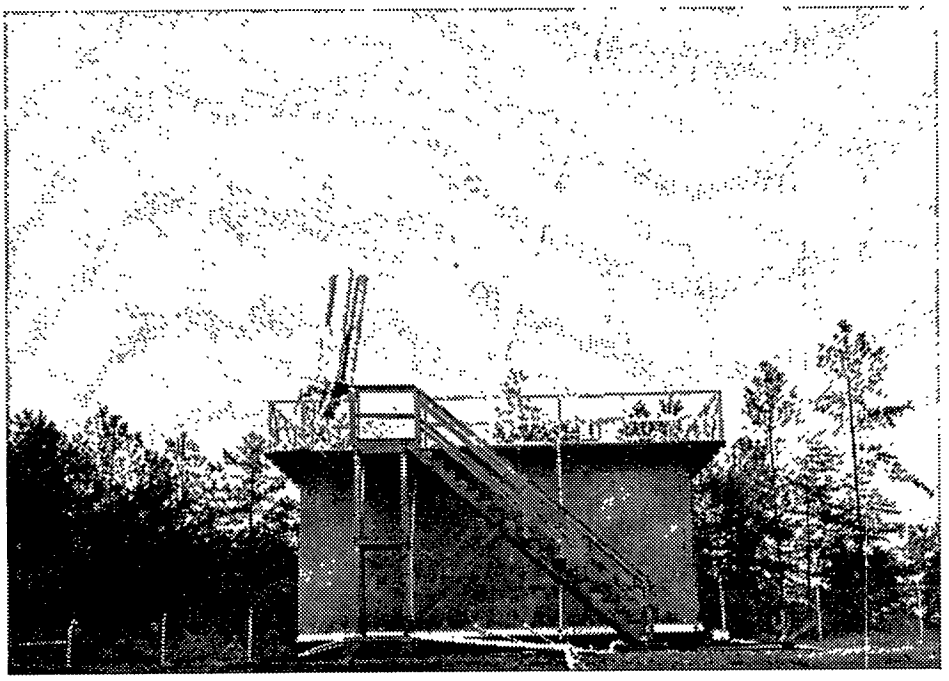

Figure 2-11. Flash 94-15 triggered to the attachment point shown in Figure 2-10b, which in this photograph is out of view behind the test structure

As was mentioned in Section 2.2, during Storm 4 a modified LPS configuration was tested to support a comparison of the effectiveness of a single mast system against one comprised of air terminals and down conductors. To obtain direct attachment of the triggered flashes to the top of the mast, the arrangement shown in Figure 2-12 was employed successfully. In this technique, the launcher was canted to an angle that forced the flight of the rocket to pass nearby the elevated tip of the protection mast. Thus, even though there was no physical connection between the rocket's trailing wire and the mast itself, the substantial electric field enhancement occurring around the tip of the elevated mast encouraged the return strokes of the triggered flash to jump from the vaporized trailing wire channel onto the top of the mast. In the figure, the braided strap conductor shown between the LTA and the sensor instrumentation box provided the path for the early streamer and wire-burn components of the triggered flash currents to flow to ground through the sensor.

2.5 Instrumentation

The same basic complement of instrumentation was employed during these tests as was used for the munitions bunker RTL test in 1991, and most of the instrumentation details are therefore documented in Reference 1. That description will not be repeated herein, although departures from the earlier versions, overall instrumentation

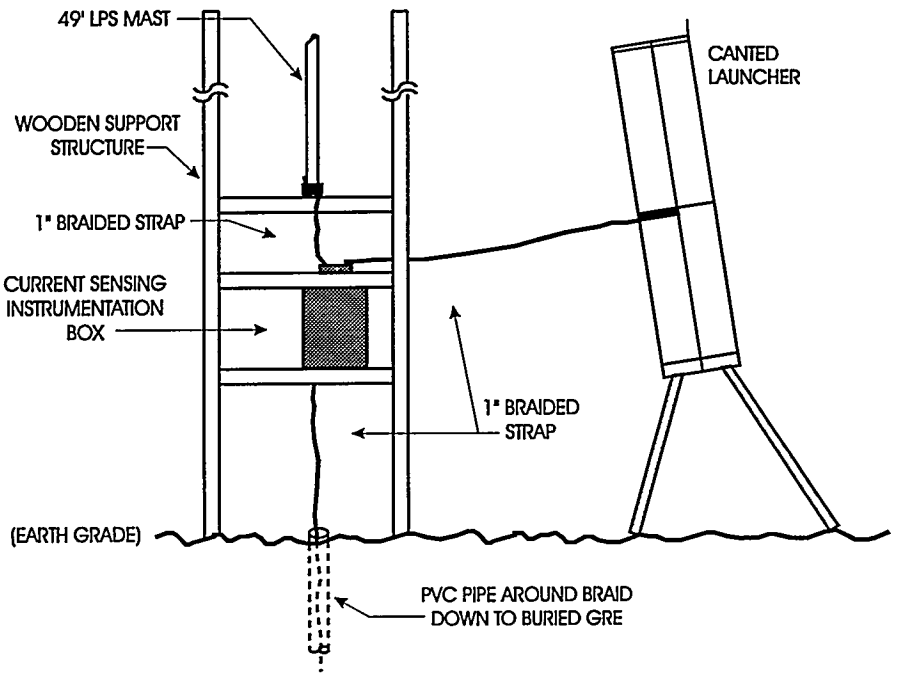

Figure 2-12. Arrangement of the LTA and base of the lightning protection mast tested during Storm 4

characteristics, and key operating parameters relevant to the present tests are summarized in what follows. The five categories of measurements that were carried out were the recording of channel-base return-stroke and continuing current components of the incident triggered lightning flashes; voltages developed between different points within the structure; currents flowing within various structural members, electrical system conduits, and LPS elements; and magnetic fields within each half of the building at floor level.

2.5.1 Incident Flash Currents

Per SNL's standard practice, the incident flash current flowing on either the launcher assembly or, as was the case during Storm 4, on the LPS mast was sensed directly using a T&M Research Model K-5000-10, 1-mΩ coaxial current viewing resistor (CVR). The CVR was mounted in an electromagnetically sealed steel enclosure, which also housed two separate fiber optic transmitters, their batteries, and pneumatically controlled actuator components. The steel enclosure was inserted physically and electrically between the base of the LTA or LPS mast and the designated attachment points as illustrated in Figures 2-9 through 2-12. The legs of the LTA are made of dielectric materials to provide high voltage electrical isolation of the launch tubes and their supporting frame from the attachment point and nearby portions of the building or earth. Thus all of the incident flash current flows through the CVR to the designated attachment point and thence to earth.

As was done during the previous RTL tests, flash current components of low amplitude, such as the wire-streamer, wire-burn, and various continuing current

components[4] were transmitted over Dymec 5717 FM fiber optic links. These signals were recorded on FM magnetic tape recording channels with an overall bandwidth from zero to approximately 400 kHz. The selected sensitivity for these channels resulted in a saturation level of approximately 2 kA and a resolution capability of approximately 20 to 30 A after post-test data processing with a 125-kHz low pass filter to reduce tape recorder noise contamination.

One change from previous procedures was that during these tests the detected signals from the high amplitude (kiloamperes to tens of kiloamperes, typically), fast rising transient return-stroke current pulses were transmitted to the LeCroy 9400A digital recording oscilloscopes in the SATTLIF shelter via two different types of fiber optic systems. The return-stroke signal from one of the LTA's was transmitted over a NanoFast 300-2 analog FOL. This is the same system that was employed previously during earlier SNL triggered lightning activities. The overall measurement 3-dB bandwidth associated with this channel was from about 5 Hz (set by the low frequency limit of the NanoFast system) to just under 6 MHz. The upper limit corresponds to the measured 60-ns 10-to-90 percent rise time of the CVR.

The NanoFast FOL, which operates by analog amplitude modulation, has the inherent drawback that optical coupling through its various fiber optic cable connectors affects the level of the signal at the receiver. While a compensation network is provided to adjust for slow changes in the optical signal level, there has remained a concern that short term perturbations due to the mechanical shock associated with the lightning strikes to the LTA might affect the measurements. Other cost and operational disadvantages associated with the NanoFast units have also been experienced during previous RTL testing. An improved alternative was therefore being sought.

The excellent performance of the Dymec FM FOL links that have been used in the SATTLIF since 1990 to record the low frequency portions of the incident current (in particular, continuing currents) favorably supported the choice of an FM system, which, among other advantages, is also immune to irregularities in optical signal levels. Such a device with adequate bandwidth to accommodate the return-stroke signals has recently become available. This is the MM-3701 video fiber optic link manufactured by Opticomm. Because of the physical size of this unit and its battery, the transmitters of both the MM-3710 system for use with the return strokes and the Dymec 5717 system for continuing currents were consolidated into a single package. As shown in Figure 2-13, the MM-3710 link itself has a measured bandwidth from just above 10 Hz to almost 10 MHz. The overall frequency response of the measurement, however, was still inherently limited to about 6 MHz because of the 60-ns rise time capability of the CVR. A block diagram of the combined return-stroke/continuing current FOL package is shown in Figure 2-14. The design and specifications of this unit are fully documented in Reference 4.

[4] See Section 3 of Reference 3, for example, for a discussion of these important components of a triggered lightning flash current and their correspondence to those of naturally initiated CTG lightning.

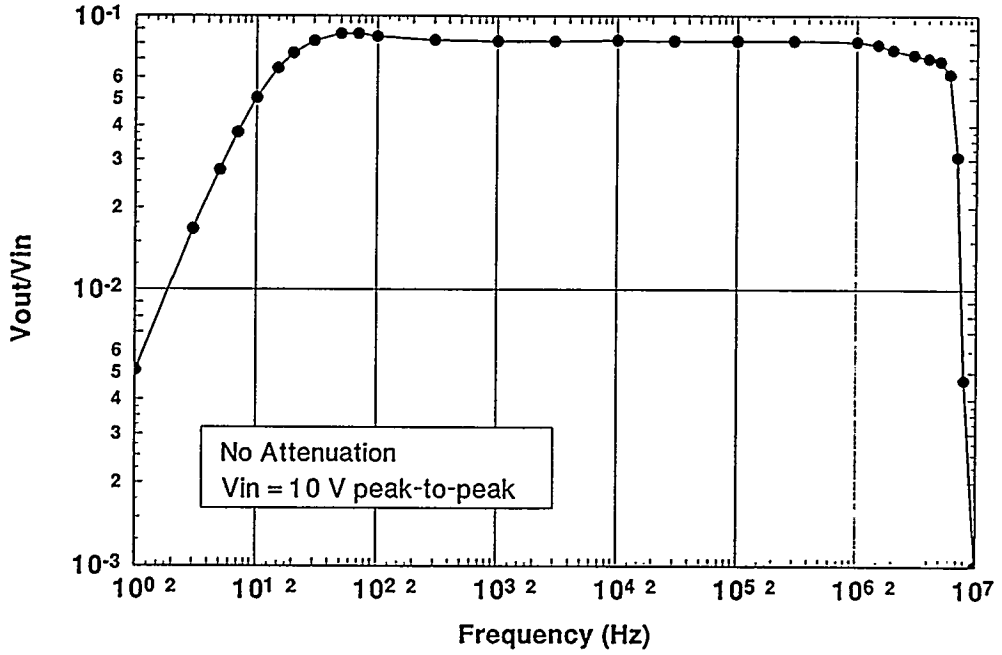

Figure 2-13. Measured bandwidth of the Opticom MM-3710 FM fiber optic link employed for the first time during the present tests to transmit the incident current signals from one of the LTAs to the recording equipment in the SATTLIF

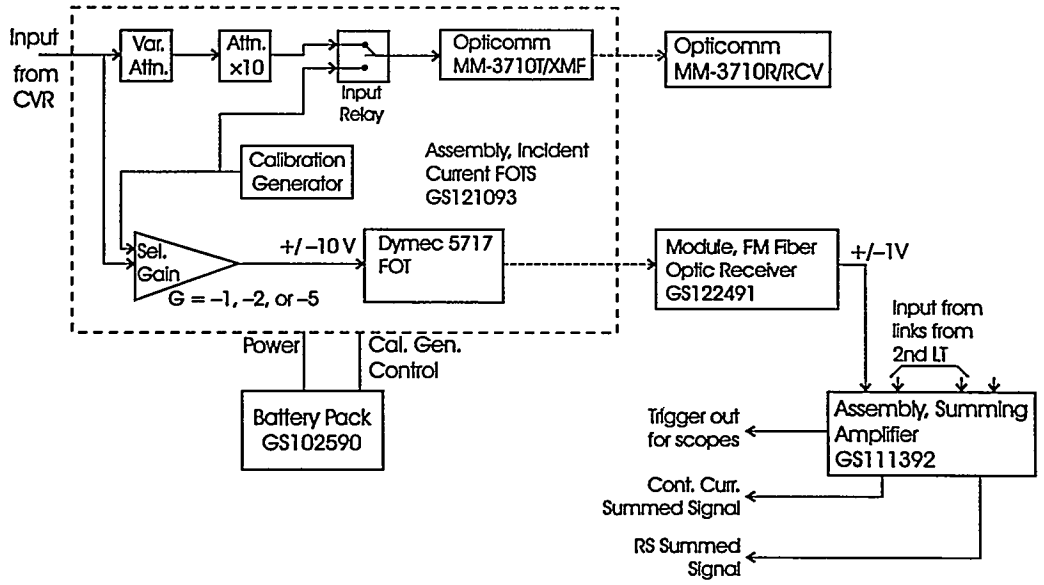

Figure 2-14. Diagram of the combined return-stroke and continuing current instrumentation channels employed during the present tests

The summing amplifier assembly shown in Figure 2-14 serves several functions. The first is to make possible the recording on the same channels of signals arriving from either one of the two deployed launchers without having to reconfigure any hardware during the course of a storm. The four indicated inputs to the amplifier correspond to the return-stroke and continuing-current data links from the instrumentation installed on each of the two launchers. A second function of the summing amplifier circuitry is to generate a common triggering signal for all of the data acquisition digitizers that are employed on a given test shot. The triggering level was set to correspond to an incident return-stroke current of 4 kA. Finally, the assembly also contains the 6-MHz low pass filter circuitry employed to improve signal-to-noise ratio and to preclude potential aliasing in the digitized data, which were sampled every 40 ns.

2.5.2 Voltage Measurements

The potentials developed across the various test points listed in Table 2-1 were sensed by means of voltage dividers of appropriate values. The installations of two of these sensors are shown in Figure 2-15. Because of the magnitudes of the anticipated responses (in some cases as high as several hundred kilovolts), special 5-MΩ resistors were employed as the voltage divider resistors in series with the 50-Ω input resistance of the fiber optic transmitter circuit. Calibrated attenuators were inserted as required at the input to the transmitter to limit the amplitude of the anticipated signal to within the ±1-volt linear range of the transmitter.

As was the case during the previous test of the munitions storage bunker, Meret fiber optic data links, with nominal bandwidth of zero to 35 MHz, were used to transmit the detected voltage transients to the recording equipment. A filter amplifier assembly was inserted between the receiver output and the recording device in each channel. The function of the filter circuitry was twofold. First, it served to limit the output of the receiver to a bandwidth of 1.6 Hz at the lower end to a 3-dB upper frequency of either 4 or 10 MHz, depending on the intended application of the particular channel. Secondly, it enabled compensation for small variations in the gain of individual units. Additional details of the Meret FOL instrumentation channels and their calibration procedures are given in References 1 and 5.

During the course of data analysis following the test, it was realized that stray shunt capacitances across the voltage divider resistors, although small, still resulted in impedances that were too small in comparison with those of the 5-MΩ resistors. This situation resulted in distortion of the measured signals due to capacitive peaking effects, and compensation therefore had to be applied during data processing.

As a first step in the compensation procedure, the shunt capacitance for each voltage measurement configuration employed during the tests was determined experimentally. This was done by recreating as closely as practicable in the laboratory the same physical and electrical voltage measurement configurations as those employed at the various test point locations in the test structure. In each case, the actual resistors used during the tests

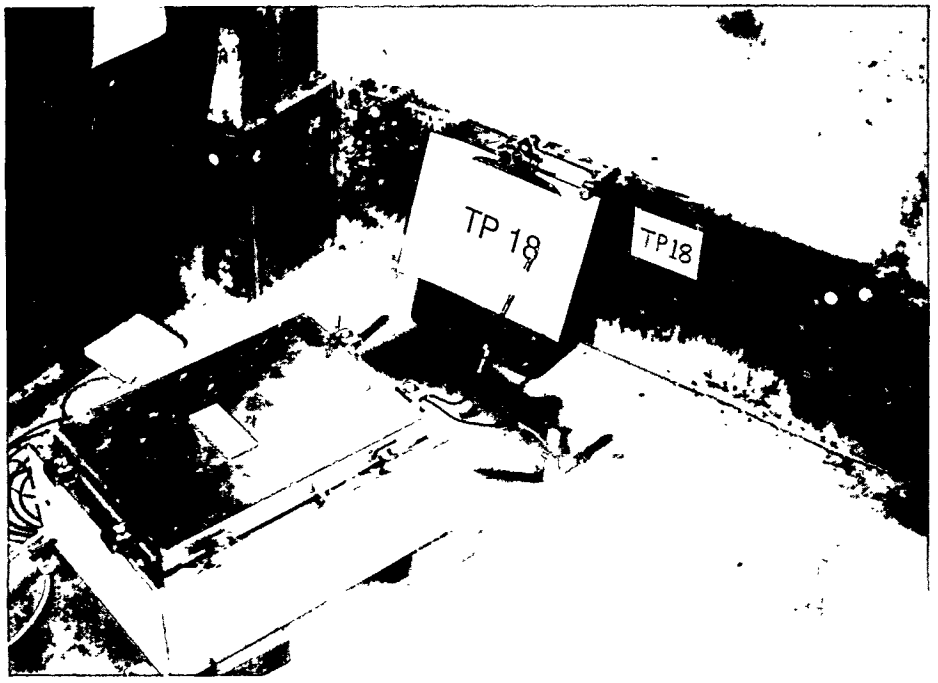

(a)

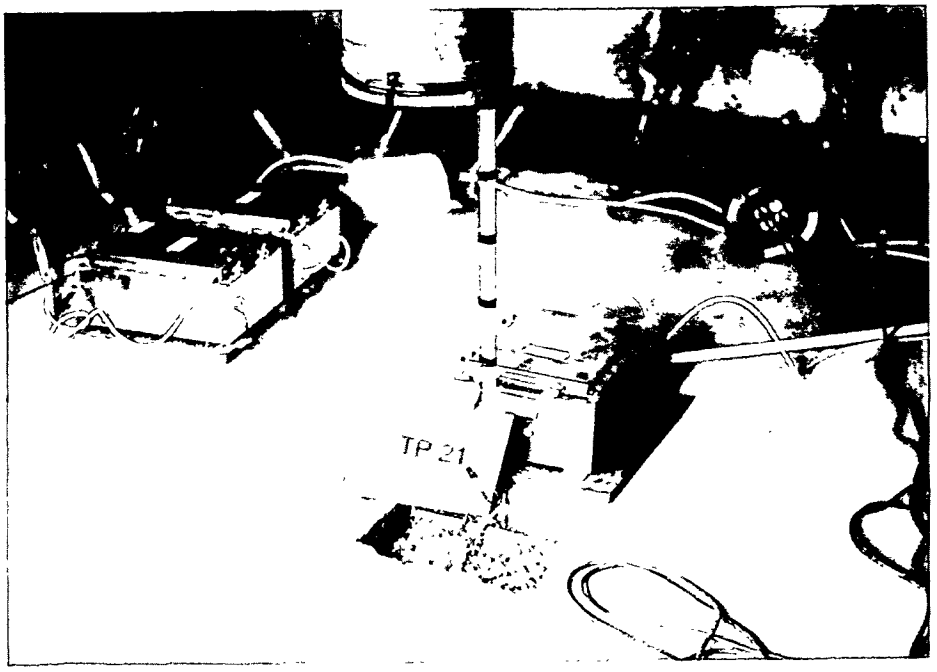

(b)

Figure 2-15. Voltage dividers used to sense transients at (a) TP18 and (b) TP21. In (a) the voltage divider consists of a single ceramic high voltage resistor in series with the 50-Ω input of the FOL transmitter. In (b) there are five resistors installed along the length of the PVC pipe.

on the building were the ones that were used in the laboratory setup. Next, the voltage transfer function of each probe was measured against frequency as indicated in Figure 2-16. From this set of measurements, an equivalent circuit model such as that shown in Figure 2-17 was derived for each test probe configuration and its individual voltage divider resistors. Three different numerical filtering compensation functions, with input parameter values as derived from the circuit model of an example probe, were then applied to sample data files from that probe, and the results were found to be essentially the same. Of the three, the step-invariant filtering function [6] was chosen for application to the remaining voltage response data files. Details of the development and application of the compensation factors are documented in Reference 7. Unless otherwise noted, all voltage measurement data presented in this report have been processed in this manner.

2.5.3 Current Measurements

Commercial current viewing transformers (CVTs) were used as the transducers for all current measurements. Pearson Model 110A CVTs were employed at the test points inside the structure, and Pearson 3025 units were used for the measurements of down conductor, ground ring electrode, and conduit currents. In each case, the sensor outputs were transmitted to their respective recording equipment over Meret FOLs. These are the same fiber optic systems that were described in Section 2.5.2, and further details are also available in Reference 1. A typical installation of these sensors at one of the wall-to-floor rebar test points is shown in Figure 2-18.

2.5.4 Magnetic Field Measurements

As was the case during previous SNL RTL tests, magnetic field measurements were obtained using commercially available EG&G MGL-4 B-dot sensors and Meret FOLs. In each channel an active integrator was inserted between the sensor and the input to the FOL transmitter so that the signal transmitted over the FOL was proportional to the incident magnetic field rather than its derivative. Additional discussion of these channels and their calibration is available in Reference 1. The installation of one of the sensors inside the test structure is shown in Figure 2-19.

2.5.5 Photography

Photographic coverage of each triggered event consisted of video records from several angles and fields of view, 16-mm framing camera movies with 3- to 5-ms time resolution, and various 35-mm still photographs. An extensive set of 35-mm photographs was obtained to document the test configurations, sensor installations, and other items of relevance to each test.

In addition to the above, a 35-mm camera was operated inside the building in the time exposure mode during the first three storms. Its purpose was to record any arcing that might occur between different parts of the interior of the structure. Such arcing was, in fact, detected and is discussed in Section 3.2.10.

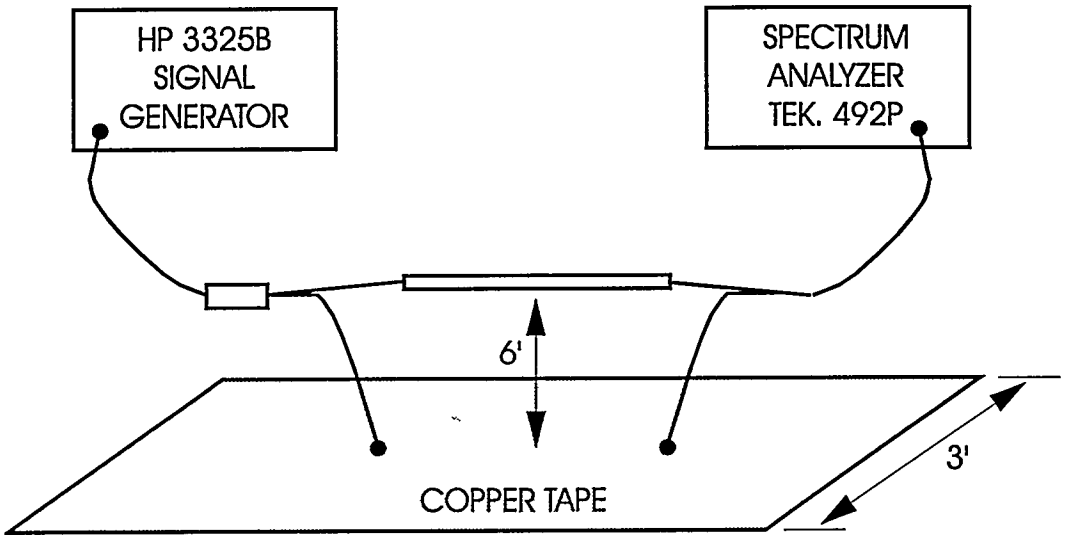

Figure 2-16. Laboratory arrangement for measuring the transfer function of the type of voltage probe shown in Figure 2-15a.

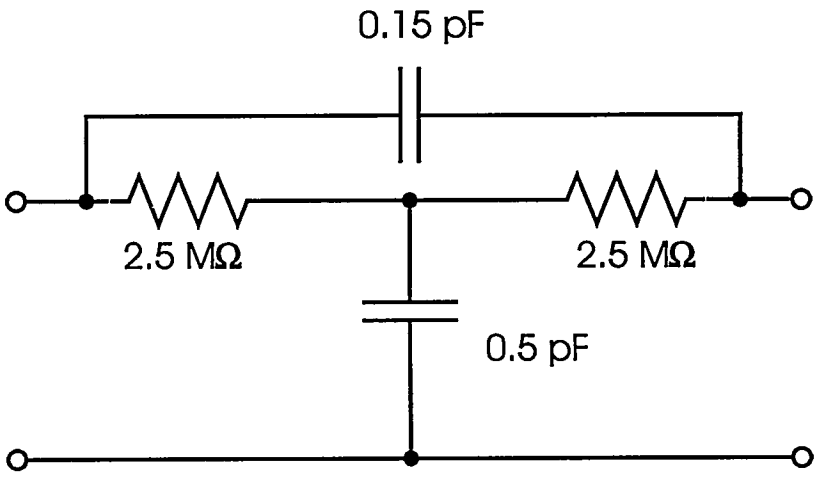

Figure 2-17. Example equivalent circuit of a voltage probe of the type shown in Figure 2-15a as derived from the transfer function measured as illustrated in Figure 2-16

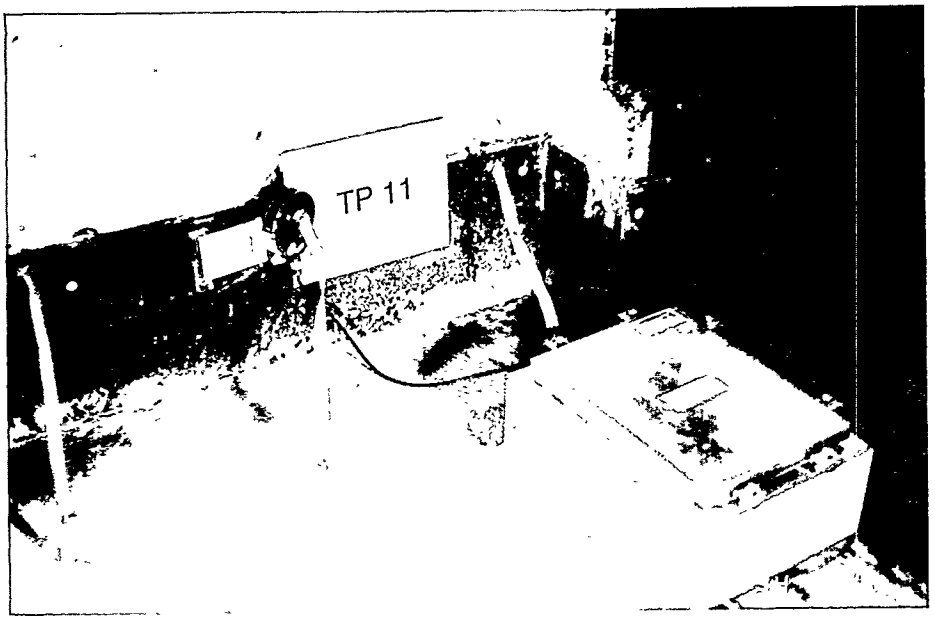

Figure 2-18. Typical installation of current sensor at one of the wall-to-floor rebar connections

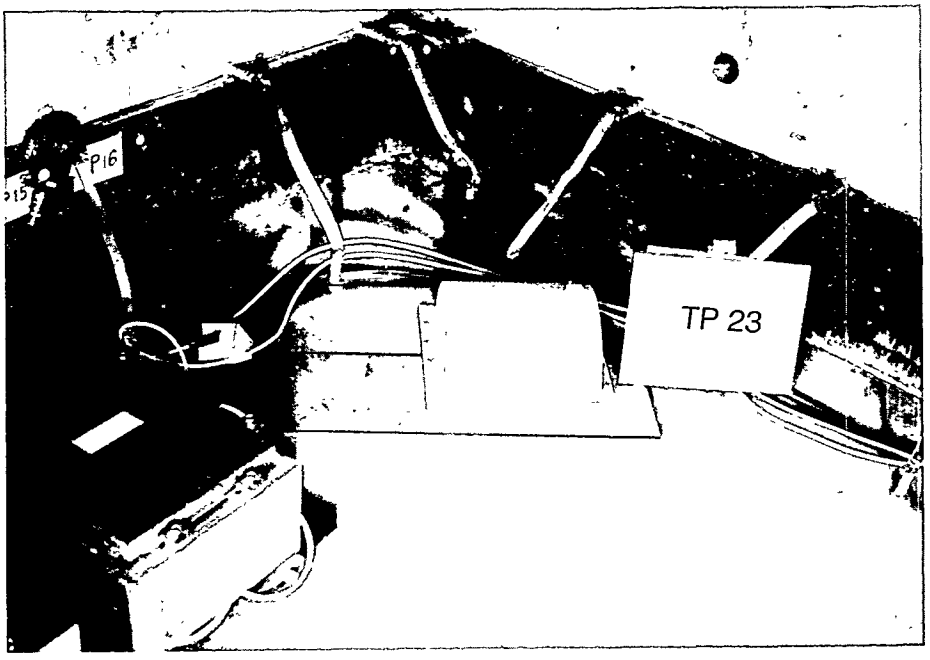

Figure 2-19. Installation of the magnetic field sensing instrumentation at TP23

2.5.6 General Instrumentation Procedures

In each test configuration of the building, up to 23 individual channels of data were acquired during each triggered lightning event. These included 10 measurements recorded on the LeCroy digitizing oscilloscopes and 13 recorded on magnetic tape. One magnetic tape channel was reserved for voice notations during each shot. Instrumentation was assigned to and installed at test points in each building configuration according to formal test [8] and instrumentation [9] plans, which took into account the nature, amplitudes, and priorities of the anticipated responses of each kind.

Each instrumentation channel employed during these tests was calibrated and operated throughout the test as an integrated unit. That is, each channel consisted of its respective sensor, signal processing assemblies, FOL (with specifically assigned cable), and recording device. Each of these system elements was uniquely identified by manufacturer's serial number or the equivalent, and the overall channel always consisted of the same physical set of components. Two aids were used to assist in maintaining this arrangement and to ensure that the installation of all sensors, external attenuators, and other components was carried out and documented properly.

The first aid was a special end-to-end "one-line" instrumentation drawing, which was developed for each test configuration. An example is shown in Figure 2-20. One such drawing was prepared for the instrumentation complement implemented during each of the four storms for which data were acquired. Included separately in each drawing is every physical component of a given channel and a simplified illustration of the test structure, in which each instrumented test point is identified. Accompanying each test point is information on the direction of each installed sensor, and the amplitudes and polarities of the predicted responses at each point. These multiple-sheet drawings, along with corresponding tabulated data sheets containing further detail on probe calibration factors and other setup information, represented the roadmaps used to guide the installation and setup of each channel.

Once the installation was completed for each test configuration, and on any occasion after that when a channel was physically adjusted for any reason, it was checked using a specially designed test pulser. The pulser could be arranged to produce an output pulse of either current or voltage of known amplitude and polarity. Pulses from this device were injected *in situ* through each installed sensor and the responses were recorded through the entire channel. In this way all cable connections were checked, and polarity factors, attenuations, and sensitivity settings were verified to have been accounted for properly.

For documentation purposes, the one-line drawing sheets for each storm configuration are included in Volume 2 of this report along with the corresponding test data.

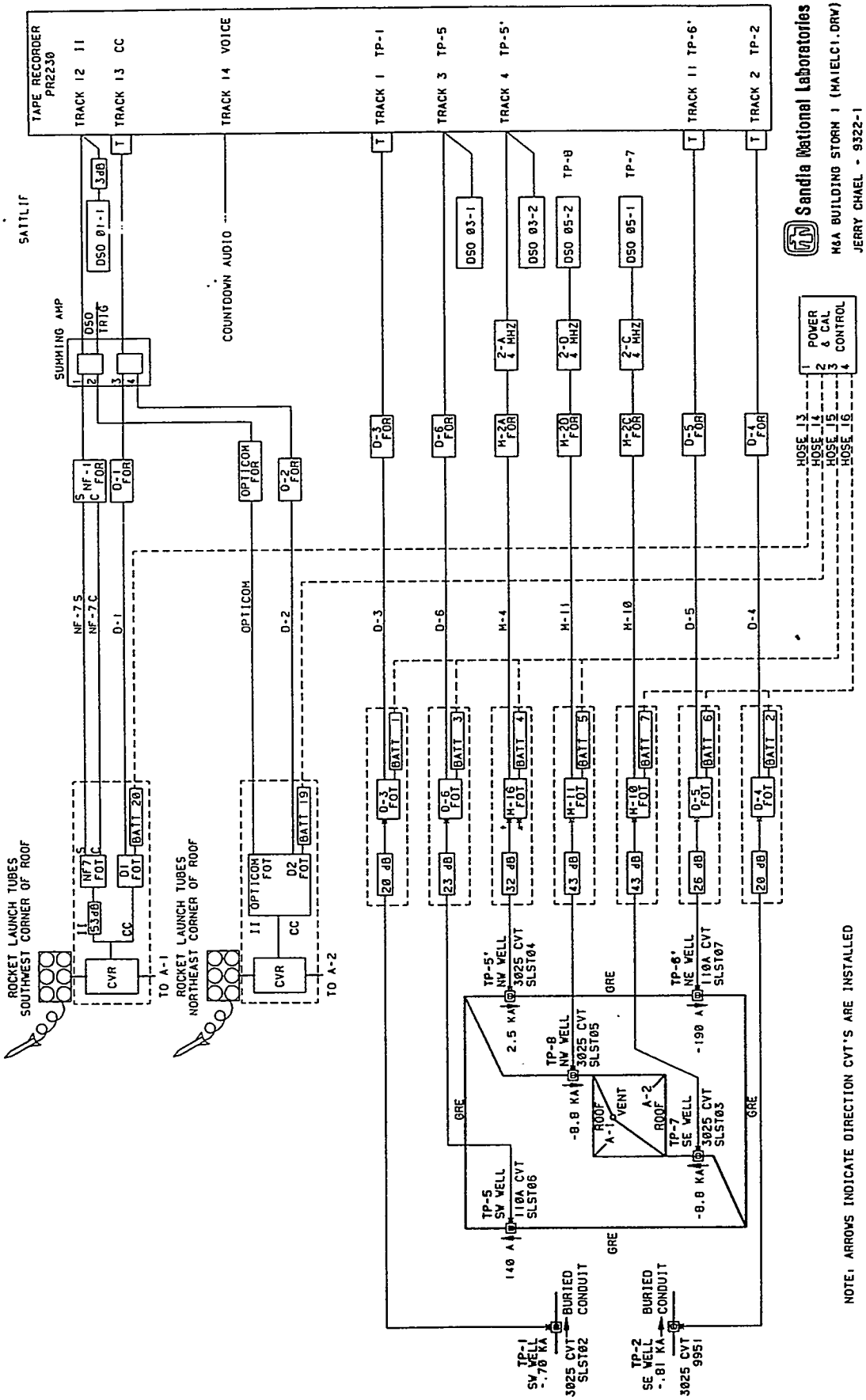

Figure 2-20. One-line drawing of the instrumentation installed during Storm 1. Similar drawings for each storm are included in Volume 2 (page 1 of 2).

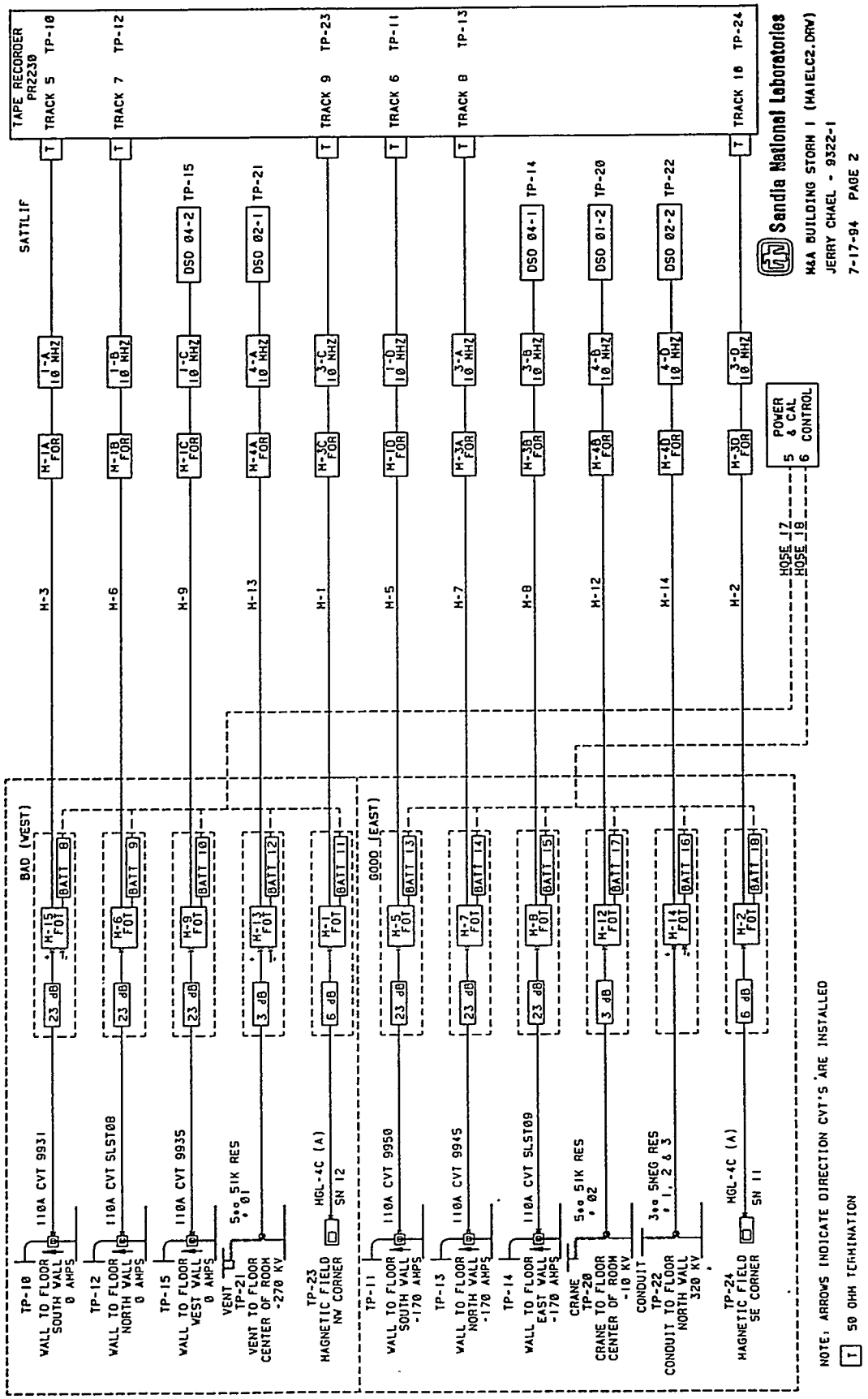

Figure 2-20. One-line drawing of the instrumentation installed during Storm 1. Similar drawings for each storm are included in Volume 2 (page 2 of 2).

3.0 Data

A total of ten fully developed lightning flashes were triggered during the course of four storms that occurred throughout the 1994 fielding period. These flashes contained 51 identifiable individual return strokes with a range of recorded peak current amplitudes of 4.2 to 29.6 kA. In this section the data acquired during the 10 flashes are summarized and discussed. Plotted waveforms of all incident return-stroke currents and the corresponding responses recorded at each of the test points being monitored during each storm are presented in Volume 2 of this report. No in-depth analyses of the data are presented; they will be addressed separately as the results become available.

3.1 Incident Flash Currents

General information related to the 10 triggered flashes is summarized in Table 3-1, and data characterizing their constituent return strokes are listed in Table 3-2. A typical return-stroke current as recorded on a LeCroy digitizing oscilloscope during the present testing is shown in Figure 3-1. The triggering threshold of the digitizing recording instrumentation was set to 4.0 kA. Therefore, any return-stroke currents occurring with peak amplitudes below that level were captured only on magnetic tape channels, the

Table 3-1. Summary of 1994 Triggered Flashes

Flash ID	Date	Time[1]	Electric Field (kV/m)[2]	No. Strokes	Attachment Point
Storm 1					
94-04	6/22	16:15:17.5	-4.7	3	NE AT
94-06	6/22	17:12:09.5	-3.6	10	SW AT
Storm 2					
94-07	6/29	16:38:17.5	-4.3	4	Vent Stack
94-09	6/29	16:59:59.6	-4.7	3	SW AT
94-10	6/29	17:25:27.1	-4.4	1	Vent Stack
Storm 3					
94-14	7/16	14:13:11.0	-5.3	4	NE AT
94-15	7/16	14:21:32.6	-3.1	3	Conduit Riser
Storm 4					
94-21	8/5	15:23:34.4	-5.8	8	LPS Mast
94-22	8/5	15:38:03.6	-4.4	3	Conduit Riser
94-24	8/5	16:07:43.3	-5.5	12	Conduit Riser

[1] Local Alabama time of wire-burn.
[2] Electric field at time launch was initiated.

Table 3-2. Incident Stroke Current Summary[1]

Flash ID	Stroke No.	Ip (kA)	τ_r[2] (μs)	di/dt[3] (10^{10} A/s)	FWHM[4]	CC[5]
94-04	1	12.7	1.2	0.72	71	N
	2	5.7	1.3	0.07	20	Y
	3	(False Trig)	—	—	—	—
	4	11.3	0.32	2.6	20	Y
94-06	1	10.9	0.50	1.6	46	N
	2	6.0	0.65	0.45	34	Y
	3	10.7	0.70	2.8	62	N
	4	4.2	0.52	0.31	23	N
	5	6.5	0.52	1.3	34	N
	6	15.7	0.28	5.0	46	N
	7	12.1	0.16	5.7	26	N
	8	7.4	0.24	2.5	34	Y
94-07	1	19.5	0.24	6.8	40	N
	2	8.8	0.12	5.0	5.7	N
	3	16.5	0.24	5.5	21	N
	4	14.6	0.26	4.2	5.9	Y
94-09	1	9.5	0.59	1.6	43	N
	2	10.9	0.16	5.1	31	N
	3	(<4)[6]	—	—	—	—
94-10	1	12.9	0.44	4.6	7.9	Y
94-14	1	24.9	0.16	14.2	35	N
	2	11.9	0.20	4.0	2.1	Y
	3	20.2	0.21	7.3	20	N
	4	10.3	0.15	5.9	1.9	Y
94-15	1	17.4	0.22	6.1	48	Y
	2	10.9	0.12	4.4	6	Y
	3	8.4	0.48	1.7	34	N
94-21	1	7.5	0.62	0.73	30	N
	2	7.2	0.76	1.2	36	N
	3	5.2	1.76	0.73	34	N
	4	16.3	0.28	4.7	29	N
	5	12.3	0.33	2.3	38	Y
	6	18.5	0.32	4.9	7.3	Y
	7	8.0	0.06	8.0	3.8	N
94-22	1	9.9	0.37	2.0	32	Y
	2	20.1	0.21	6.6	33	Y
	3	10.9	0.24	3.8	7.3	Y
94-24	1	7.8	7.0	0.02	47	Y
	2	8.1	6.0	0.04	45	Y
	3	5.7	4.0	0.03	50	Y
	4	29.6	0.18	10.8	57	Y
	5	(False Trig)	—	—	—	—
	6	9.1	5.5	0.20	39	Y
	7	11.9	0.86	0.52	40	Y
	8	19.0	0.24	5.8	5.8	Y

1 Table includes only strokes for which high resolution digital data are available.
2 Rise time between 10 and 90 percent points.
3 Average slope between 10 and 90 percent points.
4 Full Width to Half Maximum is the width of return stroke current between the 50-percent amplitude points.
5 Return stroke followed by continuing current of duration greater than 10 ms.
6 No digital data.

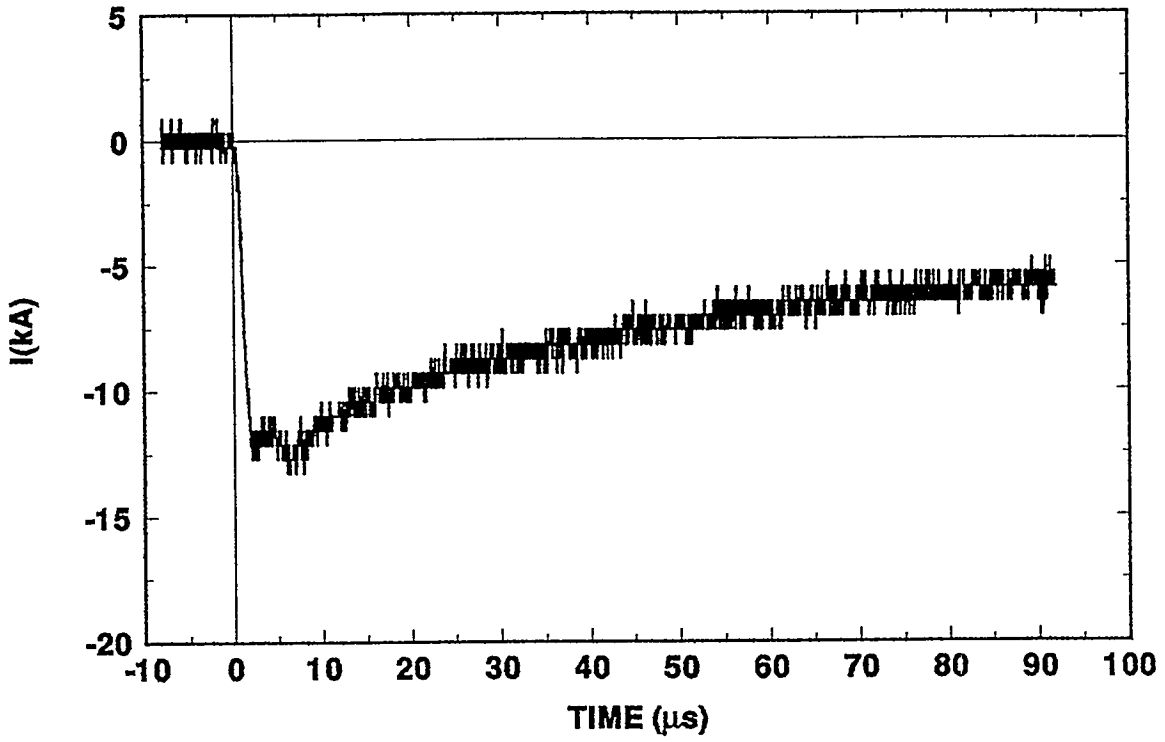

Figure 3-1. Typical return-stroke current as recorded during the present tests (Flash 94-04, Stroke 1)

primary purpose of which was to provide low amplitude continuing current data records and overall time histories of each incident flash current. An example of one of the full-flash current records obtained in this way is given in Figure 3-2. Because of the limited bandwidth of the tape channels and the sensitivity at which they were operated to obtain good resolution of the low amplitude continuing currents, these records are unsuitable for use in analyzing return-stroke current characteristics. Furthermore, since the LeCroy digitizing oscilloscopes were run in a mode that limited their recording capacity to a maximum of 8 individual events in a given sequence, digitized data from the last one or more return strokes in some flashes were not obtained. The detailed data listed in Tables 3-2 and 3-3 include only those pertaining to return strokes for which high resolution digital records are available.

Stroke statistics of particular interest are summarized in Table 3-3. These statistics are based on the generally accepted assumption that the lightning parameters listed, with the exception of strokes per flash, are log-normally distributed [10]. The results in Table 3-3 can be compared directly with those obtained during the testing of the munitions bunker in 1991 (Table 4, Reference 1) and with the more general triggered lightning data base presented in Reference 11. As indicated in Reference 11, the key characteristics of

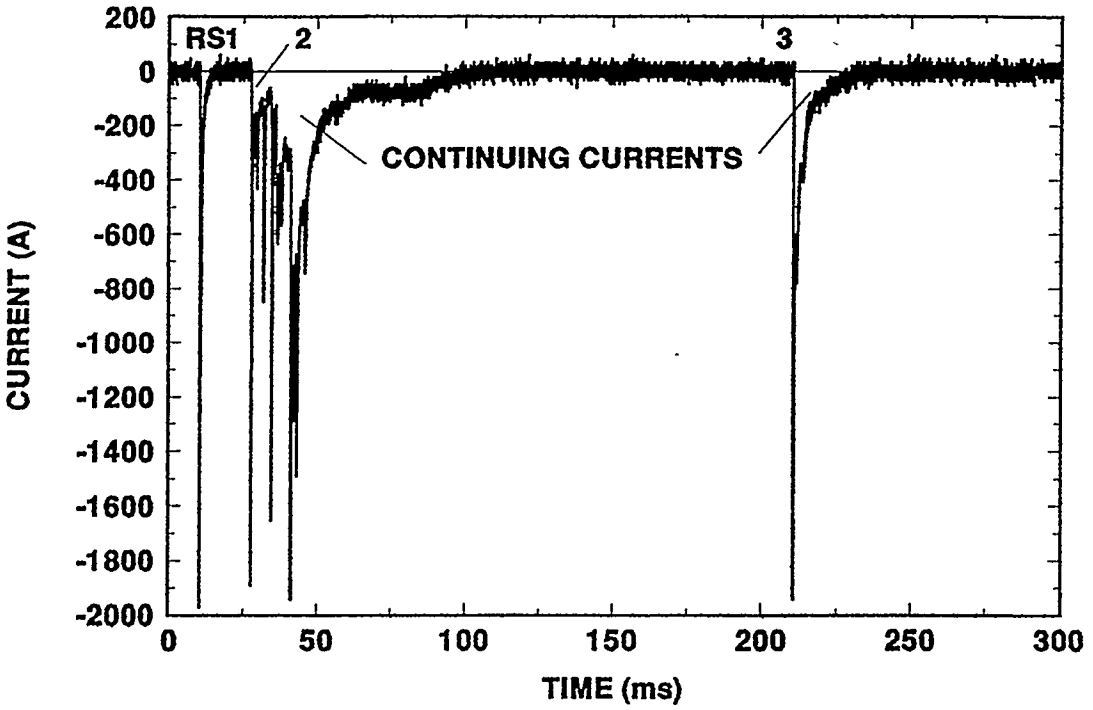

Figure 3-2. The return-stroke and continuing current portion of triggered flash 94-04 as recorded on the FM magnetic tape channel. The instrumentation sensitivity was chosen to provide resolution of the low-amplitude continuing current components of the current and therefore resulted in a saturation level of approximately 2 kA.

Table 3-3. Summary of Triggered Flash Current Statistics[1]

Parameter	n	Median (Mean)	Max	Min	Standard Deviation
Strokes per Flash	10	(5.2)	12	1	3.5
I_p (kA)	42	11.0	29.6	4.2[2]	0.19
τ_r (μs)	42	0.43	7.0	0.06[3]	-0.47
10-90 percent di/dt (kA/μs)	42	20.0	142	0.2	0.64
FWHM (μs)	42	22.1	71	1.9	0.41
Strokes followed by continuing currents: 52%					

[1] Log-normal distribution assumed for all but strokes per flash. Standard deviations for log-normally distributed quantities are the standard deviations of the logarithms (base 10) of the quantities.

[2] Triggering threshold was ~4 kA.

[3] 10 to 90 percent rise time capability of the incident current sensor was 0.06 μs.

triggered lightning return stroke currents are quite comparable to those of subsequent return strokes in naturally initiated flashes. The latter are thought to be initiated by the same processes that are responsible for producing triggered return strokes of the type occurring in the present tests.[5] As a test source for engineering purposes, triggered lightning therefore provides the highest possible degree of simulation fidelity with respect to naturally initiated lightning.

3.2 Test Structure Responses

The sheer quantity of data and number of variations in test configuration and attachment point combine to make the presentation of a concise summary of the results somewhat difficult. However, in the following sections, the data will be examined from various viewpoints, and their major implications will be discussed. Detailed analysis will require extensive future modeling activity, and the availability of more refined conclusions will have to await those efforts.

A complete set of plotted data, including both incident stroke currents and the corresponding responses measured at each of the applicable test points, is given in Volume 2 of this report. In Volume 1 the data are summarized and discussed, with examples being presented as appropriate in support of their discussion. As a beginning point, the peak values of the responses are tabulated on a storm/flash basis and are presented below in Tables 3-4 through 3-13. (The corresponding configuration of the structure tested during each storm is listed in Table 2.3.) In the following sections, patterns of behavior of the various measured currents, voltages, and magnetic fields are examined, with emphasis being given to the isolation of any discernible effects related to the LPS variations implemented during the course of the testing.

[5] Refer to Section 3 of Reference 3 for additional discussion of this point.

Table 3-4. Storm 1, Flash 94-04 Test Structure Responses, NE Air Terminal Attachment

	Stroke			
I_{inc}	12.7	5.7	11.3	kA
TP	1	2[1]	4	Units
1	>-2[2]	>-2	>-2	kA
2	-1.95	-0.5	-1.9	kA
5	-90/+225	-60/+110	-75/+160	A
5'	+800	>+300	+850	A
6'	-70/+80	-20/+40	-80/+50	A
7	-2.6	>-1	-2.5	kA
8	-2.4	>-1	-2.4	kA
10	-25	<-10[3]	-20	A
11	-45/+120	-20/+75	-30/+80	A
12	-15	<-10	-20	A
13	-60/+30	-10/+20	-30/+20	A
14	-30	-20	-40	A
15	-15/+20	<±5	-30/+20	A
20	0.64/-1.4	~0	4.7/-1.6	kV
21	-6.0	<±1	-11.2/+8.3	kV
22[4]	--	--	--	kV
23	+230/-100	+100/-40	+130/-75	A/m

1 Event 3 was a false trigger, not a stroke.
2 > sign implies saturated signal of absolute magnitude beyond indicated value.
3 < sign indicates unreadable signal of absolute magnitude below the indicated level.
4 No reliable data from TP22 during Storm 1.

Table 3-5. Storm 1, Flash 94-06 Test Structure Responses, SW Air Terminal Attachment

	Stroke								
I_{inc}	10.9	6.0	10.7	4.2	6.5	15.7	12.1	7.4	kA
TP	1	2	3	4	5	6	7	8	Units
1	>-2	>-2	>-2	>-2	>-2	>-2	>-2	>-2	kA
2	-2.0	-1.0	-2.0	-0.6	-1.3	-2.0	-2.0	-1.6	kA
5	-140/+160	-75/+80	-140/+150	-70/+50	-80/+100	-190/+260	-150/+160	-100/+110	A
5'	+1080	+530	+950	+450	+700	+1500	+1200	+800	A
6'	+160	+50	+125	+40	+75	+190	+105	+75	A
7	-2.6	-1.7	-2.4	-1.4	-1.8	-3.5	-2.8	-1.9	kA
8	-2.8	-1.6	-2.5	-1.3	-1.8	-3.7	-3.0	-2.0	kA
10	-25/+10	-20/+5	-24	-16	-20	-30	-20	-20	A
11	-110/+40	-40/+25	-105/+40	-30/+25	-60/+25	-125/+60	-105/+30	-70/+25	A
12	<-20	<-10	<-20	<-10	<-10	<-10	<-10	<-10	A
13	-70/+15	-25/+10	-60/+20	<±10	-30/+10	-90/+25	-75/+20	-40/+10	A
14	-20	-10	-20	-10	-15	-34	-20	-20	A
15	-55/+25	-30/+10	-60/+25	-20/+10	-30/+15	-75/+30	-60/+30	-35/+15	A
20	+4.6/-2.5	+1.3/-0.6	+5.2/-1.2	+0.8/-0.41	+1.2/-1.4	+8.3/-2.3	+8.6/-2.4	+5.0/-2.0	kV
21	-19.6/+4.8	-8.9/+3.3	-30.9/25.3	-3.8/+1.6	-9.1/+2.5	-27.6/28.2	-29.0/34.7	-16.4/16.5	kV
22	--	--	--	--	--	--	--	--	kV
23	+160/-90	+110/-50	+130/-90	+90/-40	+110/-60	+135/-125	+125/-80	+100/-60	A/m

Table 3-6. Storm 2, Flash 94-07 Test Structure Responses, Vent Stack Attachment

	Stroke				
I_{inc}	19.5	8.8	16.5	14.6	kA
TP	1	2	3	4	Units
1	>-7.5	-4.0	>-7.5	~-7	kA
2	-3.5	-1.3	-2.5	-1.8	kA
5	-325	-95	-160	-115	A
5'	+1250	+400	+900	+600	A
6	+1200	+350	+750	+700	A
6'	+210	+55	+160	+105	A
7	-4.3	-2.0	-3.0	-2.7	kA
8	-4.8	-2.1	-3.5	-3.0	kA
16	-160	-100	-145	-140	kV
17	-140	-60	-120	-105	kV
18	-180	-85	-145	-120	kV
19	-105	-60	-80	-70	kV
20	-205	-145	-180	-165	kV
21	--	--	--	--	kV
22	-105/95	-72/76	-90/80	-95/80	kV
23	+280/-90	+105/-20	+159/-95	+100/-80	A/m
24	+1430	+600	+1050	+870	A/m

Table 3-7. Storm 2, Flash 94-09 Test Structure Responses, NE Air Terminal Attachment

	Stroke		
I_{inc}	9.5	10.9	kA
TP	1	2	Units
1	>-7.5	>-7.5	kA
2	-1.8	-2.2	kA
5	-105	-130	A
5'	+750	+750	A
6	+600	+550	A
6'	+130	+145	A
7	-2.5	-2.5	kA
8	-2.4	-2.5	kA
16	-100	-130	kV
17	-85	-110	kV
18	-80	-75	kV
19	-60	-75	kV
20	-150	-170	kV
21	--	--	kV
22	-80/+80	-90/ 80	kV
23	+140/-80	+150/-80	A/m
24	+760	+900	A/m

Table 3-8. Storm 2, Flash 94-10 Test Structure Responses, Vent Stack Attachment

	Stroke	
I_{inc}	12.9	kA
TP	1	Units
1	>-7.5	kA
2	-2.3	kA
5	-150	A
5'	+900	A
6	+750	A
6'	+110	A
7	-3.0	kA
8	-3.2	kA
16	-151	kV
17	-110	kV
18	-117	kV
19	-74	kV
20	-180	kV
21	--	kV
22	-95/+80	kV
23	+140/-100	A/m
24	+980	A/m

Table 3-9. Storm 3, Flash 94-14 Test Structure Responses, NE Air Terminal Attachment

	Stroke				
I_{inc}	24.9	11.9	20.2	10.3	kA
TP	1	2	3	4	Units
1	>-7	-3.0	>-7	-2.0	kA
2	-4.7	-1.2	-3.1	-1.0	kA
3	-5.8	-1.8	-4.0	-1.3	kA
4	+1.1/-2.8	+0.25/-1.3	+0.9/-2.0	+0.1/-0.9	kA
5	-1.6	-0.5	-0.6	<-0.1	kA
6	+2.5	+1.7	+2.0	+1.2	kA
7	-3.8	-2.3	-3.1	-1.7	kA
8	-3.3	-1.5	-2.7	-1.0	kA
9	-1.75	-1.75	-1.75	-1.25	kA
9'	-3.0	-1.3	-2.0	-1.0	kA
16	-160	-85	-140	-80	kV
17	-170	-75	-140	-75	kV
18	-175	-95	-135	-80	kV
19	-135	-70	-115	-65	kV
20	-190	-140	-170	-120	kV
21	--	--	--	--	kV
22	-120/+120	-90/+100	-110/+100	-90/+80	kV
23	+205	+105	+180	+100	A/m
24	+1420	+800	+1320	+600	A/m

Table 3-10. Storm 3, Flash 94-15 Test Structure Responses, Conduit Riser Stub

	Stroke			
I_{inc}	17.4	10.9	8.4	kA
TP	1	2	3	Units
1	>-7	-4.25	-5.5	kA
2	+12.5	+5.2	+6.0	kA
3	+13.0	+5.0	+6.2	kA
4	-5.2	-4.0	+5.0	kA
5	0.9	-0.5	-1.3	kA
6	-7.2	-3.0	-2.7	kA
7	+6.0	+1.6	+1.4	kA
8	-1.0/+0.8	-0.8	-1.0	kA
9	+13.2	+5	+6.0	kA
9'	-5.4	-3.8	-5.2	kA
16	21/-9	-20	-20	kV
17	+61/-17	+12/-34	-24	kV
18	+12/-10	+15/-18	+10/-13	kV
19	+51/-10	+10/-33	+5/-20	kV
20	+120/-30	+20/-60	-45	kV
21	--	--	--	kV
22	+110/-150	+75/-140	+20/-145	kV
23	-190	+130	+190	A/m
24	>-2250	-2000	>-2250	A/m

Table 3-11. Storm 4, Flash 94-21 Test Structure Responses, Attachment to LPS Mast

	Stroke							
I_{inc}	7.5	7.2	5.2	16.3	12.3	18.5	8.0	kA
TP	1	2	3	4	5	6	7	Units
1	-5.0	-4.7	-2.5	-8.5	-8.0	-8.0	-1.5	kA
2	-1.0	-1.0	-0.6	-2.1	-1.5	-2.4	-1.0	kA
5	-3.0	-2.8	-2.0	-4.8	-4.4	-5.8	-2.7	kA
5'	+0.4/-0.55	+0.4/-0.49	+0.25	+0.3/-1.1	+0.3/-0.8	+0.3/-1.0	+0.3	kA
6	-3.5	-3.2	-2.6	-6.9	-5.5	-8.0	-3.7	kA
6'	-0.75	-0.70	-0.6	-1.48	-1.2	-1.6	-0.7	kA
10	<±10	<±10	~0	+25/-10	<±20	+30/-10	<±10	A
11	+240	+230	+200	+350	+340	+365	+160	A
12	~0	~0	~0	~0	~0	~0	~0	A
13	-100	-110	-60	-200	-150	-190	-50	A
14	-25	-20	-20	-40	-30	-45	-20	A
15	-5/+20	-10/+10	~0	-35/+25	-25/+20	-40/+25	-25/+15	A
20	-4/+4	-6/+4	-3/~0	-17/+3	-11/+2	-16/+3	-10/~0	kV
21	+7.5/-20	+10/-13	+6/-10	+9/-26	-21/+15	+22/-18	+9/-13	kV
22	+40	+45/-15	+35/-15	-30/+90	-25/+70	+110/-20	-25/+45	kV
23	-140/+105	-180/+20	-100	-120/+250	-130/+190	-175/+250	-130	A/m
24	~0	~0	~0	+600	~0	+685	~0	A/m

Table 3-12. Storm 4, Flash 94-22 Test Structure Responses, Attachment to Conduit Riser Stub

	Stroke			
I_{inc}	9.9	20.1	10.9	kA
TP	1	2	3	Units
1	-6.0	-11.5	-5.0	kA
2	+7.0	+14.5	+6.1	kA
5	~0	-0.3	-0.2	kA
5'	+0.2	+0.5	~0	kA
6	~0	+0.3	+0.5	kA
6'	~0	+0.3	~0	kA
10	~0	~0	~0	A
11	+375	>+500	+350	A
12	~0	~0	~0	A
13	+60	+125	+40	A
14	-70	-120	-50	A
15	~0	<±10	~0	A
20	-3/+9	-4/+13	-4/+8	kV
21	+9/-5	+6/-8	+6/-10	kV
22	-100/+20	-80/+10	-85/+15	kV
23	-90	-175	-80	A/m
24	-2100	<-2000	-1750	A/m

Table 3-13. Storm 4, Flash 94-24 Test Structure Responses, Attachment to Conduit Riser Stub

	Stroke							
I_{inc}	7.8	8.1	5.7	29.6	9.1	11.9	19.0	kA
TP	1	2	3	4	6[1]	7	8	Units
1	-6.0	-6.0	-4.8	-15.5	-6.8	-8.8	-8	kA
2	+7.5	+7.0	+5.3	>+18	+8	+11	+10.5	kA
5	-0.3	-0.3	~0	-0.5	~0	-0.3	-0.3	kA
5'	~0	~0	~0	+1.25	~0	+0.5	+0.4	kA
6	+0.3	+0.3	~0	+0.5	~0	~0	+0.1	kA
6'	+0.2	+0.2	~0	+0.5	~0	+0.2	+0.2	kA
10	~0	~0	~0	~0	~0	~0	~0	kA
11	+450	+450	+375	>+500	+460	>+500	+470	A
12	~0	~0	~0	~0	~0	~0	~0	A
13	+50	+60	+40	+200	+60	+90	+90	A
14	<-5/+50	-50/+?	-10/+80	-150/+?	-60/+?	-90/+?	-80/+?	A
15	~0	~0	~0	-10	~0	<±10	<±10	A
20	+3.5	+3.5/-1.5	~0	-7/+15	-1.5/+6	-3.5/+8	-5/+11	kV
21	-9/+2	-7/+4	~0	+17/-18	-5	+4/-10	+10/-15	kV
22	-25/+15	-30/+15	~0	-100/+20	-50/+25	-90/+20	-120/+15	kV
23	~0	-50	~0	-180	~0	-70	-110	A/m
24	-2000	-2010	-1505	>-2000	>-2000	>-2000	>-2000	A/m

[1]Event 5 was a false trigger, not a stroke.

3.2.1 LPS Down Conductor Currents

One question of particular interest is whether or not in a building in which the steel wall rebar and other steel structural members are well bonded to the metal roof the use of separate external lightning down conductors is necessary or cost effective. In the present experiments, the building was constructed to assure that there was extensive intentional electrical bonding between the metal roof structure and the rebar within the walls. At the base of the walls, special provisions were made to allow the intentional isolation of the wall and floor/footer rebar during part of the testing. During other portions of the tests, the wall and floor rebar were intentionally well bonded together at 28 points around the interior perimeter of the building. A comparison of the distribution of currents throughout the structure, including those flowing within the external down conductors themselves, should therefore offer insight into the effectiveness of the dedicated down conductors as part of the overall protection system. Furthermore, from such an assessment would follow important guidance on the criticality of the inclusion and diligent maintenance of floor-to-wall rebar bonding throughout the lifetime of the facility.

In this section the down conductor currents are examined under the different variations of wall/floor bonding and lightning attachment locations that were tested. Reference to the details given in Section 2.2 on the construction and configurational details corresponding to each storm may be helpful.

As illustrated in Figure 2.4, the LPS system included five standard air terminals (lightning rods) mounted one at each corner of the roof and one atop the vent stack. All

five terminals were interconnected by standard #1/0 gauge copper lightning protection system cable, with the down conductors themselves being located at the NW and SE corners of the building. The bases of the roof-mounted terminals were bonded to the corrugated metal roof itself. The currents flowing on down conductors were measured during each triggered flash at the base of the building above their junctions with the GRE (test points 7 and 8 in Figure 2-8.)

Let us first examine the relative amplitudes of the currents flowing on the two down conductors under varying conditions. To do so, refer initially to Tables 3-4 and 3-5. These relate to the first storm, during which the wall and floor rebar were connected together, and the incident flash currents were attached to the NE and SW roof terminals during flashes 94-04 and 94-06, respectively. Since Stroke 4 of 94-04 and Stroke 1 of 94-06 were each of similar amplitude (~11 kA), they present the opportunity for a direct comparison of down conductor currents under attachments to two different locations, all other factors being held approximately the same. The peak currents listed in the entries of interest all have values within the range of -2.4 to -2.8 kA. The data confirm that electron current flow was in the direction of cloud to ground, and that apparently both down conductors carry approximately equal shares of the current. For comparison, the corresponding response waveforms are overlaid in a single plot in Figure 3-3. In Figure 3-4, the peak amplitudes of the down conductor currents measured during the eight strokes of flash 94-06 are plotted against return-stroke current amplitude, and the results are seen to be linear.

Next, consider the effect of disconnecting the intentional bonding between the floor and wall rebar, with all other factors remaining constant. By comparing the TP 7 and 8 entries in Tables 3-4 and 3-7 under Strokes 1 and 2, respectively (both strokes of ~11-kA amplitude), we again observe that the current is approximately equal in both down conductors. Furthermore, and rather surprisingly, the removal of the intentional connection between wall and floor rebar evidently exerted no significant influence on the fraction of the incident current carried by the down conductors. As is discussed in detail in Section 3.2.2, however, unanticipated breakdown and arcing occurred in such a way as to provide a low impedance path to earth via the west buried power service conduit. The consequences of this arcing are addressed again throughout the discussions of various structure responses that follow. Furthermore, the concrete of the floor was poured over a base of crushed limestone, which prevented intimate contact between the concrete and the underlying soil. The combination of this effect and the artificial funneling of current to the conduit through the arc path may have obscured the effect of the bonding of wall and floor rebar. A further incidental observation from the results in Tables 3-6 and 3-8 is that the approximately equal distribution of currents to the two down conductors also holds for attachment to the vent stack on the roof.

In each of the above examples, it is noted that the total peak current carried by the down conductors represented something less than half that of the incident return-stroke

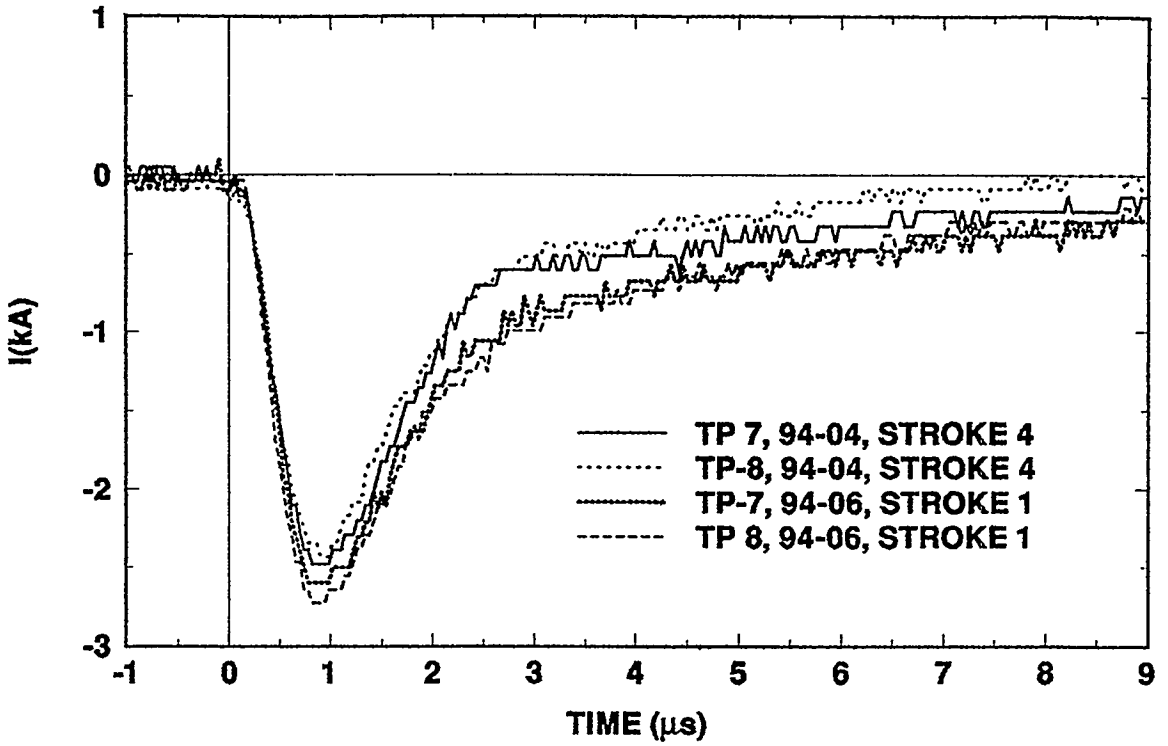

Figure 3-3. Overlay of down conductor currents measured during Flashes 94-04 (attachment to A-2) and 94-06 (A-1). The incident return-stroke currents both had peak values of about 11 kA.

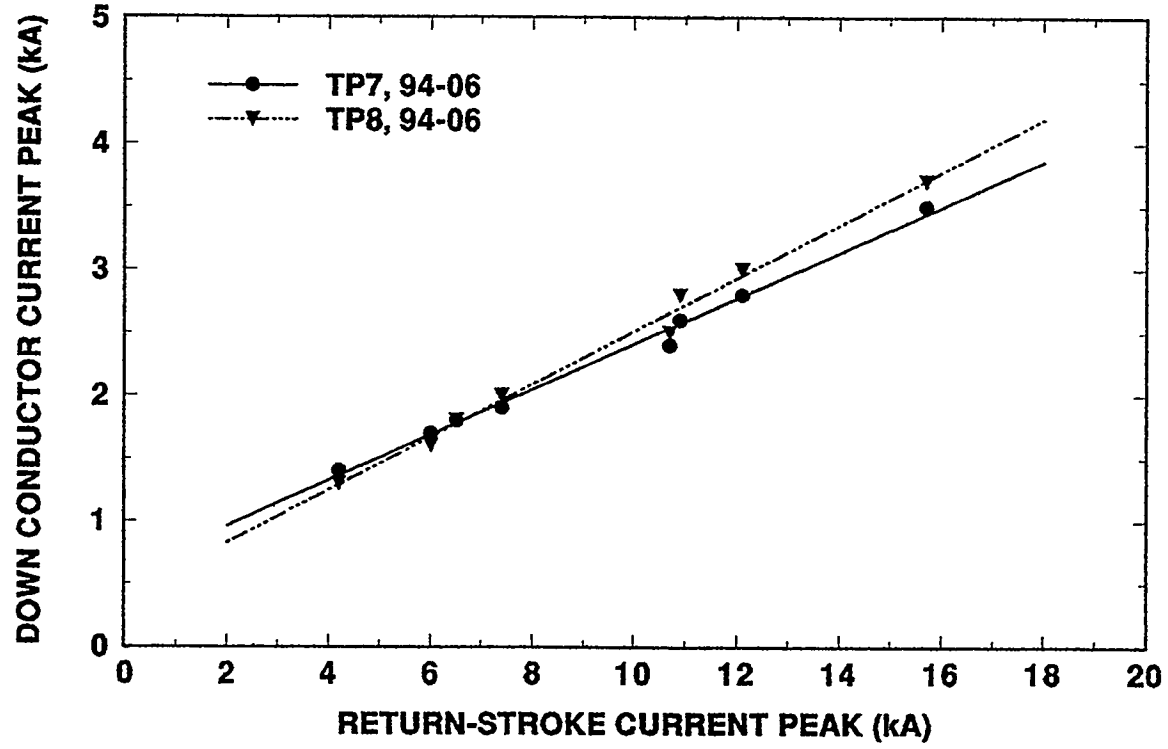

Figure 3-4. Peak amplitudes of down conductor currents plotted against the peak magnitudes of their corresponding return strokes during Flash 94-06 (A-1), which yielded 8 return strokes

current, with the implication that the remainder found its way to earth via the walls. In Figure 3-5 the differences between the stroke currents and the sums of the currents in both down conductors for Stroke 4 of 94-04 (floor/wall rebar connected) and Stroke 2 of 94-09 (rebar disconnected) are plotted together for comparison along with their respective incident stroke currents. These difference currents represent the total currents flowing to earth down through the walls for stroke currents of approximately the same magnitude and roughly the same waveshapes.

In Figure 3-6 the waveforms of the incident current and the response of one of the down conductors (TP7) during Stroke 1 of Flash 94-04 are over laid. Both have been normalized to unit amplitude for purposes of comparison. From the figure, it is apparent that the peak of the down conductor current occurs at the same time as that of the incident current. The rather distinctive waveshape of the down conductor currents results from the combination of values of the inductances and resistances to earth in the down conductor paths versus those of the path down through the walls, footers, and out the conduit to earth ground. This relationship is examined in some detail in the next section.

3.2.2 Buried Conduit Currents

Experience during the earlier RTL test of a munitions bunker showed that the buried 4-in electrical service conduit to that facility carried a substantial fraction of the incident stroke current away from the structure—a much larger fraction, for example, than did the intentional LPS grounding system [12]. It is therefore of considerable interest to examine the behavior of the currents carried by the two 100-ft-long buried conduits present in the test of the building and to compare them with their counterpart currents on the two LPS down conductors and GRE. Other aspects of interest include the effects on conduit current associated with the bonding of the wall and floor rebar and the connection of the conduits directly to the GRE.

Plotted in Figure 3-7 are the responses recorded at TP1 (west conduit) and TP2 (east conduit) during the same two strokes for which the down conductor currents were compared in Section 3.2.1. As is evident from the figure, the TP1 currents during both strokes drove the fiber optic instrumentation deep into saturation, the threshold for which was about 2 kA. The peaks of the TP2 currents just reached that saturation point.

The instrumentation settings for Storm 1 had been chosen based on predictions that assumed electrical isolation between the buried conduit and the rest of the test structure. These predictions indicated an anticipated current of less that 1 kA at both test points. However, the data in Figure 3-7, and those corresponding to all similar return strokes occurring throughout the testing, suggest that electrical breakdown and arcing took place between some portion of the structure and the west buried conduit, thereby encouraging the bulk of the stroke current to flow to earth via that conduit and driving the TP1 measurement into saturation.

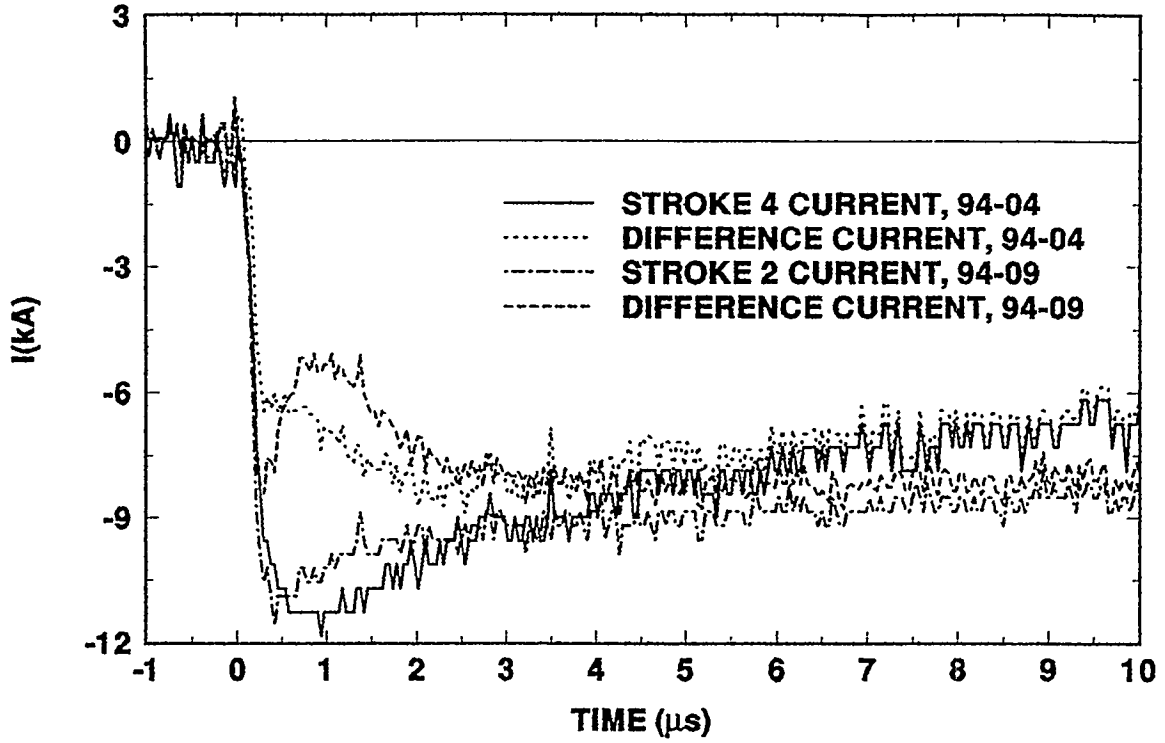

Figure 3-5. Overlays of stroke and wall currents for two flashes during which conditions were the same except for the attachment points; (Flash 94-04, A-2; Flash 94-06, A-1). Wall currents are deduced as the total stroke current minus the sum of the two down conductor currents.

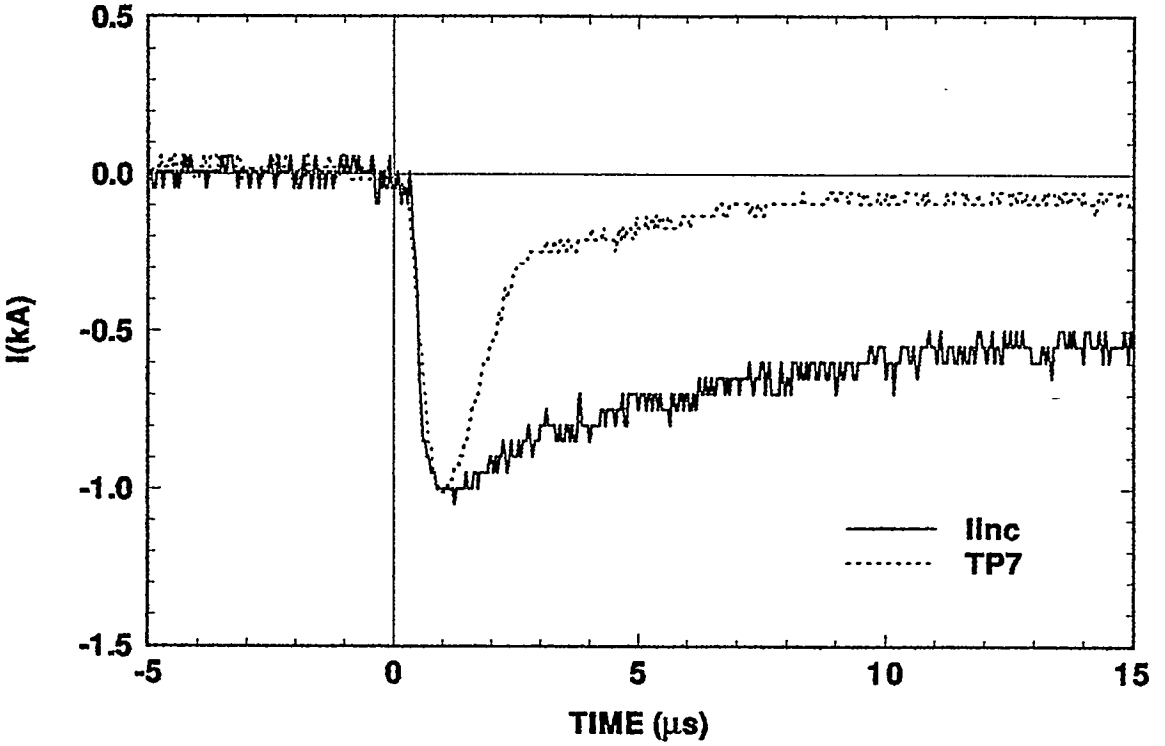

Figure 3-6. Normalized waveshapes of the incident stroke and down conductor currents measured at TP7 during Flash 94-04, Stroke 4

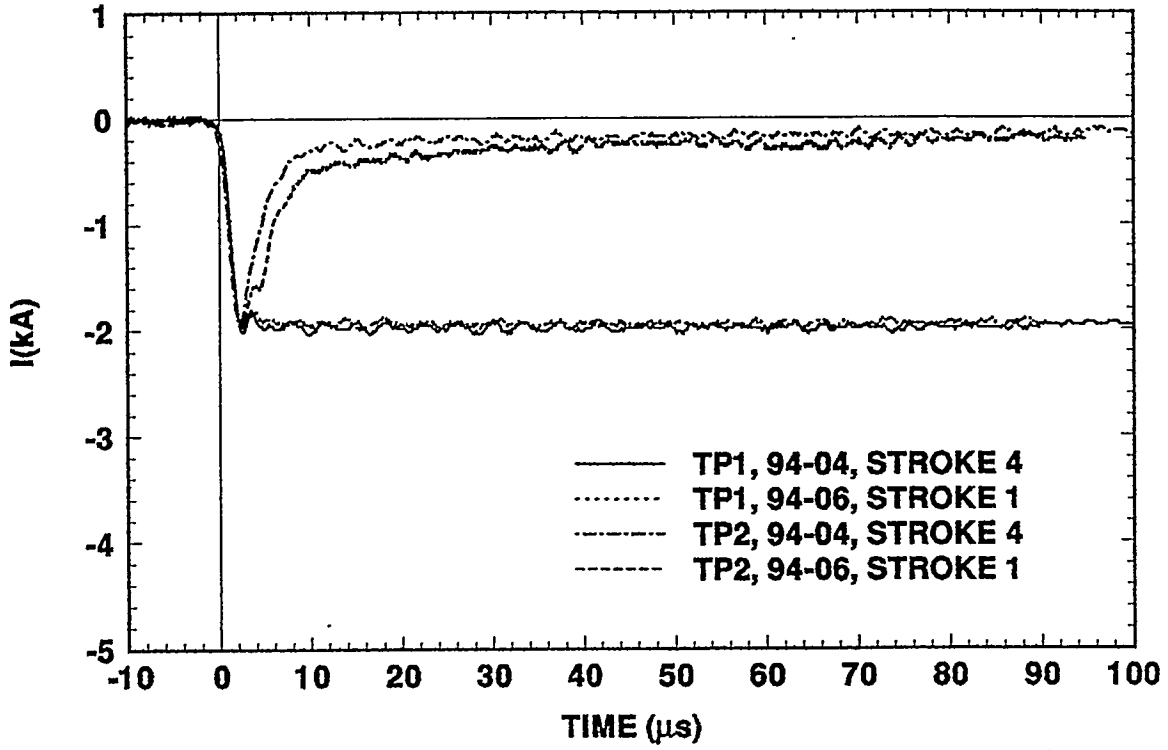

Figure 3-7. Conduit currents recorded at TP1 and TP2 during Stroke 4 of Flash 94-04 and Stroke 1 of 94-06. Both strokes were of approximately 11-kA peak amplitude

The responses shown in Figure 3-7 raise some question as to whether the TP2 data might have been affected as they approached the instrumentation saturation threshold. Based on an examination of the shapes of TP2 responses to small strokes that did not drive the TP2 currents near to the saturation level, this does not seem to be the case. This situation is shown in Figure 3-8, in which the incident stroke current and the corresponding responses at TP1 and TP2 are given for Stroke 4 in flash 94-06. The peak amplitude of this particular stroke is small, only about 4.2 kA, and the current at TP2 did not approach the 2-kA instrumentation saturation level and can therefore be considered reliable. Although the TP1 current again exceeded the saturation threshold, it did not drive the instrumentation as deeply into saturation as in the case shown in Figure 3-7. In this instance recovery took place by about 25 μs. From that point on, the TP1 current matched the stroke current (to within resolution of the plotted data) for the duration of the data records. This same situation also occurred during the second strokes of both 94-04 and 94-06, the data for which are shown in Figure 3-9.

Finally, in Figure 3-10 both conduit currents from Stroke 2 (5.7 kA) of 94-04 are shown. In that figure an "eyeball" extrapolation of the TP1 current yields a peak value that is consistent with the conclusion that the west conduit carried the bulk of the current away from the structure.

That breakdown and arcing to the west conduit occurred is unfortunate in that it tends to cloud the results of some of the comparisons that were the objectives of this particular test. To maintain electrical isolation unless otherwise intended, the conduit penetrations

into the building were specified to have been made through PVC pipe sleeves. However, during construction the sleeves were installed so that they were flush with the outer wall, rather than being allowed to extend well out away from the building. This alteration is suspected to have led to the unintended current path to the conduit but was not discovered until well into the testing when an attempt was being made to investigate where the suspected arcing might be taking place.

The next question was why, even given an arc connection to the conduit in the vicinity of the building penetration, that conduit should carry such a large fraction of the total current in comparison with the east conduit. In investigating this issue, it was discovered that at the point at which the west conduit passed under the security fence surrounding the test site approximately 40 ft from the south wall of the building, the top of the conduit came within 1-1/8" of the exposed bottom end of one of the steel fence posts as illustrated in Figure 3-11. The steel fence system, with its over 80 posts all connected together by the low inductance chain link fencing material, therefore represented the lowest impedance ground in the vicinity of the test structure. When the earth was excavated at the point where the conduit passed by the fence post, numerous substantial arcing spots were found on the top surface of the conduit confirming that arcing to the fence system had occurred consistently. A reasonable explanation for the large current flow on the west conduit during the test therefore seems to be that, early in the incident stroke pulses, arcing occurred simultaneously at both the conduit/

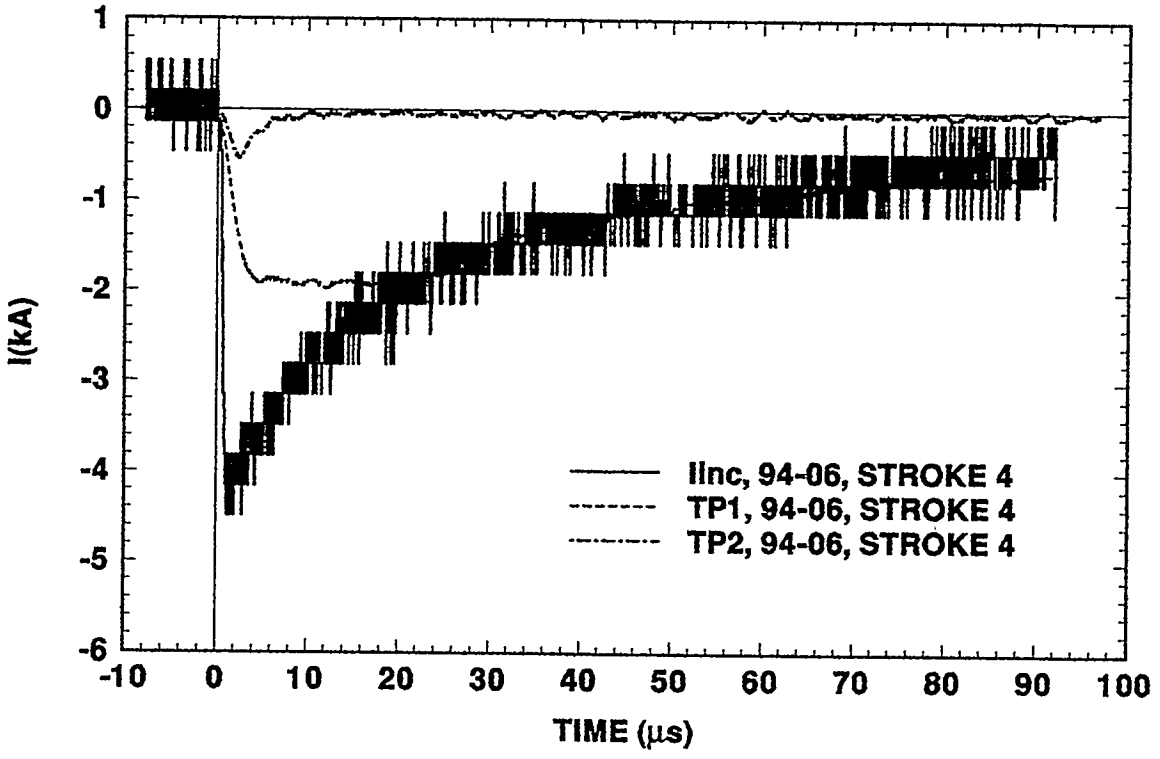

Figure 3-8. Incident stroke current and corresponding responses at TP1 and TP2 for Stroke 4 of Flash 94-06, which had a peak amplitude of 4.2 kA

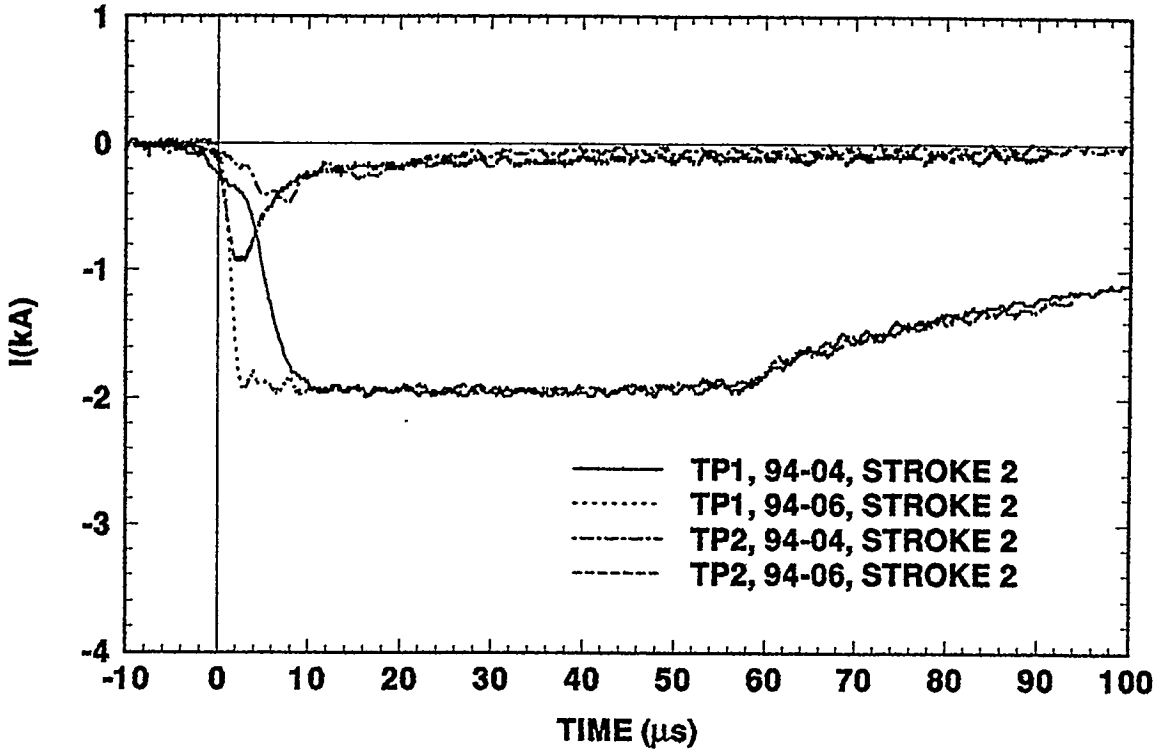

Figure 3-9. Conduit currents recorded at TP1 and TP2 for two strokes of amplitude small enough that the TP2 responses did not approach the instrumentation saturation threshold

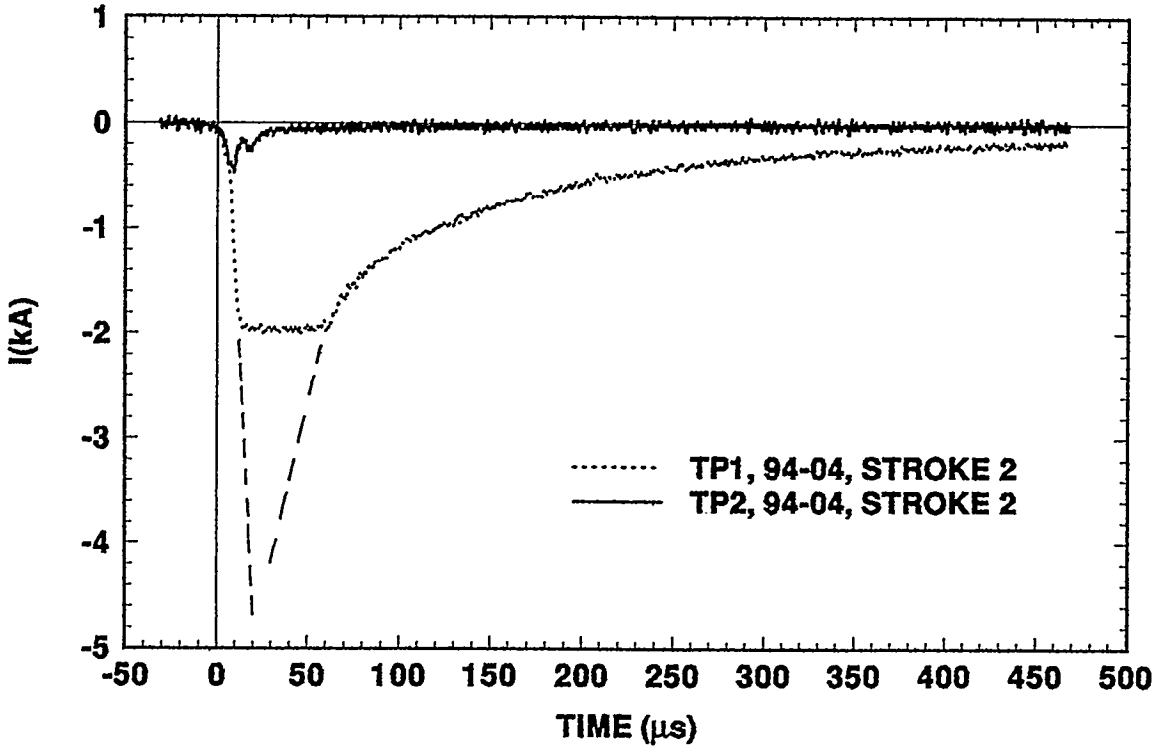

Figure 3-10. Conduit currents at TP1 and TP2 during the same stroke

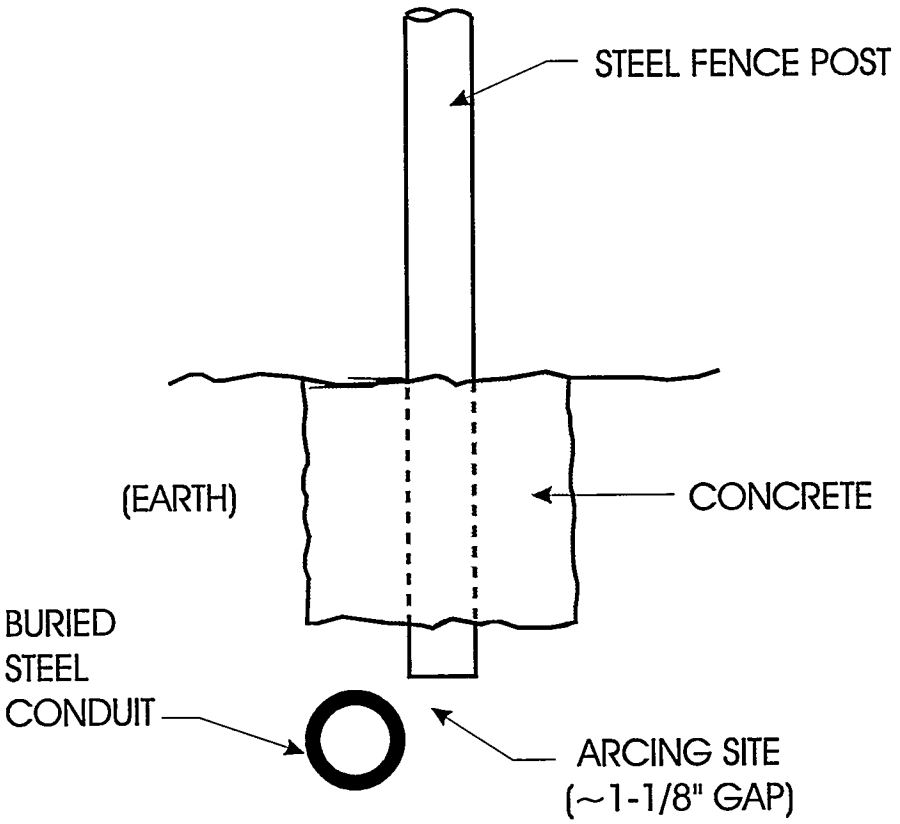

Figure 3-11. Diagram of the site where arcing took place between the west conduit and a steel fence post about 40 feet from the test structure

fence intersection and somewhere near the conduit/building penetration. As a result, the low impedance connection of the west conduit to earth potential through the fence system provided the preferred path to ground for the bulk of the incident current.

This outcome clearly demonstrates the difficulty of making definitive analytical assessments of the lightning responses of arbitrary complex structures or facilities. In the present instance every practical control was exercised during the design and construction of the test structure to implement and document known structural features. Despite these efforts, an unanticipated and, in this case, dominant current path developed. Given the structural complexities of an existing, and probably often modified and poorly documented, operational facility, great uncertainty will be inherent in the available knowledge of actual "as-built" construction details, some of which may influence the lightning responses to a major degree. Any assessment of this type of structure would therefore certainly have to be preceded by a careful site survey by a knowledgeable analyst, backed up by a set of specialized measurements to identify as many hidden factors as possible. *A priori* identification of potential arc-over points may still not be complete.

Given that the arcing described above actually occurred, a basic circuit description of the paths to ground for current attaching to the roof is shown in Figure 3-12.

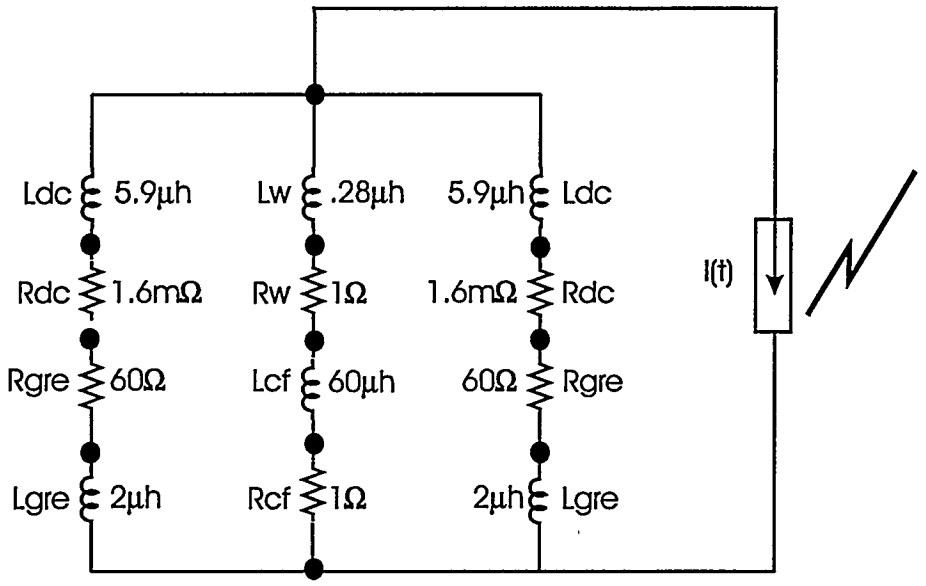

I(t) = Double exponential lightning current
dc = Down conductor
gre = Ground ring electrode
w = Wall path
cf = Conduit/fence

Figure 3-12. Electrical circuit model of current paths to earth of strokes attaching to the top of the structure

Conceptually, it consists of three parallel paths to earth: the two down conductors connected to the GRE and thence to zero ground potential through the earth; and the path down the walls, through the footers to the west conduit via the arc path, out to the fence system, and thence to zero ground potential through the earth. Using the PSPICE™ transient circuit analysis computer code, this circuit was analyzed to obtain currents corresponding to the down conductor and conduit paths to ground. A double-exponential return-stroke current of 11-kA peak amplitude, 0.5-µs rise time, and about 50-µs decay time to half value was used as the incident excitation, a reasonable approximation to the return-strokes associated with measured down conductor data shown in Figure 3-3. Values for the elements of the model circuit were determined analytically, in most cases from first principles [13, 14]. The transient responses obtained with the circuit model are given in Figure 3-13. The main characteristics of response currents are remarkably consistent with those of the down conductor currents in Figure 3-3 and the conduit current in Figure 3-10. For example, the distinctive waveshape, the times to peak, and amplitudes of the down conductor currents are all fairly well reproduced. The slower rise time of the conduit current is given, along with approximately the right amplitude, and at later times it closely follows the decay of the incident stroke current. The times to peaks of the down conductor and wall path currents, however, are too fast by a factor of about two, and the amplitude of the down conductor current is also too large by about the same factor. Variations of the different circuit elements were tried, but improvements in

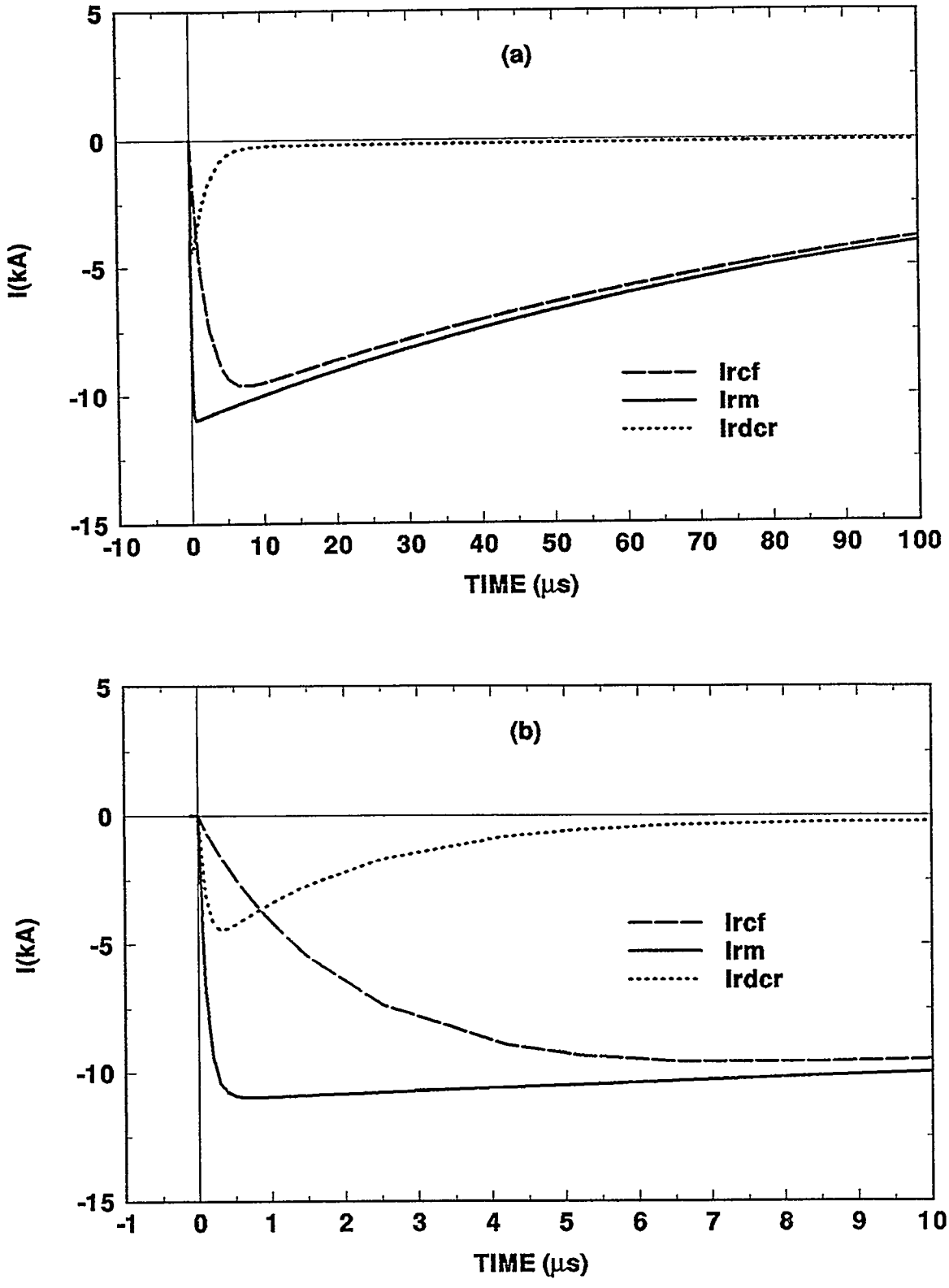

Figure 3-13. Down conductor and west conduit currents obtained from analysis of the circuit model of Figure 3-12. Assumed incident stroke current had a peak amplitude of 11 kA.

agreements in these parameters could not be reproduced without the introduction of corresponding deterioration in some of the other characteristics. Thus, it appears that the circuit model is not completely adequate, in that it, for example, ignores the path to ground associated with the east conduit, leakage resistances between the walls and floor, and several other subtleties. Nevertheless, it seems that the basic model does provide a fairly reasonable framework for the interpretation of the key building responses obtained during these tests.

Another aspect of interest is the effect of an intentional connection of the two buried conduits to the GRE. During Storm 3 both buried conduits were intentionally bonded to the GRE extensions brought into the interior of the building as shown in Figure 2-4. These stubs, which penetrated the floor through 4-in PVC pipe sleeves, were connected to the EMT conduit runs installed on the outer side walls in each half of the structure. We consider the results obtained during two flashes, during which the only configurational change was the connection of the GRE to the conduit system just described. In both cases the attachment point was the NE air terminal on the roof.

Although during Storm 3 the instrumentation settings had been adjusted to increase the threshold to 7 kA, saturation of the TP1 channel still occurred, thereby eliminating the utility of those data for present purposes. Nevertheless, some indication of the effect of the conduit/GRE connection can still be obtained from the TP2 data from Flashes 94-09 (no connection) and 94-14 (connections made). In Figure 3-14 the peak response currents at TP2 are plotted against peak return-stroke current for each flash. Aside from the issue of the apparent zero offsets displayed in the two fitted lines, the effect of the parallel path to ground due to connection of the conduits to the GRE shows up as a discernible overall reduction in response current on the east conduit. No definitive explanation for the non-zero intercepts has as yet been pursued.

Finally, the effect of connecting the wall and floor rebar together is of interest because of its implications regarding the surge impedance of the floor system to earth in comparison with that of the conduits. Unfortunately, once again the comparison is somewhat obscured by the inadvertent introduction of the enhanced path to ground presented by the west conduit and the "super ground" of the fence system. But again some insight can be obtained from the data from the east conduit current. In this case, consider Flashes 94-04 and 94-09, during which the only configurational change was the removal of the bonding straps between the wall and floor rebar during the latter flash. The response data are plotted together in Figure 3-15 and are seen to exhibit a systematic reduction of about 20 percent in the current flow out the east conduit when the wall and floor rebar are connected together. This situation provides a discernible parallel path to earth via the system of floor rebar and concrete, but the dominant preferred path continues to be away from the structure via the conduit. It is probable that, in the absence of the arc connection to the west conduit discussed in the previous section, the effect would have been more marked.

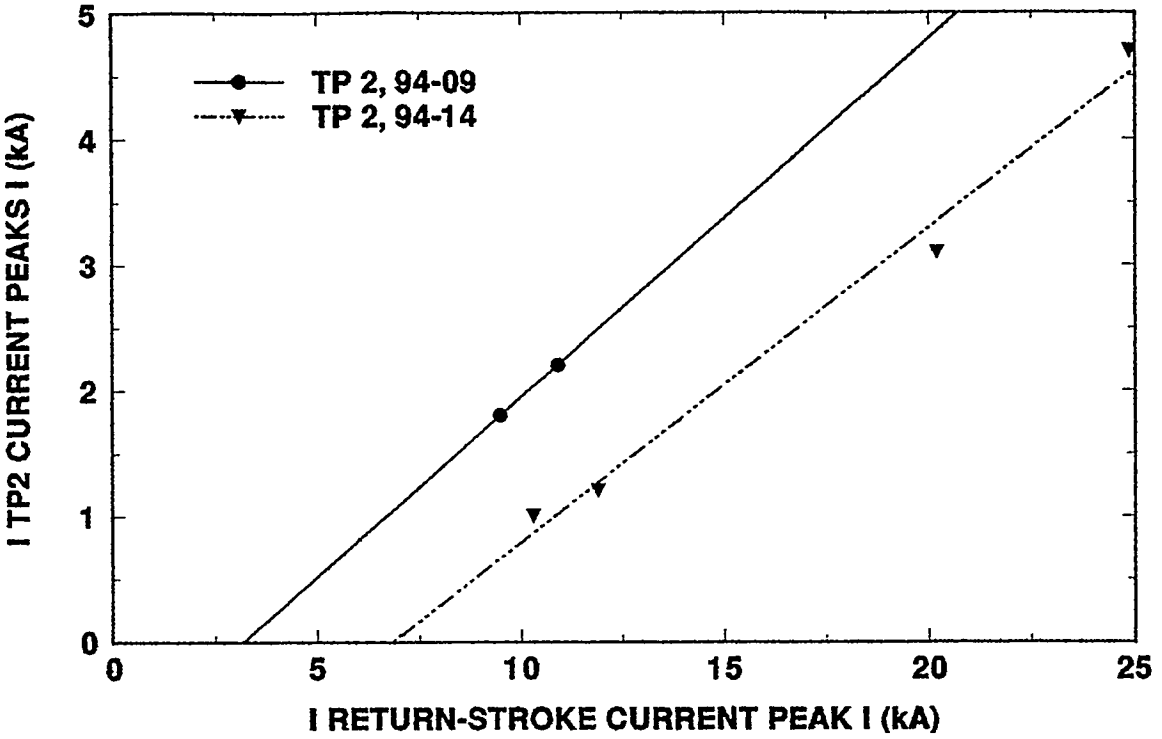

Figure 3-14. Peak amplitudes of east conduit currents as a function of peak return-stroke current amplitude for conditions in which the conduit was disconnected from the GRE (94-09) and intentionally connected to it (94-14)

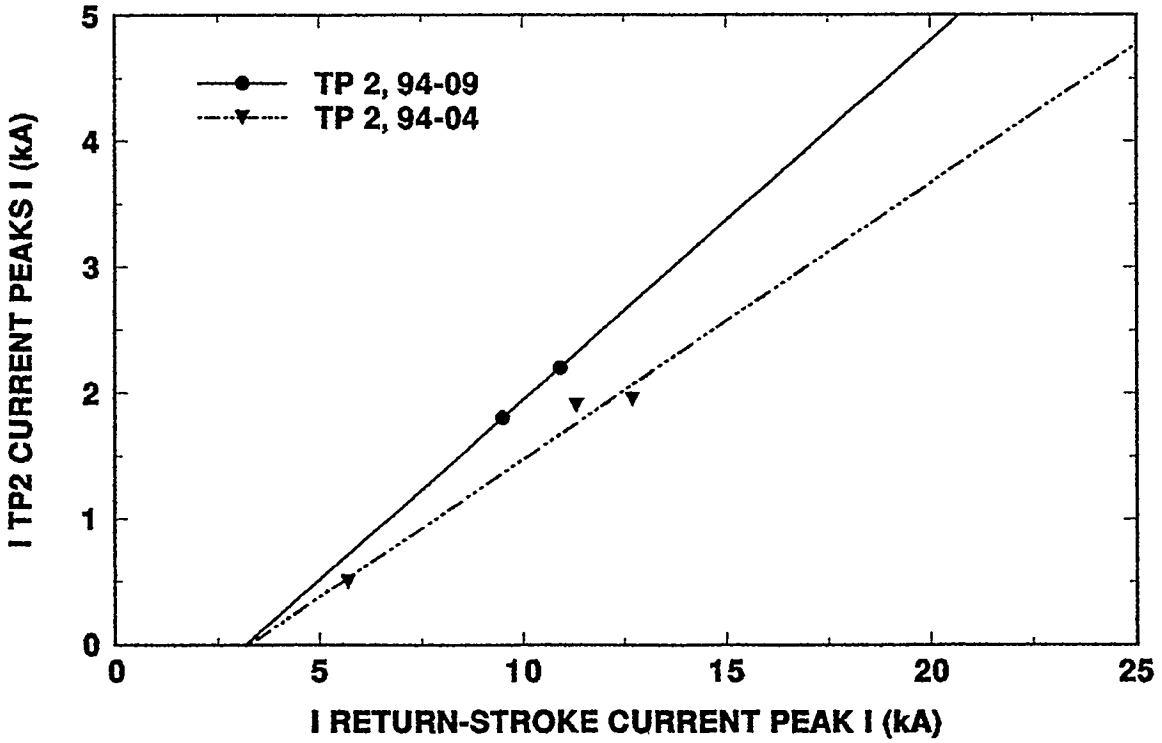

Figure 3-15. Peak amplitudes of east conduit currents as a function of return-stroke current with (94-04) and without (94-09) bonding of wall and floor rebar

3.2.3 Wall Currents

The response currents flowing through the bonding straps between the matching exposed ends of wall and floor rebar at six locations around the interior perimeter (Figure 2-8) were measured during attachments to different points on the building (Table 2-3). Of particular interest are the effects on overall current distribution due to variations of the attachment point, comparisons of the current amplitudes flowing in the good and bad sides of the structure (refer to Section 2.2), and comparisons of the currents at a given location under different attachments.

As was previously indicated during the discussion of the LPS down conductor current in Section 3.2.1, the wall system as a whole provided the preferred path to earth for most of the stroke current incident on any of the roof terminals. Reference to Figure 3-5, for example, indicates that at and prior to the peak of the incident current, more than half of the current was carried by the wall system, presumably because its total impedance is significantly lower than that of the two intentional down conductors. At later times, during which the derivatives of the stroke currents were small, essentially all of the current flowed through the lower resistance path of the wall system.

The currents recorded at the various test points exhibit a variety of waveforms. Some are bipolar or peculiarly structured as shown, for instance, in Figure 3-16, evidently as a result of the superposition of currents flowing in different directions at that location. Some insight into the general distribution of the current flow throughout the building can be obtained from an examination of the data shown in Figures 3-17 through 3-19, acquired during Storm 1 flashes to the NE (94-04) and SW (94-06) roof terminals. In general, the results reveal a pattern of higher currents at the test points located in the good side than at the corresponding locations in the bad side. It will be recalled that "good" and "bad" relate to the degree of enforced electrical connection between the intersections in the wall rebar grids. Hence, in general, the data confirm a pattern of distinctly higher currents in the well bonded, or good, side than at the counterpart points in the poorly bonded side. The only notable exception appears to be that the current at TP 15 (side wall in the bad side) during 94-06 exceeded that at TP14, its counterpart location in the good side. This may simply be a ramification of the fact that the location of TP 14 was so far away from the attachment point during that particular flash. Or, alternatively, TP15 is closer to the west conduit, on which, as was discussed in Section 3.2.2, was concentrated a large fraction of the current exiting from the building.

A comparison is given in Figure 3-20 of the currents flowing at each of the test points located in the good side during attachments to the NE (good side) and SW (bad side) terminals. In general there are no large effects at any given test point associated with a change in attachment point, and those effects that do show up seem to be consistent with intuition. One exception appears to occur at TP13 in that slightly smaller currents were recorded during attachment to A-2, located on the same side as the test point in question, than during attachments to A-1, which is much farther away.

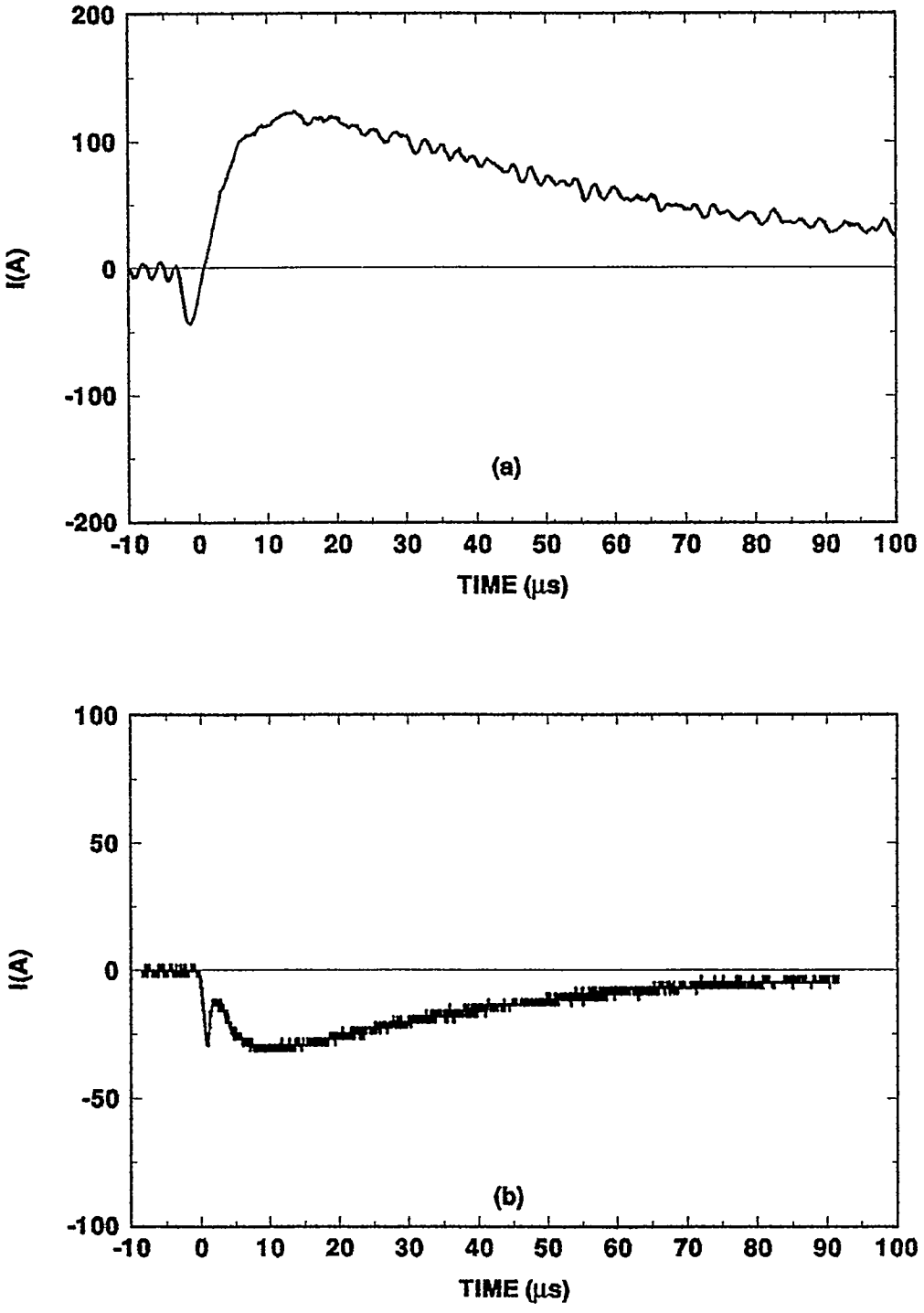

Figure 3-16. Example wall current waveforms; (a) TP11 and (b) TP14 during Flash 94-04 to the A-2 terminal on the roof

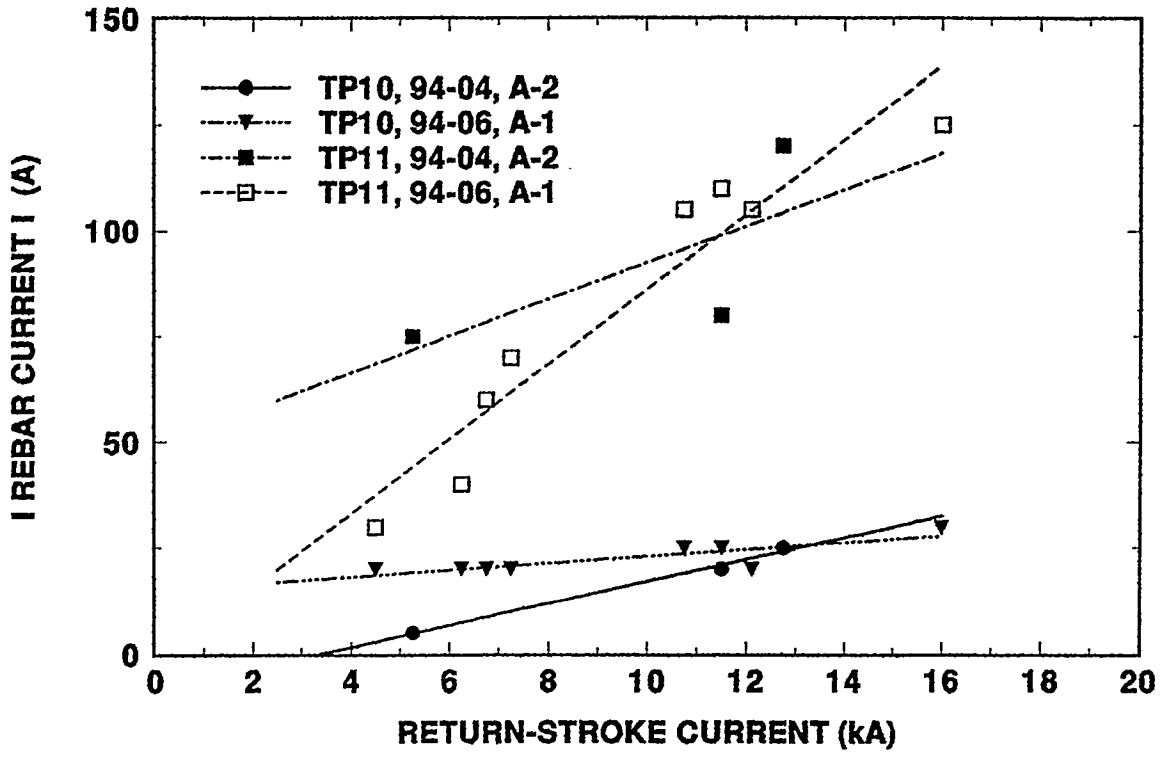

Figure 3-17. Comparison of front wall currents in good and bad sides for attachments to the SW (A-1) and NE (A-2) LPS roof terminals

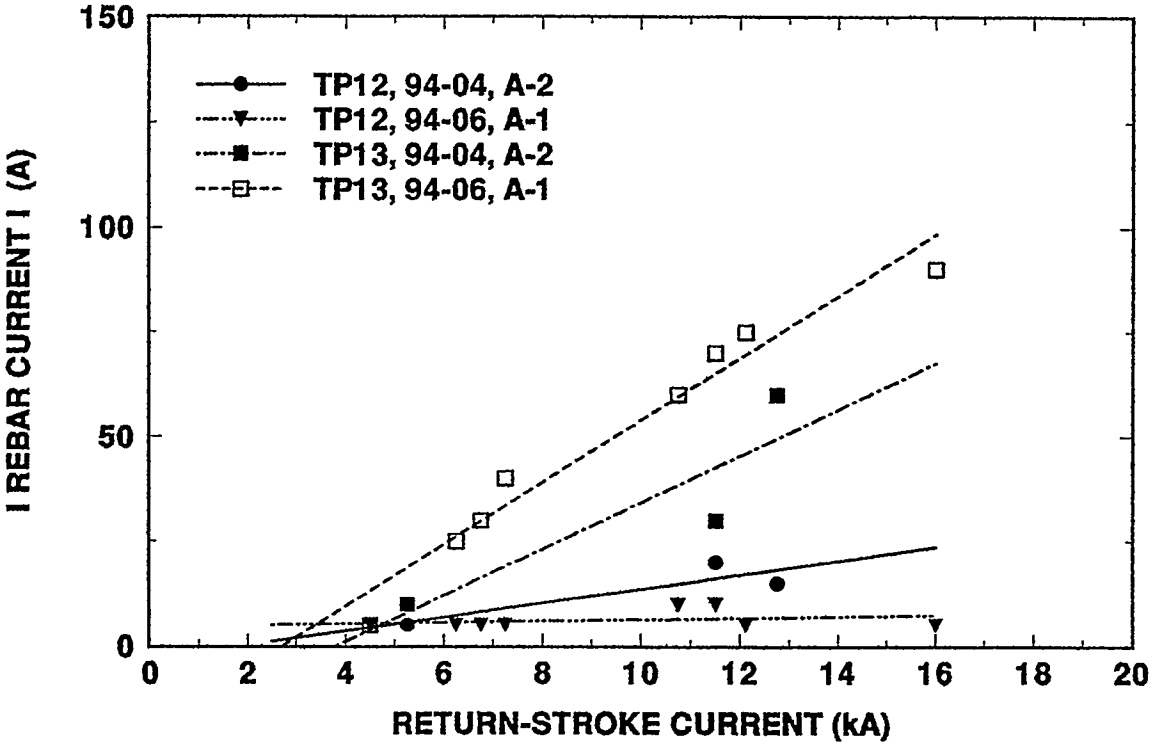

Figure 3-18. Comparison of rear wall currents on good and bad sides for strikes to the SW (A-1) and NE (A-2) LPS roof terminals

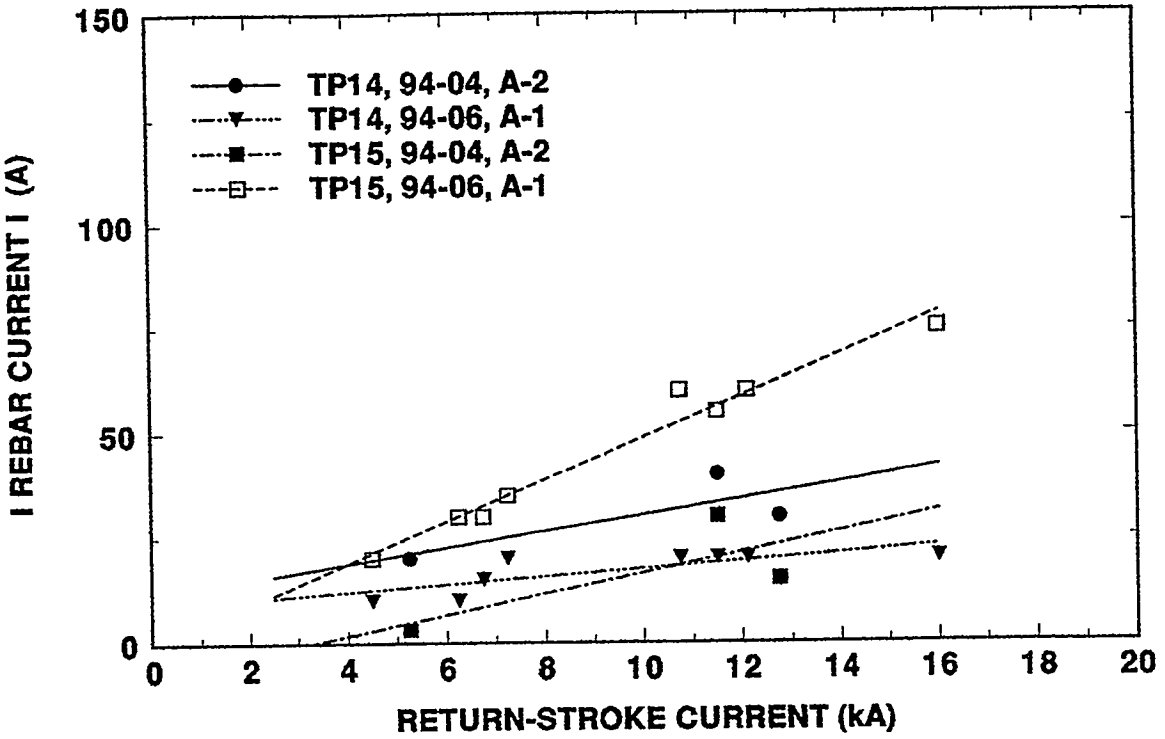

Figure 3-19. Comparison of side wall currents on good and bad sides for strikes to SW (A-1) and NE (A-2) LPS roof terminals

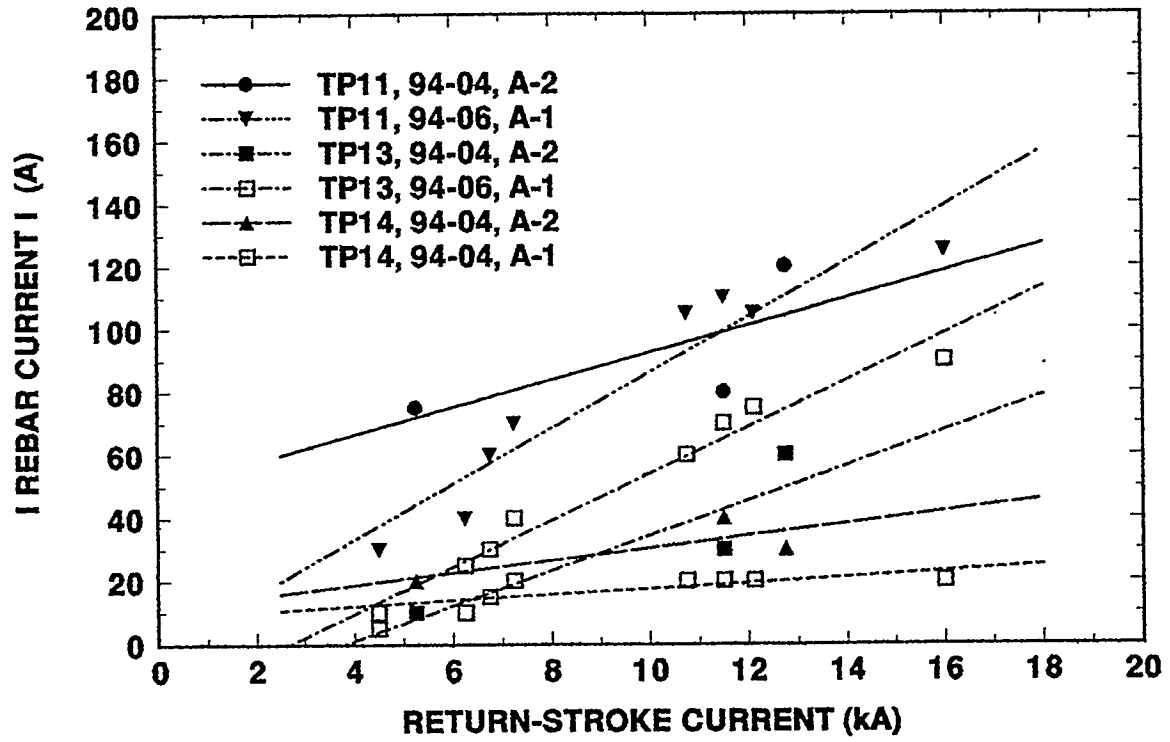

Figure 3-20. Comparison of wall currents at different locations in the good side for strikes to the SW (A-1) and NE (A-2) LPS roof terminals

3.2.4 GRE and EMT Currents

The currents flowing on the buried GRE cable were recorded at four locations (TPs 5, 5', 6, 6') during various flashes throughout the test period. During Storm 1 the first three of the listed test points were monitored under attachments to two different air terminals, the NE and SW, on the roof (see Figure 2-8). The data from TPs 5, 5', and 6 corresponding to two strokes of comparable amplitude in Flashes 94-14 and 94-15 are shown in Figures 3-21 through 3-23. The waveforms of the currents at the various monitoring locations around the buried cable are seen to be distinctly different from one another, but at any given location the waveshapes are not much different under the two attachments. The data make it clear that the current on the GRE consists of various components flowing in different directions and combining by superposition somewhat differently at the various monitoring points, probably as a result of asymmetries in the locations of the measurement points with respect to the two down conductors. At TP5' the waveform is quite similar to but with only about 30 percent of the amplitude of the down conductor current flowing at the nearby TP8. The polarity of the signal at TP5' is also consistent with the injection of electron current onto the GRE at its junction with the NW down conductor. At TP5, the waveform is quite similar to the wall current recorded at TP11 (Figure 3-16a), but no obvious relationship to account for this similarity is evident. In comparison to the other test points on the GRE, the largest amplitude by a significant margin always occurred at TP5', regardless of the attachment point.

During Storm 3, the GRE extensions shown in Figure 2-8 were connected to the EMT runs along the sidewalls in each half of the structure. As shown by the overlays in Figure 3-24a, the currents at TPs 4 and 9' are virtually identical, as would be anticipated. Interestingly, however, the similar comparison of currents at TPs 3 and 9 in Figure 3-24b reveals that the peak of the current at TP9 is flattened, although at times later than about 10 μs, the two currents are the same. This same phenomenon occurs on all strokes of Flash 94-14, and the explanation is thought to be related to arcing that developed between the EMT and a cut-off steel stud in the cement wall very near the location of TP22 in the good side of the structure. This arcing was detected photographically during Flash 94-14 and others and is discussed in more detail in Section 3.2.10. On Flash 94-15 the attachment point was the riser stub on the buried east conduit 50 ft from the front wall of the building. During this flash, no arcing was detected inside the building, and, as indicated in Figure 3-25, the currents at TPs 3 and 9 are the same.

3.2.5 Wall-to-Floor Voltages

During Storms 2 and 3 the bonding straps between the 28 pairs of exposed wall and floor rebar ends were removed, and the transient voltages between the wall and floor rebar were measured as described in Section 2.5.2 at the four locations identified in Figure 2-8 by the designations TP16 through TP19. As was discussed in Section 2.5.2, peaking effects in the raw recorded data due to shunt capacitances across the voltage divider resistors of the probe used at each test point were removed from the raw data by means of digital filtering. The applied filtering functions were derived from equivalent

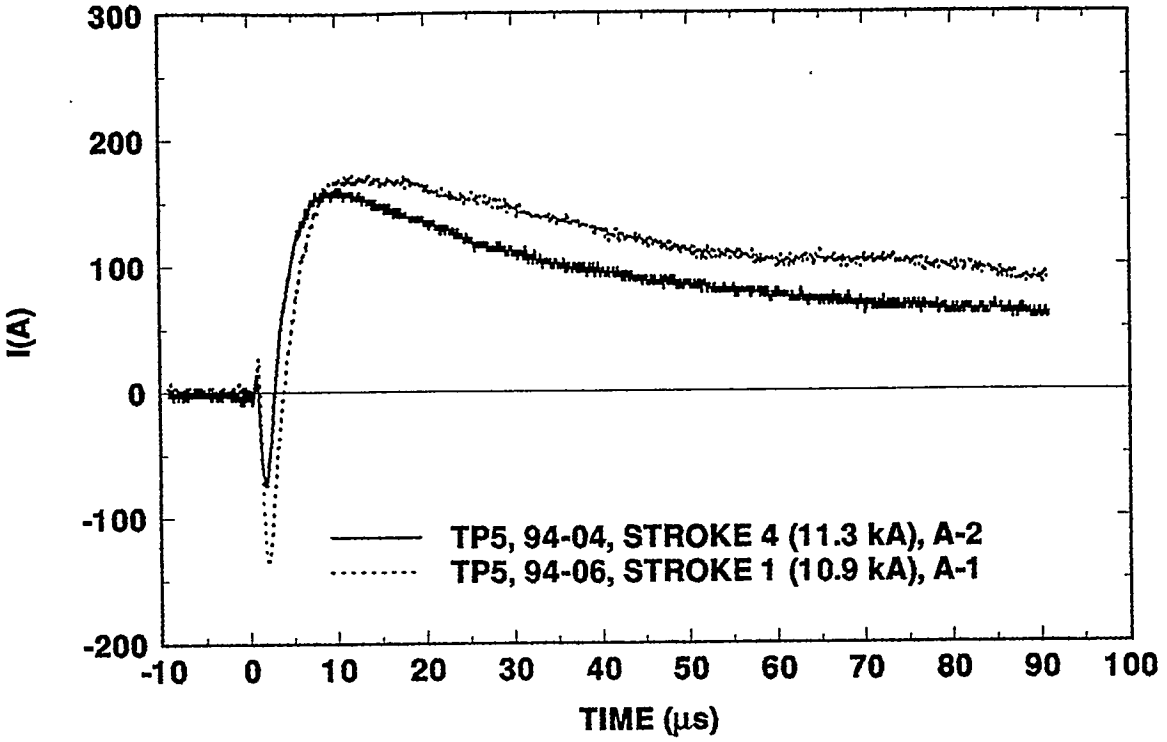

Figure 3-21. Comparison of GRE currents at TP5 for strikes of comparable magnitude to SW (A-1) and NE (A-2) LPS roof terminals

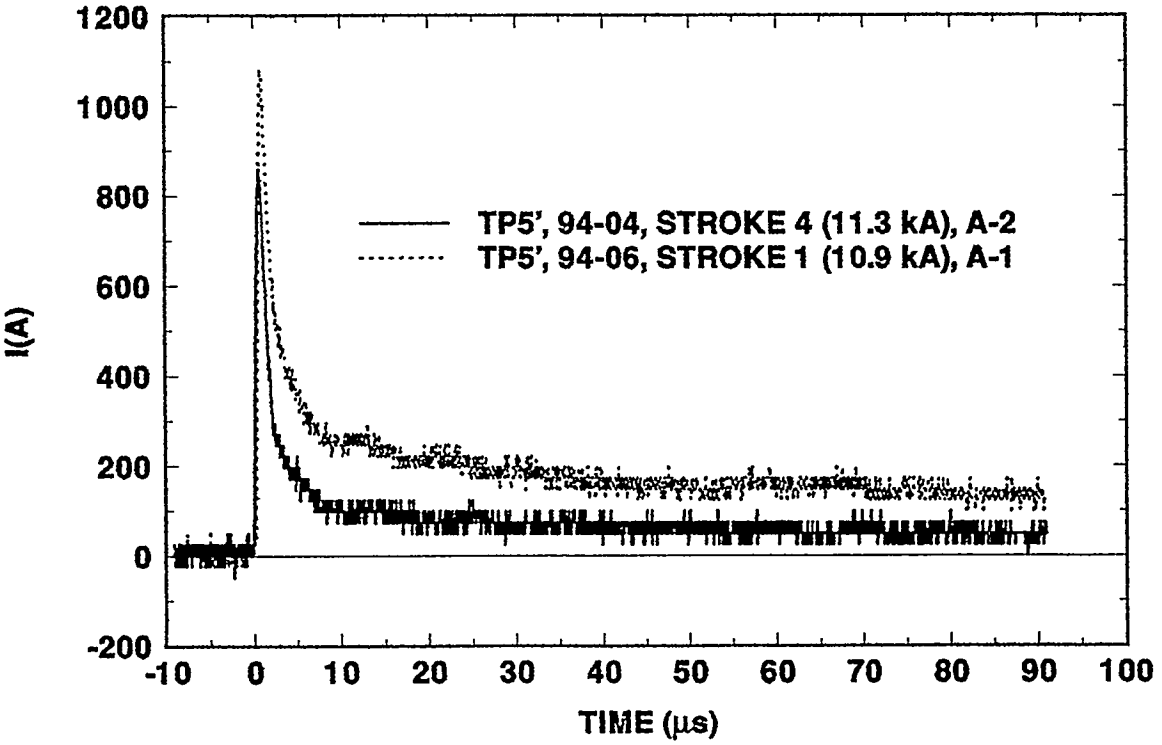

Figure 3-22. Comparison of GRE currents at TP5' for strikes of comparable magnitude to SW (A-1) and NE (A-2) LPS roof terminals

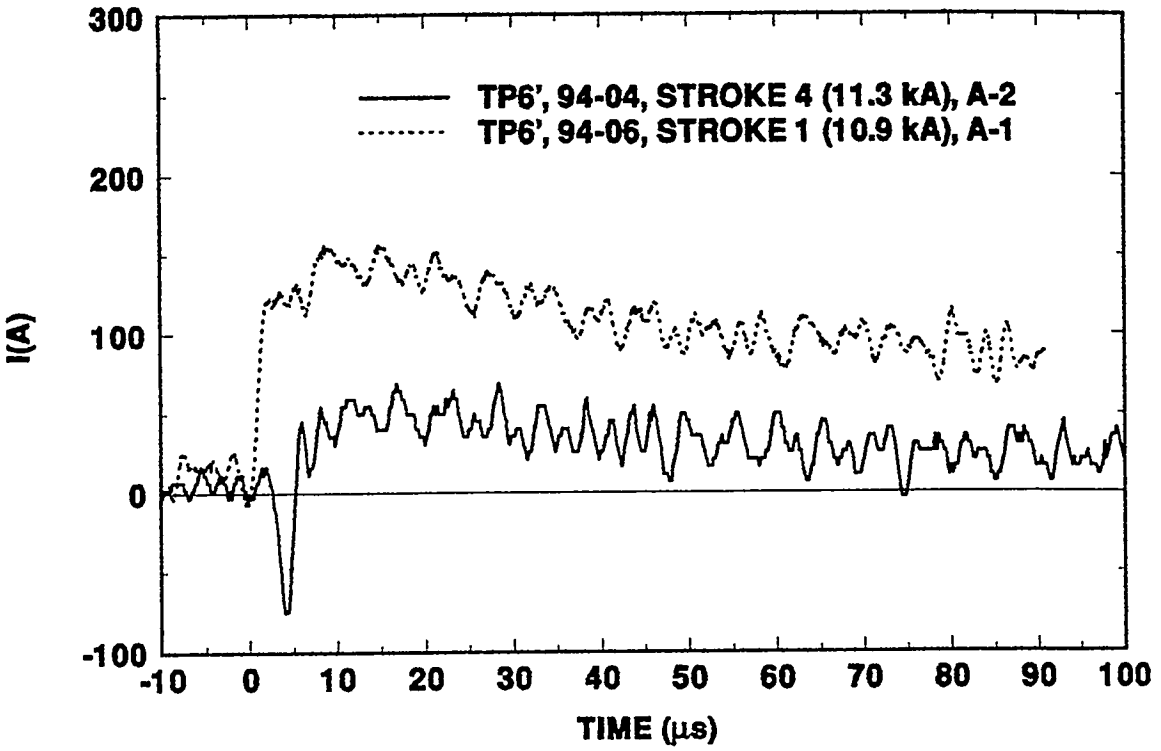

Figure 3-23. Comparison of GRE currents at TP6' for strikes of comparable magnitude to SW (A-1) and NE (A-2) LPS roof terminals

electrical models of each voltage measurement probe determined on the basis of laboratory measurements of each probe configuration. All the voltage entries in Tables 3-4 through 3-13 correspond to data that have been processed in this manner.

Flashes 94-07 and 94-10 were each triggered to the vent stack air terminal on the roof of the building. The results from these two events provide a set of 5 data points at each test point of interest obtained under exactly the same configuration. Similarly, Flashes 94-09 and 94-14 were each triggered to the NE air terminal on the roof. However, those two flashes occurred during Storms 2 and 3, respectively. Since modification was made to the GRE/buried conduit system between those two storms, the lumping of their data is less desirable than in the case of the former flashes.

It can be noted from the entries in Tables 3-6 and 3-8 for TPs 16 through 19 that, for a given stroke, the magnitudes of the response voltages at each of the four different test points are all within a factor of two of each other. In general they are all of the order of 100 kV. Interestingly, however, these voltages are not primarily due to the inductances of the down conductors and the wall system, but appear to be predominantly resistive. According to an inductive model, the measured voltages should scale linearly with the derivative of return-stroke current. In Figure 3-26 the voltages measured at each test point are plotted against the derivatives of the return-stroke currents that produced each

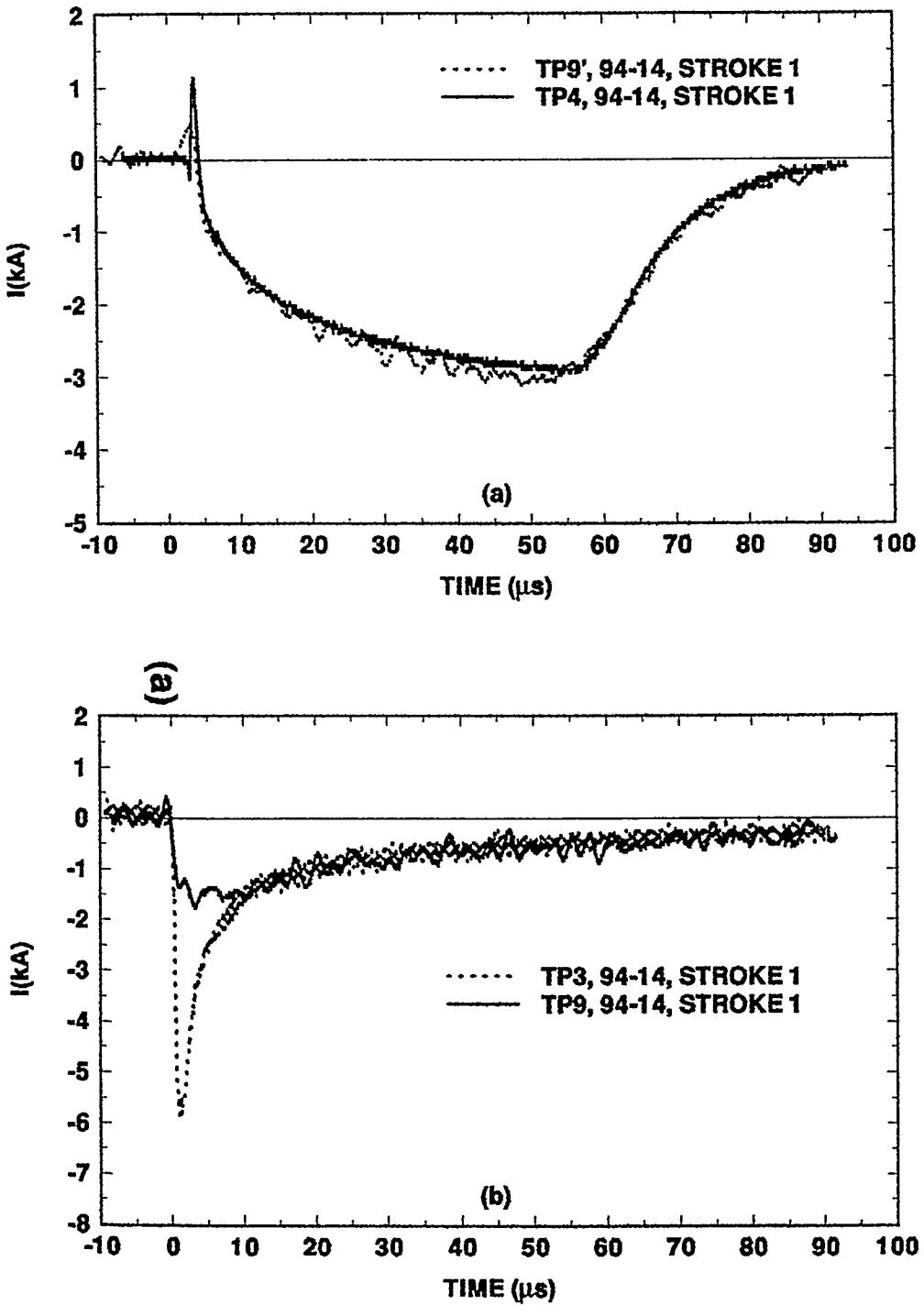

Figure 3-24. Comparison of currents at (a) TP4 and (b) TP9' for the same stroke in Flash 94-14, during which the GRE was connected to the east and west buried conduits. Flash 94-14 was attached to the NE (A-2) LPS roof terminal.

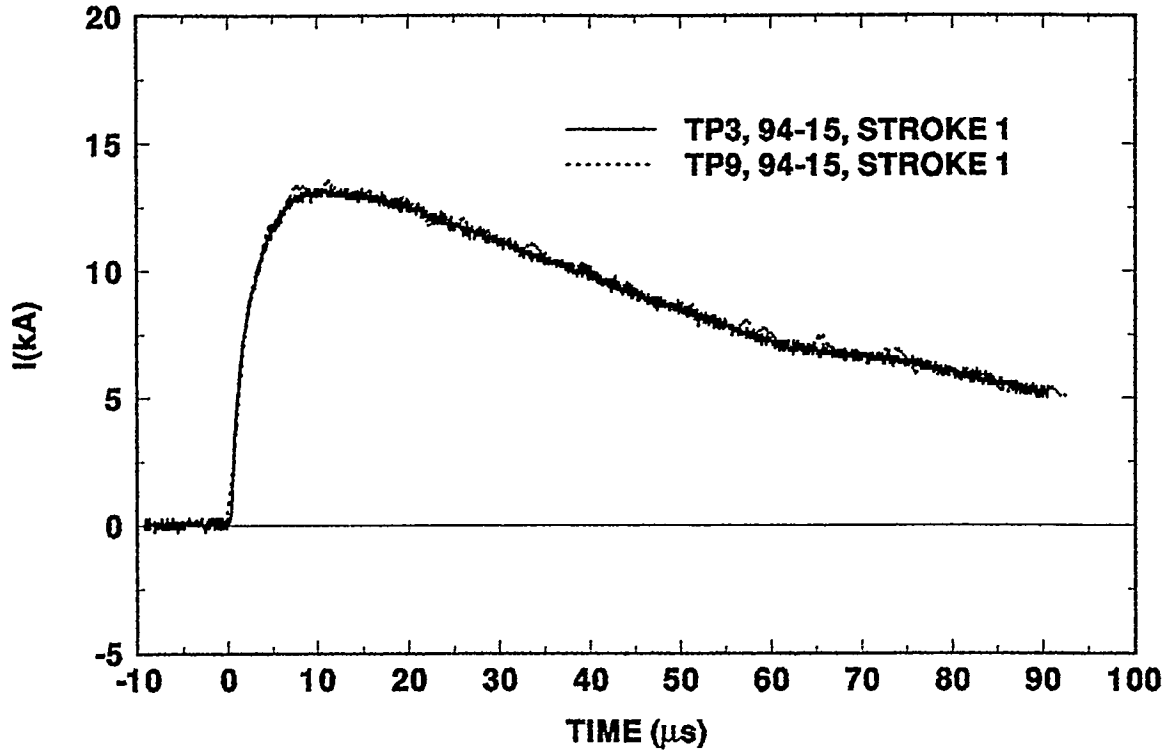

Figure 3-25. Comparison of currents at TP3 and TP9 during the same stroke in Flash 94-15, during which the GRE was connected to the east and west buried conduits. Flash 95-15 was attached to the east conduit riser stub (A-4).

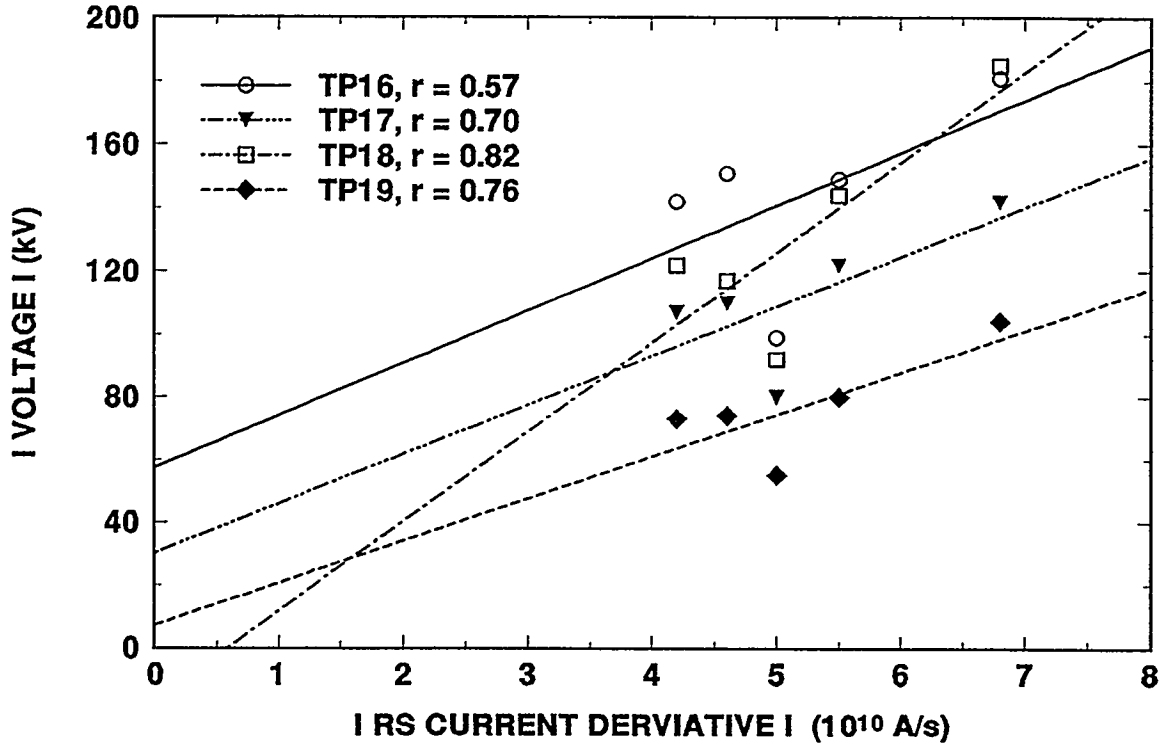

Figure 3-26. Peak magnitudes of wall-to-floor voltages as a function of wavefront rise rate of incident stroke current for Flash 94-07 to the vent stack LPS terminal (A-3)

response. The derivatives were obtained as the average slope between the 10-to-90 percent points on each return-stroke current wavefront. The correlation parameters r of the indicated regression lines range from 0.57 to 0.82, suggesting that the data are only modestly linearly correlated to return-stroke current derivative. However, as is evident from Figure 3-27, the peak of the voltage measured at TP16 occurs simultaneously with that of the return-stroke current, a feature that suggests a resistive relationship between the stroke current and the resulting voltage between the wall and floor. This implication is further confirmed by the data shown in Figure 3-28, in which the peak voltages at each test point are plotted against peak return-stroke current amplitude. Here the values of the correlation parameters of the regression lines range from 0.93 to 0.98, revealing a much stronger correlation with peak return-stroke current than with its derivative.

3.2.6 Simulated Crane and Vent Stack Voltages

The transient voltages between the simulated overhead crane rail (electrically bonded to the metal roof structure) and the floor rebar (TP20) on the good side were measured during each storm and hence under every combination of building configuration and attachment point location that was tested throughout the program. As with the other voltage data, the results presented here have undergone post-test signal processing to compensate for capacitive effects in the measurement probes that were employed.

In general the results appear to be consistent with intuition and compatible with the rest of the body of voltage data acquired at other test points. For example, for the configuration in which the floor and wall rebar were disconnected from each other and stroke attachment was made to any of the roof terminals, the results at TP20 are quite similar in waveform and amplitude to the corresponding wall-to-floor voltages discussed in Section 3.2.5. (Refer to Tables 3-6 through 3-9.) An example comparison of waveforms is given in Figure 3-29. In tests in which the wall and floor rebar were bonded together, such as during Storm 1, the response waveforms were bipolar in shape and, as would be expected, of amplitudes smaller by factors of 30 to 50 than under conditions in which the floor and walls were not connected together.

Two other fundamentally different cases were represented during Storms 3 and 4. Flashes 94-15 and 94-22 were attached to the riser stub on the east buried conduit, which was located at a distance of 50 ft from the front of the structure. The resultant responses at TP20 under these conditions were similar in magnitude to those that occurred during attachments to the roof when the floor and walls were connected together. In this case, however, the polarities of the bipolar responses were inverted. For comparison, the voltage measured during Stroke 4 of 94-06 (10.9 kA) is shown in Figure 3-30 along with that obtained during Stroke 3 of 94-22 (also 10.9 kA).

The remaining case of particular interest is the one in which attachment was made to the 49-ft LPS mast, the base of which was connected to the buried GRE at the front center of the structure. This configuration was tested during Flash 94-21 (Table 3-11), and

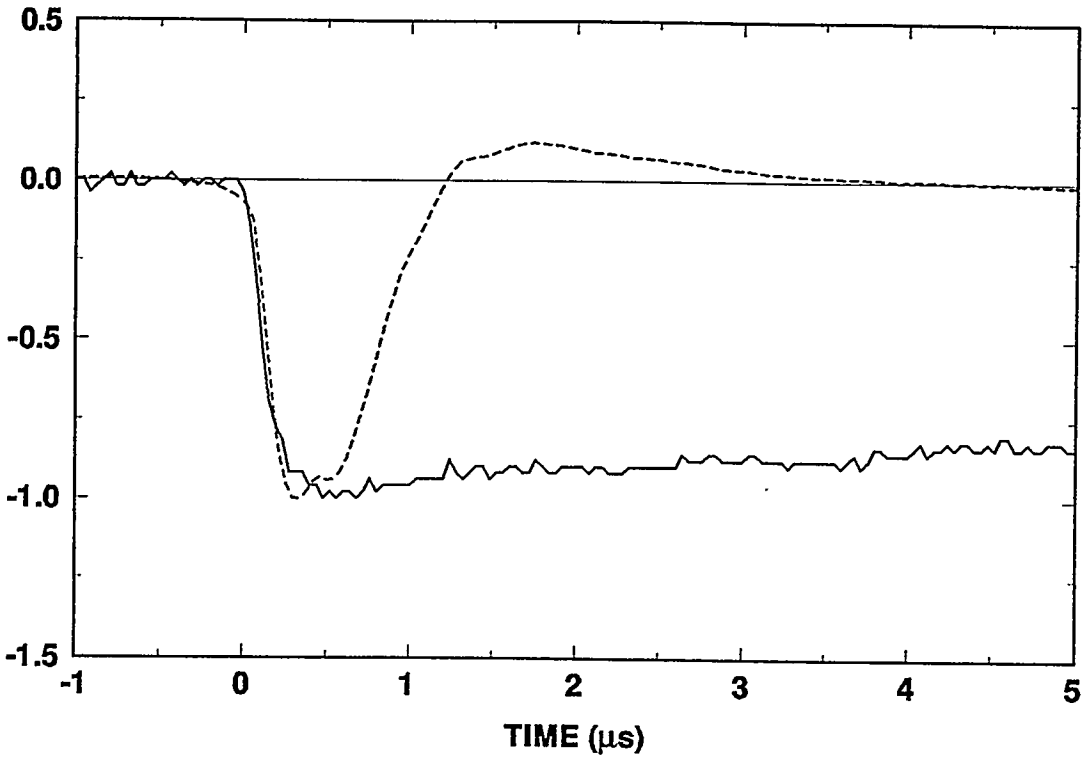

Figure 3-27. Comparison of incident stroke current and wall-to-floor voltage at TP16 during Stroke 1 of Flash 94-07 to the vent stack LPS terminal. Both waveforms have been normalized to unity amplitude for comparison purposes.

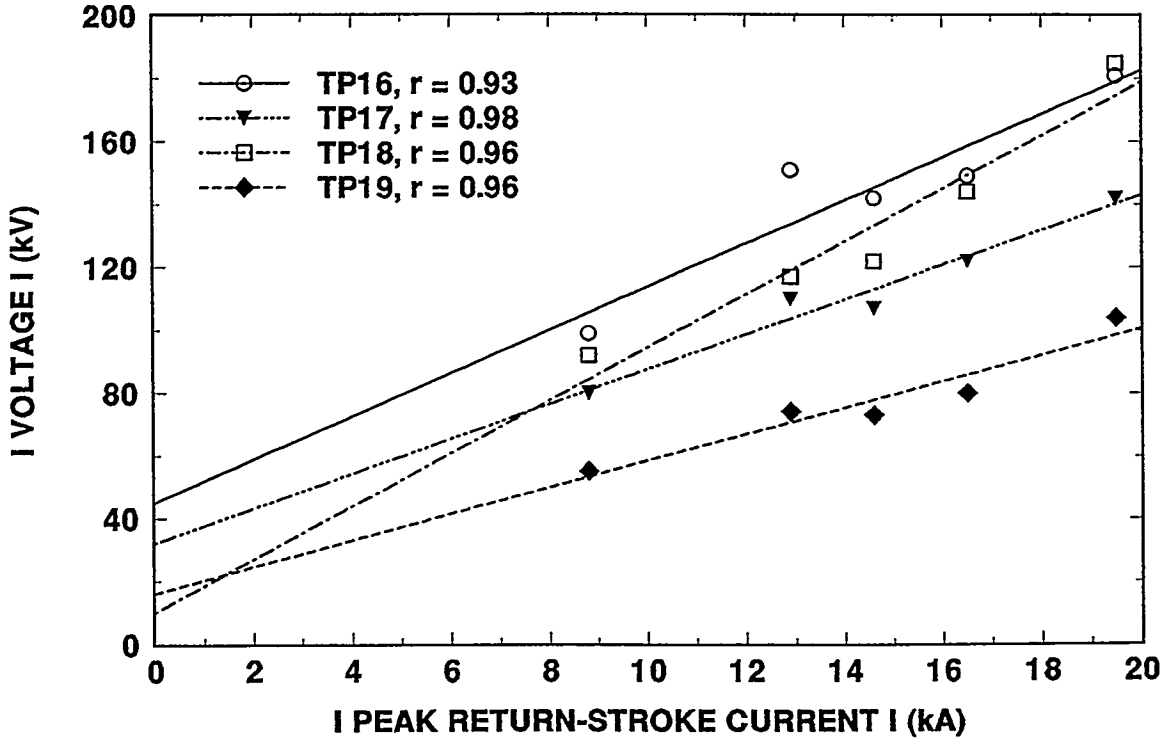

Figure 3-28. Peak magnitudes of wall-to-floor voltages as a function of return-stoke current for flashes attaching to the vent stack LPS terminal

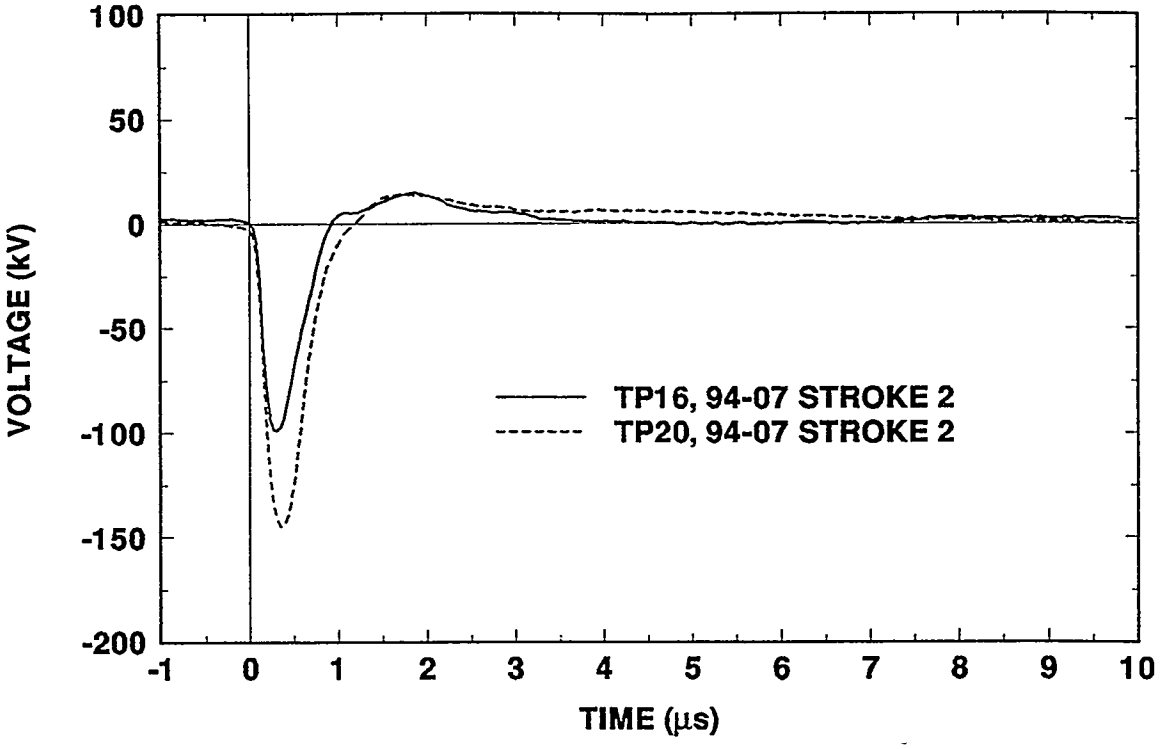

Figure 3-29. Comparison of crane rail and wall-to-floor voltages for the same stroke during Flash 94-07 to the vent stack LPS terminal

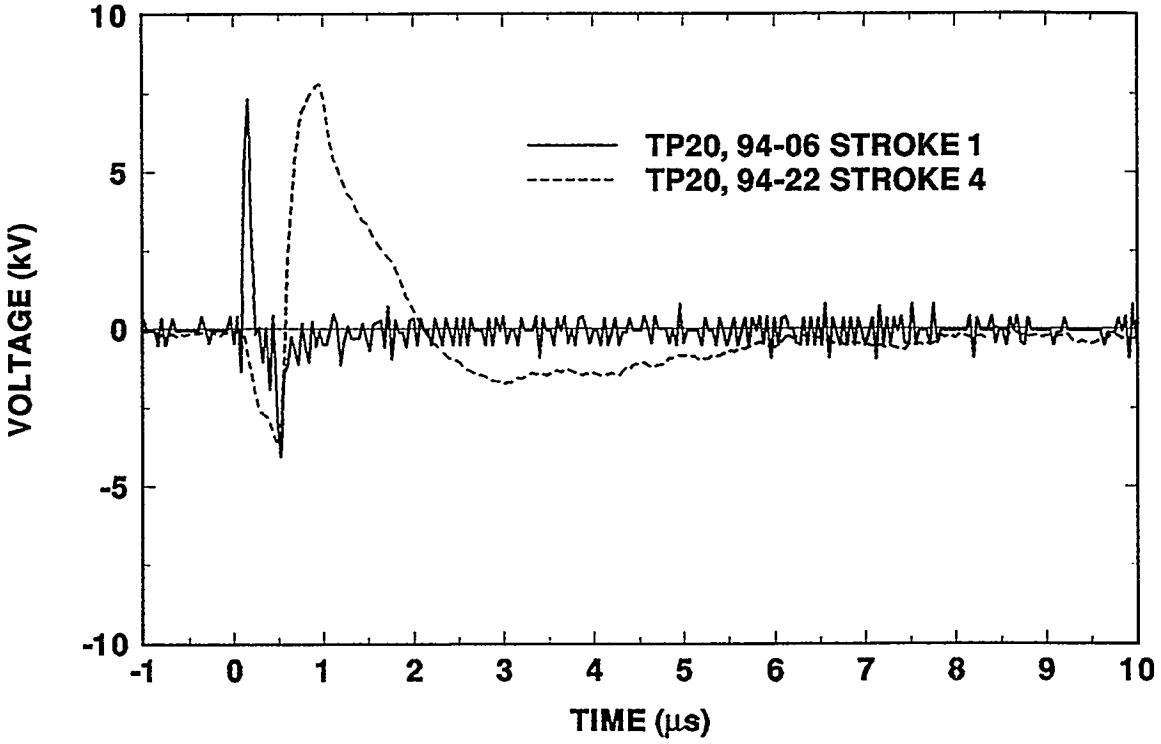

Figure 3-30. Comparison of crane rail voltages for strokes of comparable magnitude to the SW LPS roof terminal (94-06) and to the conduit riser stub (94-22)

the responses at TP20 are somewhat similar to those for attachment to the conduit riser stub. These two cases might be viewed in principle as being similar, since in both instances the introduction of return-stroke current onto the building structure takes place via its buried grounding network.

The voltage was also measured at TP 21 between the base of the vent stack duct, which was about 3 ft above the floor, and the floor rebar directly under the stack. Because of instrumentation problems, no reliable data were obtained during Storms 2 or 3 at this location. The data from Storm 1 (walls and floor rebar connected) were bipolar in waveform with peak amplitudes of the order of ±10 to 30 kV (Tables 3-4 and 3-5). These data were also characterized by a ringing structure at about a 5-MHz rate. An example is given in Figure 3-31.

During Storm 4 data were acquired at TP21 under attachments to the LPS mast (Table 3-11) and to the east conduit riser stub (Tables 3-12 and 3-13). As might be expected, these situations produced relatively small voltage transients between the stack and the floor. Responses for attachments at both locations were bipolar and of somewhat complex structure, with peak amplitudes of about ±10 kV, and durations of 10 to 20 μs. Examples of vent stack responses for attachments to the riser stub and the LPS mast are given in Figure 3-32.

3.2.7 EMT-to-Floor Voltages

To simulate an electrical power distribution system throughout the structure, steel conduits were run along the wall in both halves of the structure about 3 ft above floor level. One end in each case was connected to its respective steel power service panel box mounted on the front wall. The bottom of each panel box was connected to its respective 3½-in conduit that exited through the floor on each side and extended out from the building on each side. The EMT power distribution conduits were anchored to the walls by dielectric fasteners to ensure that they were not in direct contact with the wall rebar.

The transients developed between a service outlet box on the back wall and the floor rebar were recorded at TP22 (Figure 2-8) during Storms 2, 3, and 4 by means of the voltage divider network described in Section 2.5.2 and shown in Figure 2-15. The resistors that made up the voltage divider chain were taped to 3/4-in PVC pipe to provide physical support.

During Storm 2, the wall and floor rebar were disconnected from each other and lightning was attached to the LPS terminals on the roof, twice to the vent stack and once to the NE corner. The resultant responses at TP22 (Tables 3-6 through 3-8) were bipolar in shape, of amplitude range from ±80 to ±150 kV, and of duration of 10 to 20 μs. As is the case with all of the voltage measurements, the raw data were processed post-test to compensate for capacitive peaking effects associated with the measurement probe.

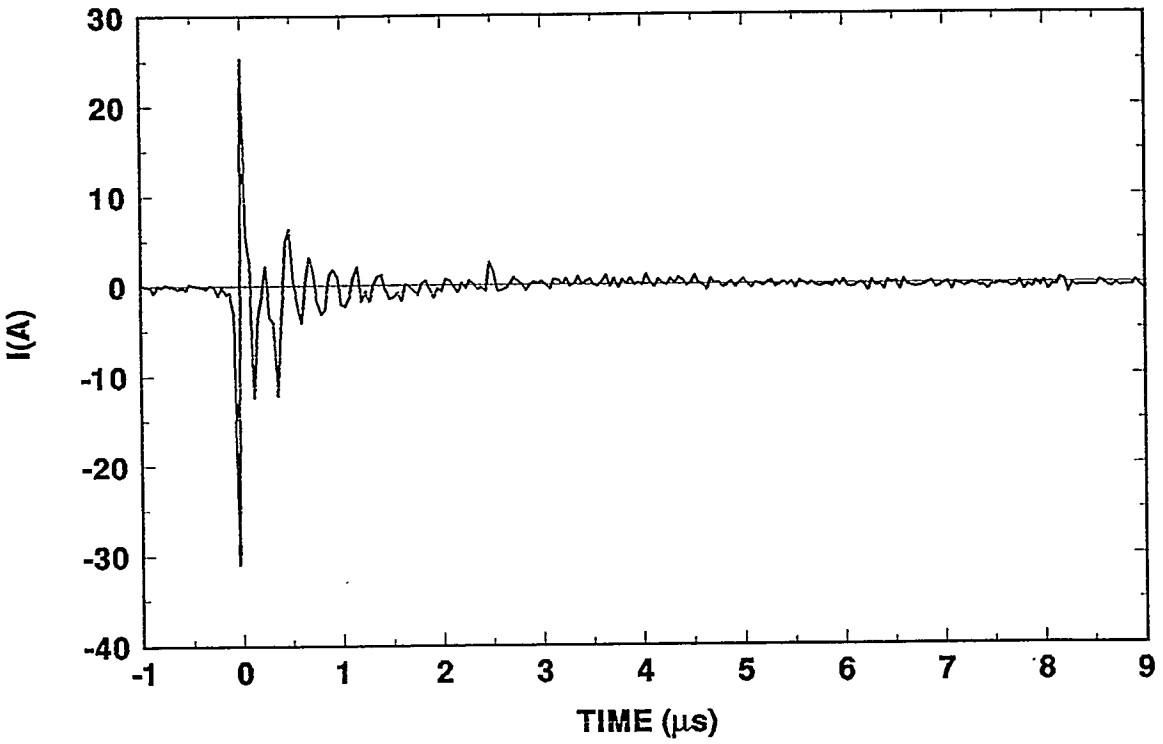

Figure 3-31. Example vent stack voltage measured during Stroke 3 of Flash 94-06 with the wall and floor rebar bonded together

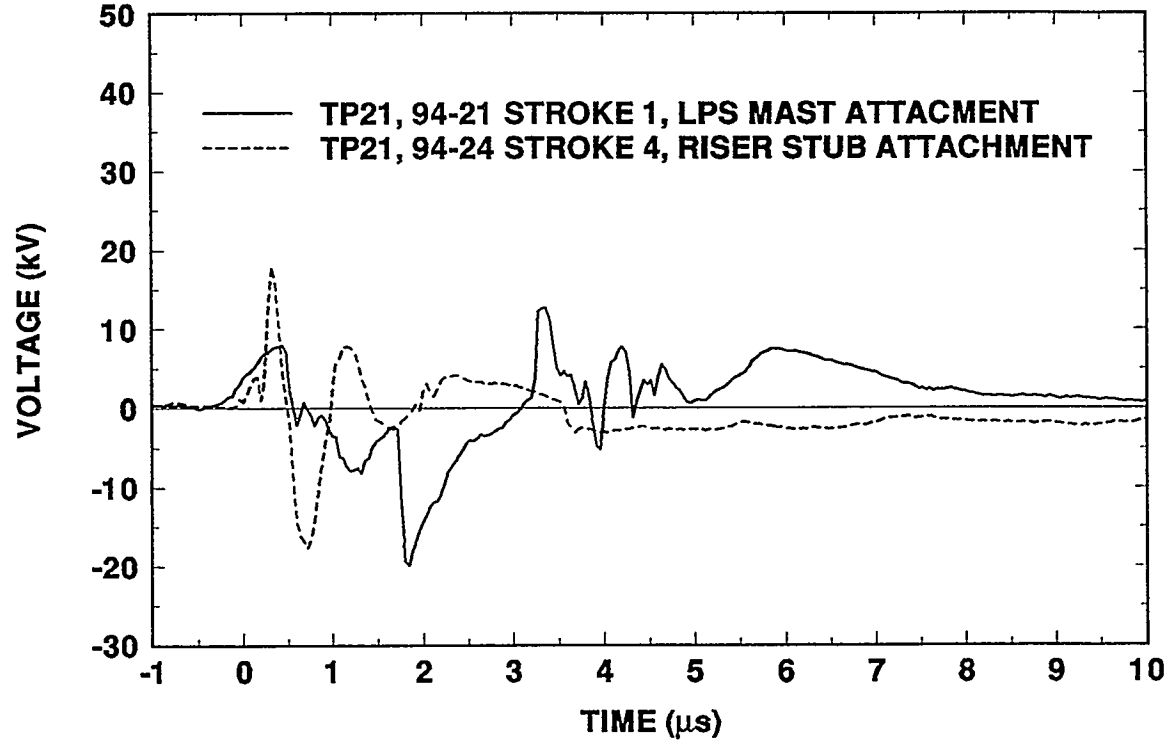

Figure 3-32. Comparison of vent stack voltages for strokes of comparable magnitudes during strikes to the east conduit riser stub (94-24) and to the LPS mast (94-21)

An example of a raw data record from TP22 is shown in Figure 3-33 along with an overlay of the compensated data trace. In the latter, the dotted line corresponds to that portion of the curve which is contaminated to some degree by the effects of the saturation of the positive and negative peaks in the raw data. Because of this clipping, the peak amplitudes reflected in Tables 3-6 through 3-13 represent underestimates, but the order of magnitude of the actual maximum responses would still be 100 kV.

During Storms 3 and 4 the voltages at TP22 were also recorded for lightning attachments to the east conduit riser stub. For Storm 3 the GRE was bonded to the EMT conduits about halfway along the side wall in each section of the building. This intentional connection was removed for Storm 4. Under both configurations the results at TP22 were approximately equal in terms of amplitude, but the waveshapes were different. Examples of the responses under similar amplitude return strokes to the riser stub for each case are presented in Figure 3-34.

A factor of significance concerning the response at TP22 was the repeated occurrence of substantial arcing from the EMT on the east wall to a cut-off steel stud embedded nearby in the concrete of the wall. This arcing was detected photographically during every flash for which a camera was in operation inside the building, with the one exception being during Flash 94-21, which was triggered to the LPS mast. This arcing is discussed in detail in Section 3.2.10. Its effect on the ultimate peak responses on the power distribution system that might have occurred in its absence is, of course, unknown. However, the limit on voltage amplitude anywhere within the structure can probably be taken to be the maximum voltage observed on either the vent stack or the crane rail during strikes to the roof. The maximum such voltage observed during the present tests was about 200 kV.

3.2.8 Magnetic Fields

Magnetic field transients were recorded inside the building at floor level approximately 1 ft from the walls in each of the corners corresponding to the location of the exterior down conductor cables from the roof. The maximum responses occurred at TP24, located in the southeast corner immediately in the vicinity of where the east buried conduit rose vertically from the floor to connect to the service panel box. The highest amplitudes were those on flashes attached to the riser stub on the east conduit. Referring to Table 3-10 (Flash 94-15), it can be seen that a substantial fraction of the current incident on the riser stub flowed back to the structure on the conduit (TP2), up to the service box (TP3), onto the east EMT conduit, and down onto the GRE (TP9) via the GRE extension connected to the EMT. (Refer to Figure 2-8.) Although, unfortunately, the TP24 signal was driven far past its instrumentation saturation point of about 2 kA/m (Figure 3-35), some estimate of the peak amplitude can be derived using Ampere's law applied to the 13 kA current flowing on the vertical section of the 3½-in conduit in the corner. Accordingly, the peak amplitude of the magnetic field was about 7 kA/m on Stroke 1 of 94-15.

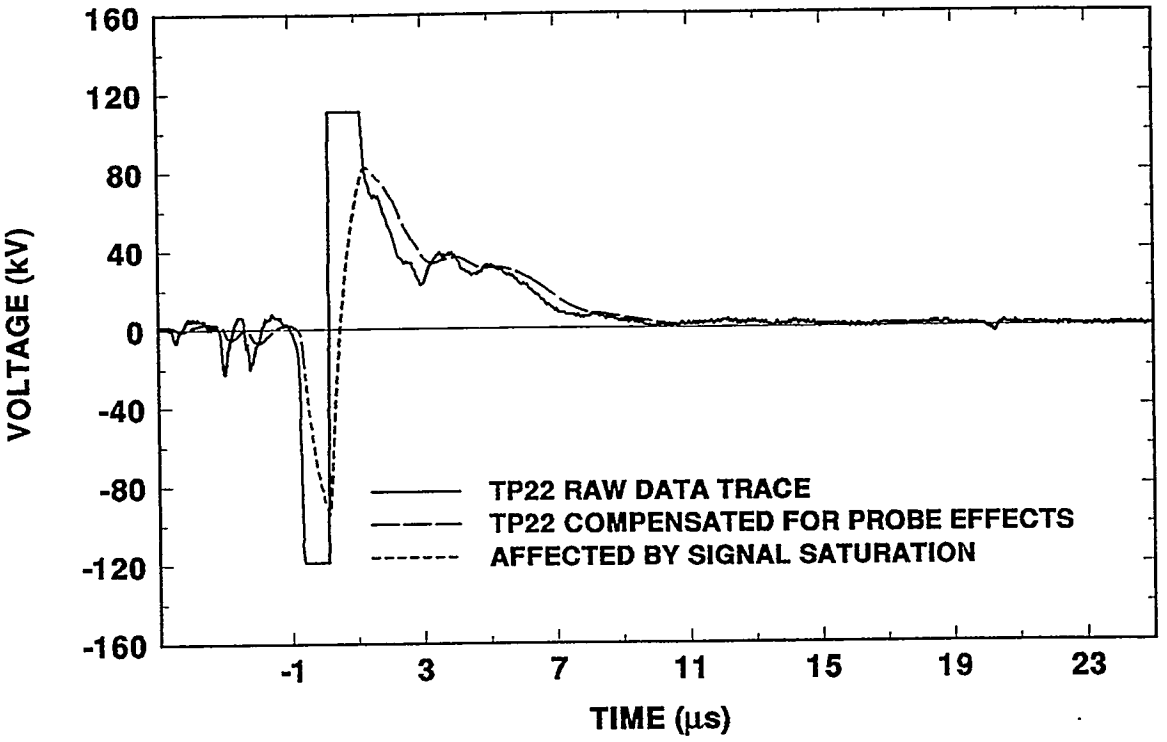

Figure 3-33. Example of raw recorded EMT voltage data trace and version processed to compensate for capacitive effects in the measurement probe

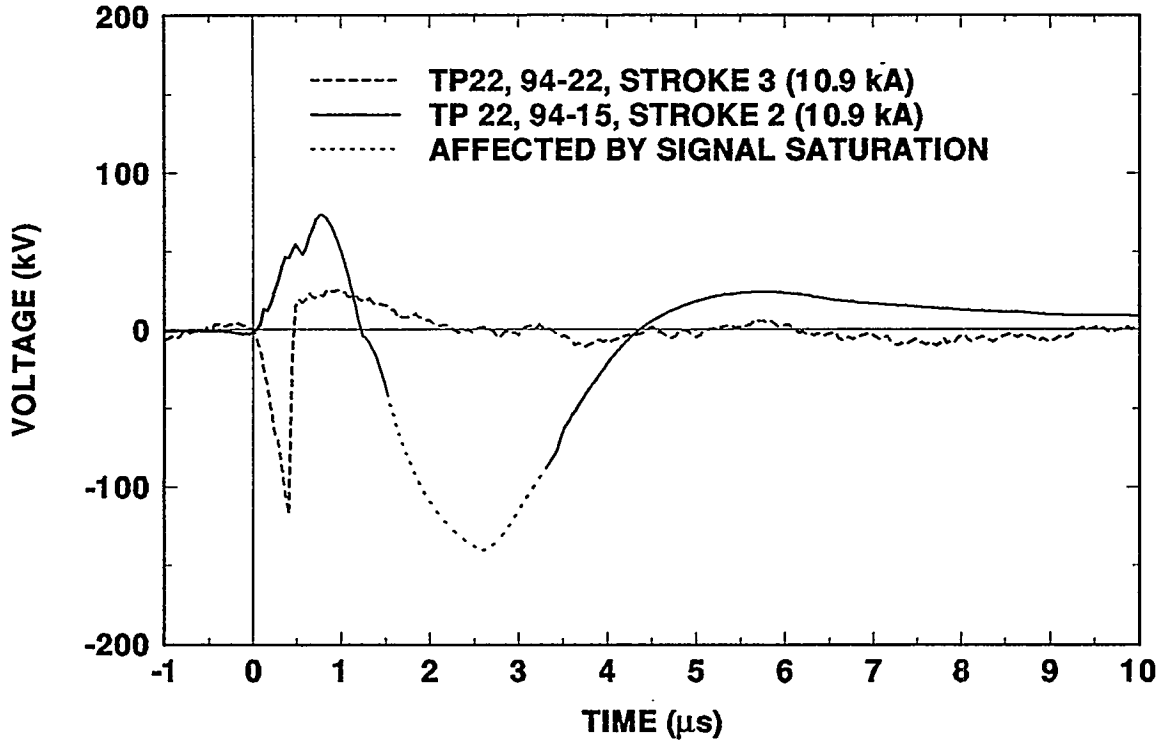

Figure 3-34. Example voltage transients on the interior power distribution conduit system measured during strikes to the east conduit riser stub. During Flash 94-15 the GRE and EMT were bonded together; during 94-22 they were not intentionally connected.

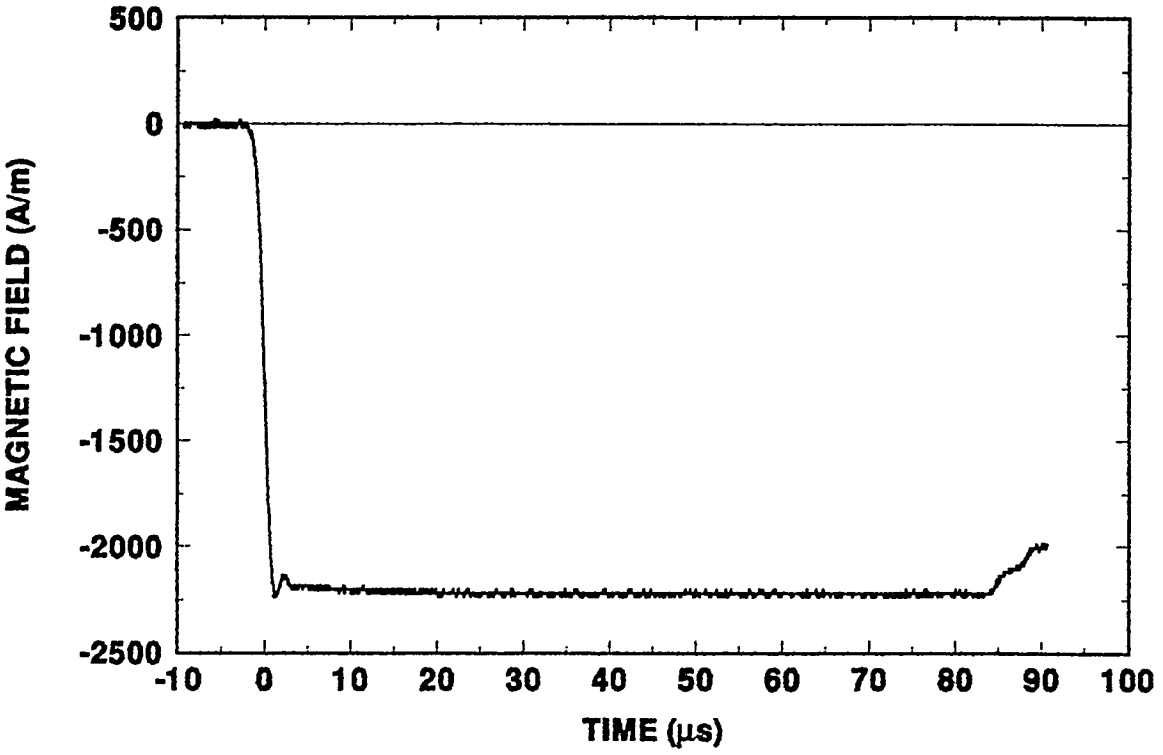

Figure 3-35. Magnetic field record from TP24 during Stroke 1 of Flash 94-15 to the east conduit riser stub

During Storm 4 the GRE extensions were disconnected from the EMT conduits. Therefore, the route to earth traced above for currents attaching to the riser stub was not available during Flashes 94-22 and 94-24. Nevertheless, from the results tabulated in Tables 3-12 and 3-13, it is apparent that much of the incident current still flowed back to the structure on the buried east conduit (TP2). Unfortunately, due to scheduled changes in the instrumentation of test points for the Storm 4, it is not possible to identify the path to earth that the stroke currents took after passing TP2.

On flashes attaching to the roof, the maximum observed magnetic field peak was about 1.4 kA/m. This response occurred at TP4 during Stroke 1 of Flash 94-07 (19.5 kA), which attached to the vent stack terminal. On every flash for which data are available at both magnetic field test points, the responses at TP24 are significantly higher that those at TP23. Setting aside the special case in which attachment was to the east conduit riser stub, these are interesting results. Since the down conductor currents are approximately the same at both corners of the building, the higher fields at TP24 must be related to higher currents flowing in the wall rebar on the good side, in which higher connectivity was enforced at the rebar intersections. From this viewpoint, then, "good" is bad, because the enforced rebar connections yielded a higher magnetic field environment inside the building.

3.2.9 Single Mast Lightning Protection System

The lightning protection system was modified prior to Storm 4. The changes included removal of the five air terminals mounted on the roof and their two associated down conductors. A 49-ft high radio antenna mast was erected as a lightning protection rod about 7 ft out from the wall at the front center of the structure. The base of the mast was instrumented to sense incident stroke currents and connected to the buried GRE as described in Section 2.4 and depicted in Figure 2-12. Seven strokes were triggered to the top of the mast during Flash 94-21, with peak amplitudes from about 5 to 19 kA.

Some insight into the overall relative effectiveness of the two different protection approaches can be obtained by comparing responses at the same points throughout the building for flashes to the roof terminals against those occurring during strokes to the mast. It is particularly instructive to carry out this comparison for strokes of comparable peak amplitude and rate of rise of the incident current. For convenience in doing so, the responses are listed in Table 3-14 for Stroke 7 (12.1 kA peak amplitude, 5.7×10^{10} A/s rise rate) of Flash 94-06 to the SW roof terminal during Storm 1 and for Stroke 5 (12.3 kA, 2.3×10^{10} A/s) of Flash 94-21 to the mast.

Table 3-14. Comparison of Responses Under Comparable Strokes: Roof Terminal Attachment and LPS Mast

I_{inc}	12.1	12.3	kA
TP	94-06	94-21	Units
1	>-2	-8.0	kA
2	-2.0	-1.5	kA
5	-.15/+.16	-4.4	kA
5'	+1.2	+0.3/-1.0	kA
6	---	-5.5	kA
6'	+0.11	-1.2	kA
10	-20	<±20	A
11	-105/+30	+340	A
12	<-10	~0	A
13	-75/+20	-150	A
14	-20	-30.0	A
15	-60/+30	-25/+20	A
20	+8.6/-2.4	-11/+2	kV
21	-29.0/+34.7	-21/+15	kV
22	--	-25/+70	kV
23	+125/-80	-130/+190	A/m
24	--	~0	A/m

Working through the list, it is observed that the currents on the buried conduits (TPs 1 and 2) are approximately equivalent, as are those at the various wall-to-floor rebar connections (TPs 10 through 15). Also comparable are the magnetic fields at TP23 (TP24 data were lost during Storm 1), and, the crane and vent stack voltages (TPs 20 and 21).

These results at first seem to be surprising in that, by design, there were no intentional connections made during Storm 4 between the buried GRE and the rest of the building. One possible explanation, illustrated in Figure 3-36, is that magnetic field coupling from the incident current flowing down the mast to the GRE sets up an opposing current due to magnetic field coupling in the cross section loop made up of the walls, roof and floor of the building. Some confirmation of this behavior is evident in the data of Table 3-14. For example, not only is the amplitude of the wall current at TP11, near the front of the building close to the LPS, high during Flash 94-21, but it is also of reversed polarity in comparison with Flash 94-06, during which attachment was directly to the roof. The same is true of the crane voltage, TP20, and magnetic field at TP23. Other test point responses that might be expected to follow suit, however, are less clearly supportive of the postulated explanation.

Maximum lightning protection is achieved by minimizing within the volume to be protected the electrical and electromagnetic environments that attend any strike to the structure or its protection system. As suggested by the data in Table 3-14, a single mast system, at least one close to the structure to be protected, does not result in a significantly lower overall set of electrical environments within the structure. If the postulated explanation for this as given above is valid, it suggests that a catenary system, with symmetric paths to ground for the incident, current might be superior. In that case, the magnetic fields surrounding the currents in each down conductor would tend to cancel one another in the center volume in which the building is located.

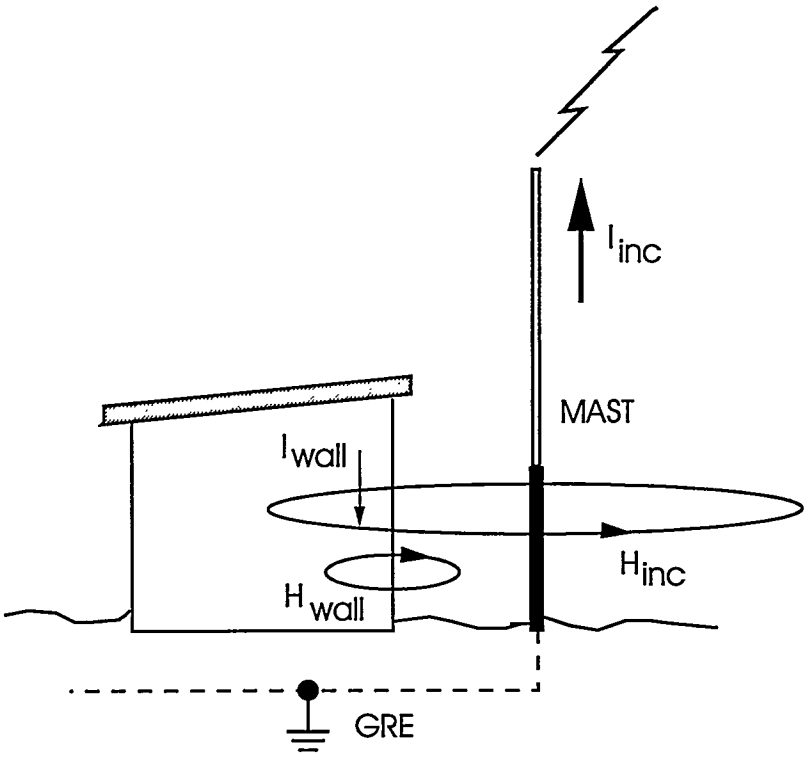

Figure 3-36. Mechanism for current flow within test structure due to strike to LPS mast

3.2.10 Arcing Inside the Test Structure

During all but the final storm a 35-mm still camera with 3200 speed black and white film was operated inside the (light-tight) building during each test event. The shutter was opened by remote control by means of a fiber optic link from the SATTLIF shelter prior to each rocket launch and was left open for the duration of the flash. Film advancement was automatic following shutter closure. The purpose of this camera was to detect any arcing that might take place during strikes to the building. The camera, equipped with an 18-mm wide angle lens, was sighted to provide maximum coverage of the interior. Prior to each storm it was installed at exactly the same spot on a stand about 5 ft above the floor near the southwest corner of the structure. The film back was equipped with a time stamp device so that each exposed frame was permanently marked for correlation with its respective test event.

Significant arcing at one spot within the building was detected during every flash triggered to the air terminals on the roof or to the east conduit riser stub. The site of the arc in each case was from a spot on the simulated power distribution system running along the east wall to the exposed end of some sort of steel stud that was cut off flush with the concrete wall about 1-½ in from the conduit. In Figure 3-37 the arc shows up as the larger bright spot just to the right of center in the photograph. The smaller bright spot to the left of the arc location is a reflection from the face of the electrical outlet box mounted on the back wall. Figure 3-37 was actually obtained from the superposition of two separate frames. The first, which makes the interior of the building visible for reference, was taken with the aid of auxiliary lighting prior to the beginning of the testing. To obtain Figure 3-37, the negative showing the arcing that occurred during Flash 94-14 was carefully superimposed on the reference frame at the time of printing.

This arcing repeatedly took place from a spot on the back side of the EMT to the steel stud in the concrete. By design, the conduit was mounted to the concrete wall on pads of woven phenolic dielectric material, which was in turn fastened to the wall using nylon bolts and anchor plugs. The purpose of this arrangement was to maintain intentional isolation of the EMT from the wall so that the bounding voltage response of the power distribution system in this type of building could be measured. Following the first storm, steps were taken to try to suppress further arcing at this location. A sheet of dielectric material was inserted between the EMT and the wall at the site of the arc. This turned out to be unsuccessful, and recurring arcing was observed throughout the first three storms. Finally, during one of the attachments to the riser stub during the fourth storm, the arcing was sufficiently energetic to tear the nylon anchor from its bed in the concrete wall. This can be seen in the photographs shown in Figure 3-38.

No other arcing was detected anywhere within the building during the course of the testing.

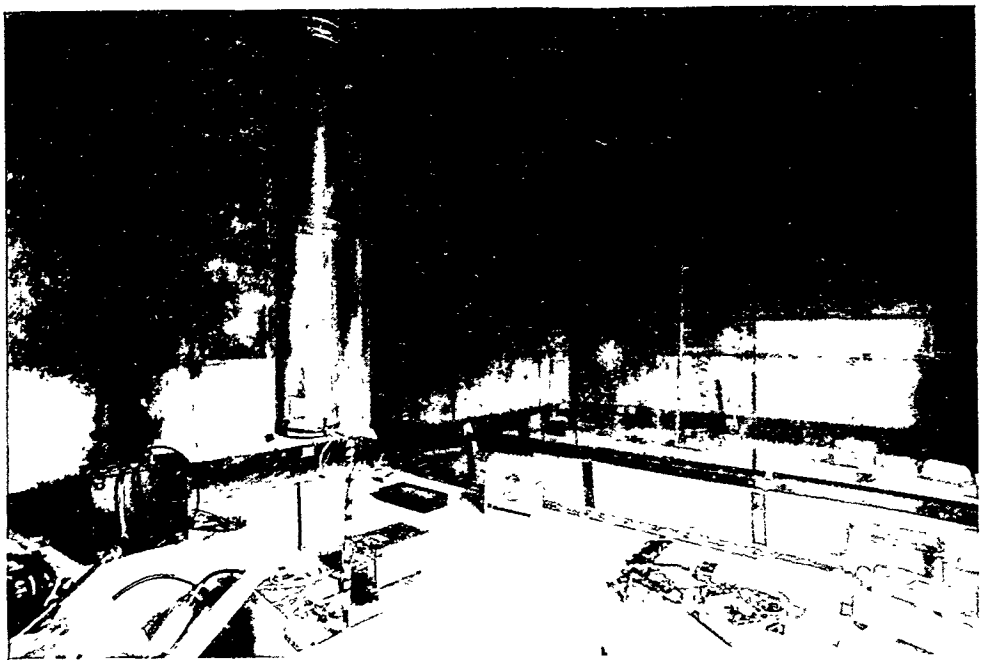

Figure 3-37. Arcing between EMT conduit and a nearby metal stud in the concrete wall. The arc is seen as the bright spot to the right of the center of the photograph. The smaller bright spot to its left is a reflection of the former from the metal plate on the outlet box mounted on the rear wall.

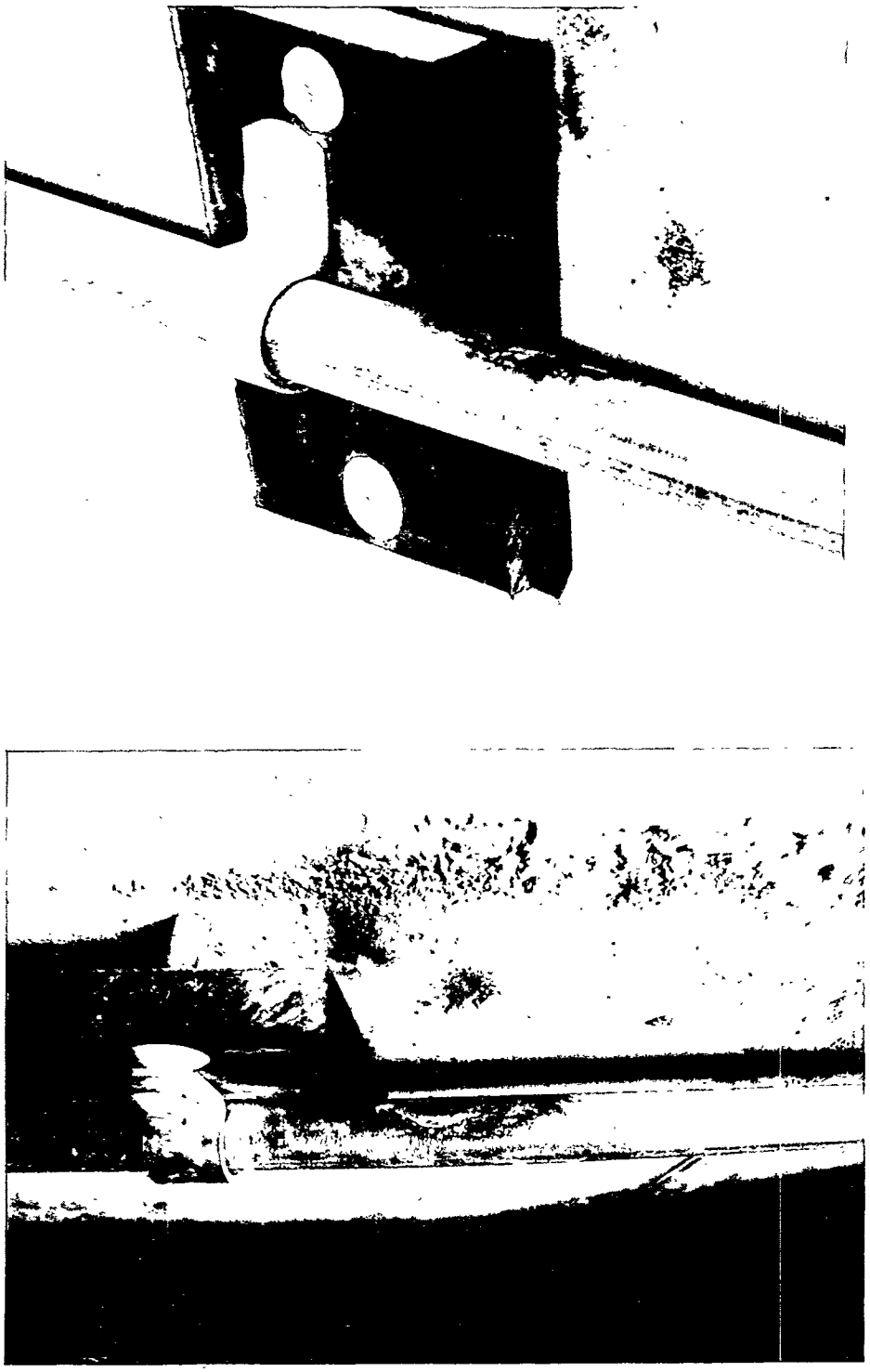

Figure 3-38. Two views of the site of arcing between the EMT conduit and the wall. Repeated arcing at this location was detected throughout the test period, but it was during the final storm that the energy of the arc caused the nylon anchor to be pulled from its bed in the concrete wall.

4.0 Conclusions and Recommendations

Presented in this report is a description of the design and construction of a test building, a description of the rocket-triggered lightning test conducted thereon, and a summary of the resulting measured response currents, voltages and magnetic fields at 24 different test points located throughout the structure and its lightning protection systems. The test building was specially designed to incorporate or simulate key features of a class of munitions maintenance and assembly buildings that are commonly in use throughout the Department of Defense complex. The structure was comprised of steel-reinforced concrete walls and floor, metal roof and supporting structure, and two types of lightning protection systems. Its design included simulated buried electrical power service conduits and interior electrical distribution system, as well as a simulated overhead crane rail and metallic ventilation duct.

Several difficulties were encountered during the testing which to some degree clouded the results of various of the direct comparisons of responses under different conditions that constituted some of the objectives of the tests. In some instances, responses substantially larger than what were anticipated caused loss of data through instrumentation saturation. In other cases, the occurrence of breakdown and arcing to the west buried conduit created an unintentional but dominant current path to earth that upset the planned comparison symmetries. In still other cases, measurement probe effects somewhat degraded the accuracy of some of the voltage measurements. Nevertheless, a very large body of reliable and highly interesting data was acquired, constituting the only known data base of its kind. The large majority of the results seem to be consistent with pretest expectations and intuition, but exceptions exist for which definitive explanations will have to await further detailed analysis, modeling and painstaking comparison of results on a location-by-location basis under the full range of test variations that were carried out. In some instances, resolution will also depend on results from follow-up testing.

The initial data reduction and analyses reported herein have led to a number of preliminary conclusions, which can be summarized as follows:

1. In this type of steel-reinforced concrete structure, structural members carry to earth the major fraction of incident lightning current. In the present case, the structure was specifically designed to allow the division of current between the building's LPS system and the embedded structural steel to be controlled. With wall-to-floor bonding jumpers removed, it was expected that the majority of the current would be carried to earth by the down conductors. In fact, this path carried no more than one-third to one-half of the incident stroke current. Modeling results have shown that in typical concrete structures protected by the integral type of system, roughly one-tenth or less of the incident stroke current is carried by the external LPS system.

2. Bonding of the floor and wall rebar resulted in only minimal effect on the percentage of current carried by the walls to earth. For this particular structure, the concrete floor was poured over a 6-in-thick layer of dry limestone gravel, a situation that is not universal for buildings of this type. The presence of this somewhat insulative

layer and the development of a shunt path to earth via arcing to one of the buried power conduits appear to have combined to reduce the effect of bonding between the floor and wall rebar. However, for structures in which the floor is in intimate contact with the underlying earth, electrical bonding between wall and floor is of key importance.

3. As might be expected, multiple LPS down conductors carry approximately equal shares of incident stroke current.

4. As a result of the development of arcing between the footer and the west buried conduit, the LPS ground ring electrode earthing system carried only a minor fraction of the incident stroke current away from the structure in comparison with the two buried simulated electrical power service conduits. Unless this preferential ground path is removed and the building is re-tested, no definitive statement about the value of the LPS grounding system can be made.

5. The development of breakdown and arcing created a dominant current path that was unanticipated prior to testing. In an actual operational facility, it may be virtually impossible to identify or predict such paths *a priori*. Thus the definitive assessment by analysis of complex existing facilities becomes tenuous. In any event, the analysis must be preceded by a comprehensive site examination backed-up by specialized pulse testing to eliminate as many uncertainties about electrical interconnections as possible.

6. The flow of current in the walls is complex and exhibits considerable bipolar structure.

7. In general, but not without exception, the enforced electrical connectivity at rebar intersections resulted in a pattern of higher wall currents in the "good" side of the test structure. Unfortunately, due to the development of arcing to the buried conduit, the true differences between the good-side and bad-side bonding practices may have been obscured by the arcing to the buried conduit.

8. Significantly high voltage transients with respect to the floor, of the order of 200 kV, were recorded on the vent stack, the simulated crane rail, and the metal conduit of the interior electrical distribution system. These transients represent hazards both to personnel and to munitions safety under readily imaginable combinations of circumstances that could occur within such a facility.

9. Peak voltages were similar at various locations throughout the structure and were found to correlate moderately well with the rise rate of incident stroke current ($0.57 \leq r \leq 0.82$). Much stronger linear correlation was found with peak amplitude of stroke current ($0.93 \leq r \leq 0.98$), and the wavefronts of voltages closely followed those of the incident currents. Hence, contrary to expectations, roof-to-floor voltages appear to be predominantly resistive in nature rather than inductive.

10. Surprisingly, the electrical responses throughout the matrix of common test points were generally comparable in magnitude, though of somewhat different waveform and polarity, during strikes to roof-mounted air terminals and strikes to the single 49-ft high protection mast. This behavior is postulated to result from the coupling or

the magnetic field from the incident current on the mast to the loop formed by the roof, walls, floor of the nearby structure.

A follow-up set of tests on the same structure are planned for the 1995 lightning season. Based on the results of the first tests presented herein, the following recommendations are made for the next tests:

1. A comprehensive set of resistance measurements should be made using the Biddle Megger. Of specific interest are resistances such as

   - floor-to-wall, with and without electrical bonding to each other
   - roof- to-wall base (from various points on the roof)
   - floor-to-fence
   - conduit at its exit point from the building to the fence system
   - GRE-to-buried conduit
   - GRE-to-fence
   - ground rod-to-fence, with ground rod disconnected from GRE

2. The buried conduits should then be completely removed, and the resistances re-measured.

3. An attempt should be made to clarify some of the intended comparisons that were clouded by the repeated development of the arc path to ground via the west conduit during the 1994 tests. Therefore, an abbreviated repeat series of triggered lightning measurements should be made with the conduits removed completely. Since only one storm will be allocated for these tests, all measurements should be concentrated in the good side of the building. One flash should be attached to the roof. The major test points of interest during that flash are

   - floor-to-wall voltage
   - crane-rail-to-floor voltage
   - down conductor currents
   - ground rod current
   - magnetic fields, center and corners

4. One flash should be allotted to confirming the postulated explanation for the observed responses associated with attachments to the LPS mast during the 1994 tests. This flash should be triggered to earth near the front of the structure to a stub coming up from the GRE at the same location as the mast was located during 1994. Two conducting loops, perhaps of 1/2-in copper tubing or similar material, should be constructed around the inside perimeter of the cross section of the building so that their planes are parallel with the side walls. One loop should be instrumented to measure open-circuit voltage, and the second to measure short-circuit current. To minimize their effects on one another, the short-circuited loop should be located in one side and the open-circuited loop in the other.

5.0 References

1. Schnetzer, G.H. and R.J. Fisher, *1991 Rocket-Triggered Lightning Test of the DoD Security Operations Test Site (SOTS) Munitions Storage Bunker*, Ft. McClellan, Alabama, Volume 1, SAND91-2343, February 1992.

2. Fisher, R.J. and G.H. Schnetzer, *1993 Triggered Lightning Test Program: Environments Within 20 Meters of the Lightning Channel and Small Area Temporary Protection Concepts*, SAND94-0311, March 1994.

3. Fisher, R.J. and G.H. Schnetzer, *1990 Sandia Rocket-Triggered Lightning Field Test at Kennedy Space Center, Florida*, SAND90-2926, March 1991.

4. Schnetzer, G.H., "SATTLIF Equipment: Incident Current Fiber Optic Links, Issue A," February 23, 1994.

5. Schnetzer, G.H., "SATTLIF Equipment: Meret Fiber Optic Link System, Issue A," June 8, 1993.

6. Stearns, S., Digital Signal Analysis, Hayden Book Co., Rochelle Park, NJ (1975).

7. Schnetzer, G.H., "Resistive Probe Corrections," October 28, 1994.

8. Fisher, R.J. and G.H. Schnetzer, "Technical Plan: Triggered Lightning Test of a Facsimile Weapons Maintenance and Assembly Building, ISSUE A," April 30, 1993.

9. Schnetzer, G.H., "Instrumentation Plan: RTL Test of Mockup M&A Building and Temporary Lightning Protection Systems, ISSUE B," March 31, 1994.

10. Uman, M.A., The Lightning Discharge, Academic Press, New York (1987).

11. Fisher, R.J., G.H. Schnetzer, R. Thottappillil, V.A. Rakov, M.A. Uman, and J.D. Goldberg, "Parameters of Triggered Lightning Flashes in Florida and Alabama," *J. Geophys. Res.*, Vol. 98, No. D12, December 20, 1993.

12. Morris, M.E., R.J. Fisher, G.H. Schnetzer, K.O. Merewether, and R.E. Jorgenson, "Rocket-Triggered Lightning Studies for the Protection of Critical Assets," *IEEE Trans. on Industry Applications*, Vol. 30, No.3, May/June 1994.

13. Merewether, K.O., L.K. Warne, and K.C. Chen, "Equivalent Circuit Parameters for the Army Maintenance and Assembly Building," SNL Technical Memo, May 9, 1995.

14. Warne, L.K., K.O. Merewether, and K.C. Chen, "Equivalent Circuit Parameters for the Fence at the Army Maintenance and Assembly Building," SNL Technical Memo, May 9, 1995.

Distribution

1 Roger E. Baldwin
Building D3, Room 003
Culham Laboratory
Abingdon
Oxfordshire OX14 3DB
United Kingdom

1 Mr. Brian Burrows
5 Willow Lane
Milton
Abingdon
Oxfordshire OX14 4EG
United Kingdom

1 Dr. Vernon Cooray
Institute of High Voltage Research
Uppsala University
Husbyborg
S-755 92 Uppsala
Sweden

1 Dr. Rajeev Thottappillil
Institute of High Voltage
Uppsala University
Husbyborg
Uppsala S7528
Sweden

1 Dr.-Ing. Wolfgang Zischank
Universitat Der Bundeswehr Munchen
Institut ET/7
Werner-Heisenberg-Weg 39
D-8014 Neubiberg
Germany

1 Prof. Matt Darveniza
Department of Electrical Engineering
University of Queensland
Brisbane, Australia 4072

1 Andre Eybert-Berard
ST1/LASP
C.E.N.G. Avenue Des Martyrs
85X 38041 Grenoble Cedex
France

Distribution (Continued)

1 AFGL
PL/GP/LYA
Attn: Dr. John Willet
Hanscom AFB, MA 01720

5 Commander
USA Armament Research, Development,
and Engineering Center
Attn: SMCAR-FSN
SMCAR-AEC-IM
SMCAR-FSN-T
Picatinny Arsenal, NJ 07806-5000

1 Commander, US Army Armament, Munitions and Chemical Command
Attn: AMSC-MAY-W
Picatinny Arsenal, NJ 07806-5000

1 Office of the Assistant to the Secretary
of Defense (Atomic Energy)
Room 3E1074, The Pentagon
Washington, DC 20301-3050

3 Director
Defense Nuclear Agency
Attn: R. C. Webb
LTC Wayne Andrews
J. V. Brackett
Washington, DC 20305

1 Commander, Naval Sea Systems Command
Department of the Navy
Attn: Nuclear Weapons/Munitions
Sec Div (SEA-643)
Washington, DC 20360

1 Commander, Naval Sea Systems Command
Theater Nuclear Warfare Program (PMS 423)
Attn: T. Rosling
Washington, DC 20362-5101

Distribution (Continued)

4 Director, Strategic Systems Projects
Department of the Navy
Attn: B. Hannah
R. M. Jones
M. Whittaker
Ruth Ann Lee
Washington, DC 20376

1 US Department of Energy
Office of Military Applications
Attn: DP-22
Washington, DC 20545

2 Navy EOD Technology
Attn: Richard Burdette
Indian Head, MD 20640

2 Commander
NATC
Attn: M. Whitaker (SY84)
Patuxent River NAS, MD 20670

1 Commander, US Army Nuclear and Chemical Agency
Attn: MONA-MS (G. Long)
7500 Backlick Road
Springfield, VA 22150

1 Dr. William Maurits
DDESB-KT
Hoffman Bldg. 1/Rm 856-C
2461 Eisenhower Ave.
Alexandria, VA 22331-0600

1 Commander
Naval Surface Weapon Center
Attn: B. Franklin
Dahlgren, VA 22448

1 Commander
Attn: HQ AFCESA (Fowler)
Tyndall AFB, FL 32403-6001

Distribution (Continued)

1 Commander
Attn: ASO/YQI (C. Churillo)
Eglin AFB, FL 32542

1 Commander, US Army Missile Command
Attn: Technical Library
Redstone Arsenal, AL 35898-5690

3 DoD SOTS
SMCAR-FSN-M
Attn: K. Haynes
Ft. McClellan, AL 36205-5300

1 Commander, US Army Armament, Munitions and Chemical Command
Attn: AMSMC-ASN-N
Rock Island, IL 61299-6000

1 National Severe Storms Laboratory
Storm Electricity and Cloud Physics
Attn: Dr. W. D. Rust
1313 Halley Circle
Norman, OK 73069

2 Field Command Defense Nuclear Agency
Attn: CDR F. T. Walker
Kirtland AFB, NM 87115-5000

1 US Department of Energy
Albuquerque Operations Office
Attn: NESD/WSSB
P.O. Box 5400
Albuquerque, NM 87115

4 Weapons Laboratory
Attn: D. Ulibarri/NTSW
M. Harrison/NTCA
LTCOL D. Stone/PL-LMI
Kirtland AFB, NM 87117-6006

1 Commander
NWEF
Attn: Jeff Stickney
Kirtland AFB, NM 87117

Distribution (Continued)

1 RDA
Attn: Art Barondes
6940 S. Kings Highway
Alexandria, VA 22310

1 Logicon RDA
Attn: Bill Kehrer
P. O. Box 9377
Albuquerque, NM 87119

1 Los Alamos National Laboratory
Attn: Technical Library
M. G. Wheeler, WX-1
P.O. Box 1663
Los Alamos, NM 87545

1 Commander, White Sands Missile Range
Bldg. 21225
Attn: Technical Library
White Sands Missile Range, NM 88002

1 Headquarters
Air Force Inspection and Safety Center
Attn: SEWV (Blount)
Norton AFB, CA 924097

1 Electric Power Research Institute
Project Manager/Distribution Program
Attn: Ralph Bernstein
P. O. Box 10412
Palo Alto, CA 94303

3 University of California
Lawrence Livermore National Laboratory
Attn: Technical Info. Dept.
R. T. Hasbrouck
Bill Hubbel, L-125
R. A. Woelffer, L-125
P.O. Box 808
Livermore, CA 94550

5 Richard J. Fisher
1797 Pleasant Grove Road
Claysville, PA 15323

Distribution (Continued)

3 University of Florida
Attn: Martin A. Uman
Dept. of Electrical Engineering
University of Florida
216 Larsen Hall
Gainesville, FL 32611-6200

1 Mr. Leon Byerly
2744 E. 5th St.
Tucson, AZ 85716

1 Prof. Vince Idone
State University of New York, Albany
1400 Washington Ave.
Albany, NY 12222

1 Mr. Bill Jafferis
4140 Hickory Hill Blvd.
Titusville, FL 32780

1 Professor E. P. Krider
Institute of Atmospheric Physics
University of Arizona
Tucson, AZ 85721

1 Mr. J. A. Plumer
Lightning Technologies, Inc.
10 Downing Parkway
Pittsfield, MA 01201

1 Mr. Jake Struck
45 Esplanong Rd.
Lake Hopatcong, NJ 07849

1 Dr. Chuck Weidman
Institute of Atmospheric Physics
University of Arizona
Tucson, AZ 85721

Distribution (Continued)

1 MS 9006 E. E. Ives (Org. 5200)
1 MS 9215 C. T. Yokomizo (Org. 8007)
1 MS 9004 M. E. John (Org. 8100)
1 MS 9031 J. E. Marion (Org. 5302)
1 MS 9202 L. E. Dighton (Org. 8116)
1 MS 9202 C. M. Furnberg (Org. 8116)
1 MS 9005 J. B. Wright (Org. 5300)
1 MS 9013 R. G. Miller (Org. 5366)
1 MS 9014 D. L. Gehmlich (Org. 5371)
1 MS 9203 E. B. Talbot (Org 5354)
1 MS 9014 J. L. Mitchell (Org. 5371)
1 MS 9033 R. A. Pearson (Org. 5362)
1 MS 9203 S. J. Vasey (Org. 5354)
1 MS 9006 D. J. Bohrer (Org. 5203)
1 MS 9033 G. E. Dietel (Org. 5362)
1 MS 9034 D. J. Beyer (Org. 5363)
1 MS 9035 G. C. Story (Org. 5365)
1 MS 9056 C. A. Skinrood (Org. 8102)
1 MS 9013 K. A. Mitchell (Org. 5366)
1 MS 9014 J. R. Hogan (Org. 5371)
1 MS 9021 R. E. Martinell (Org. 8535)

1 MS 0465 J. F. Ney (Org. 5003)
1 MS 0490 S. D. Spray (Org. 12331)
1 MS 0492 G. A. Sanders (Org. 12332)
1 MS 0490 P. E. D'Antonio (Org. 12324)
1 MS 0761 P. E. Rexroth (Org. 5822)
1 MS 0492 J. F. Wolcott (Org. 12332)
1 MS 0492 D. Loescher (Org. 12332)
1 MS 0459 T. S. Edrington (Org. 5205)
1 MS 1181 J. M. Hoffman (Org. 1208)
1 MS 1153 L. D. Bacon (Org. 1248)
1 MS 0513 H. W. Schmitt (Org. 2000)
1 MS 0311 R. F. Ellison, Jr. (Org. 2671)
1 MS 1007 J. F. Jones, Jr. (Org. 2172)
1 MS 0511 G. N. Beeler Org. 2500)
1 MS 1073 P. V. Dressendorfer (Org. 2277)
1 MS 0319 S. B. Martin (Org. 2641)
1 MS 0865 J. H. Barnette (Org. 2905)
1 MS 0527 L. A. Andrews (Org. 2235)
1 MS 0523 R. D. Holt (Org. 2251)
1 MS 0507 K. G. McCaughey (Org. 2700)
1 MS 0753 T. D. Hund (Org. 6218)
50 MS 0865 M. E. Morris (Org. 2753)
1 MS 0865 K. C. Chen (Org. 2753)

Distribution (Continued)

1 MS 0865 R. D. Jones (Org. 2753)
1 MS 0865 R. E. Jorgenson (Org. 2753)
1 MS 0865 K. O. Merewether (Org. 2753)
3 MS 0865 G. H. Schnetzer (Org. 2753)
1 MS 0865 L. K. Warne (Org. 2753)
1 MS 0570 C. W. Childers (Org. 5900)
1 MS 0447 R. E. Kreutzfeld (Org. 5111)
1 MS 0447 J. O. Harrison (Org. 5111)
1 MS 0447 J. S. Clabaugh (Org. 5111)
1 MS 0447 H. T. Lehman (Org. 5111)
1 MS 0436 G. L. Maxam (Org. 5147)
1 MS 0467 K. D. Nokes (Org. 5091)
1 MS 0482 K. Oishi (Org. 5161)
1 MS 0455 G. R. Otey (Org. 4100)
1 MS 0560 D. F. McVey (Org. 5408)
1 MS 0755 H. W. Church (Org. 6612)
1 MS 0971 G. H. Mauth (Org. 9203)
1 MS 1165 J. E. Powell (Org. 9300)
1 MS 1166 J. H. Renken (Org. 9301)
1 MS 1166 G. J. Scrivner (Org. 9352)
1 MS 1166 C. D. Turner (Org. 9352)
1 MS 0908 C. N. Vittitoe (Org. 9225)
1 MS 0768 J. W. Kane (Org. 5806)
1 MS 0765 D. E. McGovern (Org. 5808)

1 MS 9018 Central Technical Files (Org. 8523-2)
5 MS 0899 Technical Library (Org. 13414)
1 MS 0619 Print Media (Org. 12615)
2 MS 0100 Document Processing (for DOE/OSTI) (Org. 7613-2)